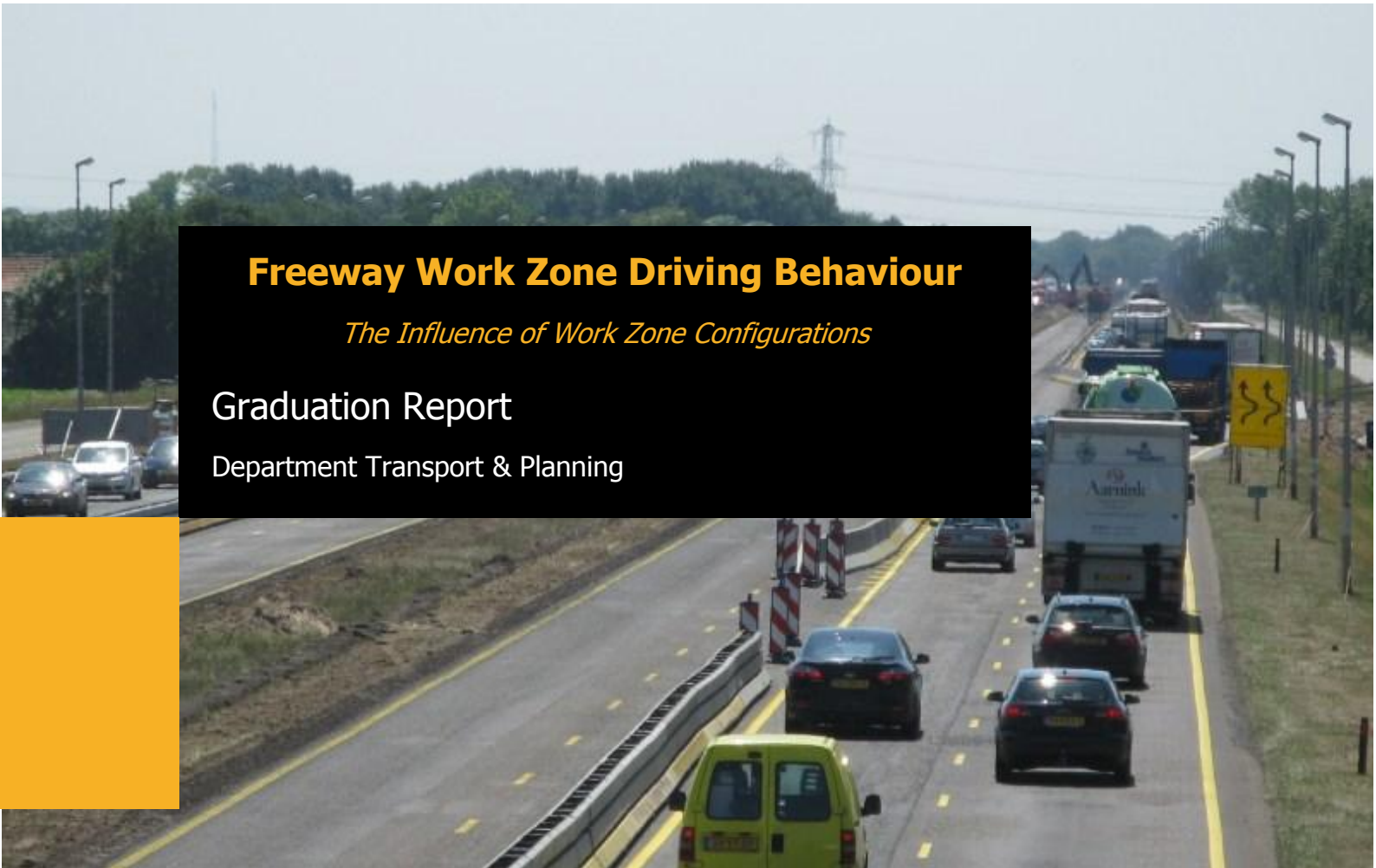


Freeway Work Zone Driving Behaviour

The Influence of Work Zone Configurations

Graduation Report

Department Transport & Planning



FREEWAY WORK ZONE DRIVING BEHAVIOUR

The Influence of Work Zone Configurations

Graduation research report

AUTHOR

R. Voorrips (Rosco)

Delft University of Technology

THESIS COMMITTEE

Prof.Dr.Ir. S.P. Hoogendoorn	Professor T&P	TU Delft
Ir. P.B.L. Wiggeraad	Coordinator T&P	TU Delft
Dr. R.G. Hoogendoorn	Daily supervisor T&P	TU Delft
Dr.Ir. R. Happee	Guest member BME	TU Delft
Ir. M. Meijs	Daily supervisor	Mourik Groot-Ammers B.V.

DATE

Januari 2013

Preface

In this graduation report, performed research with regard to longitudinal driving behaviour in work zones is presented. This research is the last step in finishing my master study at the faculty of Civil Engineering at Delft Technical University (TU Delft). This research has been done at the department of Transport & Planning in cooperation with Mourik Groot-Ammers B.V.

Mourik is a Dutch contractor who is originally specialized in cables and pipes for infrastructure above and in the underground, but over the last decennia Mourik has become an important player in the Dutch civil engineering sector, for example in the field of large road (re)constructions.

Mourik offered full possibilities to successfully complete this graduation study, and therefore I would like to thank Mourik as a company and my daily supervisor Mathijs Meijs for supporting me during this period. Furthermore, I would like to thank the other members of my thesis committee for their assistance and comments on my work during this research study as well as the IT section of the faculty of Civil Engineering and Geosciences for giving full cooperation to use complete computer rooms during weekends to be able to carry out the stabilization process.

Finally, I would like to thank my girlfriend, parents and friends who supported and encouraged me during this long graduation process.

Content

Preface	i
Summary	v
Samenvatting	ix
1 Introduction	1
1.1 Background	1
1.2 Problem definition.....	7
1.3 Research objective.....	7
1.4 Research questions.....	7
1.5 Research approach and report outline.....	7
2 Determinants of driving behaviour	11
2.1 Determinant analysis	11
2.2 Selection of research determinants	14
2.3 Conclusions	17
3 Analysing methods	19
3.1 Adaptation effect on different driving task levels.....	19
3.2 Analysing adaptation effects in driving behaviour.....	19
3.3 Conclusions	28
4 Data collection	29
4.1 Required data for analysing individual driving behaviour	29
4.2 Data collection methods	29
4.3 Configurations of observed locations.....	36
4.4 Conclusions	38
5 Data processing	39
5.1 Step 1: Image pre-processing.....	39
5.2 Step 2: Detecting and tracking vehicles.....	45
5.3 Conclusions	50
6 Analysis Results	51
6.1 Analysing empirical car following behaviour	51
6.2 Simulating individual driving behaviour	79
6.3 Conclusions	86
7 Conclusions and recommendations	89
7.1 Conclusions	89
7.2 Practical recommendations.....	92
7.3 Recommendations for future research.....	94
References	95
Appendixes	101

Summary

The performance of work zones with specific layouts cannot be accurately determined, because changes in individual driving behaviour at work zones are unknown and therefore cannot be modelled. Therefore, the research objective of this graduation research is: *"Gain insight into possible adaptation effects related to the layout of work zones, in empirical individual driving behaviour and subsequent in macroscopic effects, by presenting the applied method"*.

Determinant analysis and selection

Firstly, factors (e.g. determinants) that influence driving behaviour have been investigated by a state-of-the-art, after which researched determinants could be selected. The determinants were divided into two main groups, static and dynamic determinants, and further divided into cross-section, alignment and signage for static determinants and traffic dependent or independent for dynamic determinants. The selection of research determinants was based on two criteria:

- How specific is the determinant for work zones?
- Can authorities and contractors influence the determinant value?

Based on these criteria, lane width, speed limit, type of channelizing device, and the presence of contra flow/reverse curves have been selected as research determinants.

Methods to analyse changes in individual driving behaviour and macroscopic effects

Empirical driving behaviour can be described as real time observed vehicle movements of individual drivers including the influence of interaction with other drivers. This behaviour in work zones can be described best by microscopic analysis at a tactical level, which includes empirical driving behaviour, such as speed and following distance. Selected analysing methods analyse empirical variables, such as headway distributions, speed distributions and the speed - following distances relationship. Macroscopic effects can be analysed using macroscopic variables, such as intensities and densities, which are important for the general performance of work zones. These variables can be investigated by using empirical data and results from simulating individual driving behaviour.

So, by calibrating an individual driving behaviour model, the relationship between adaptation effects in individual driving behaviour and macroscopic effects can be investigated. Using individual driving behaviour models (in this particular research the Extended IDM), simulations can be performed from which macroscopic data can be collected.

Data collection

To collect required data, a method has been chosen that collects required variables for doing the analysis. Based on the analysing methods, it is required to observe positions of the present vehicles during a specific period. To reduce costs for data collection, the choice is made to collect data by an innovative method: the unmanned helicopter (instead of a manned helicopter).

For the five observed locations, three are fully elaborated. Specific determinant values of these three locations are given in the table below.

Configuration		Location		
		2	4a	4b
Speed limit (km/h)		90	90	90
Contra Flow		No	No	No
Channelizing Device	Left	Guard rail	Barrier	Barrier
	Right	Guard rail	Guard Rail	Guard Rail
Hard Shoulder		Yes	Yes	Yes
Lane width (m)		2x3.5	3.25-3.00	3.25-3.00
Reverse Curve		No	Yes (small)	No

Determinant values of worked out locations.

Data processing

After collecting the raw imagery by unmanned helicopter, two main steps in data processing have to be performed:

- Image pre-processing;
- Detecting & tracking vehicles.

The first step should have stabilized moving imagery to stable isolated frames, but included many errors. This resulted in many short stabilized parts, which had to be handled separately. These many parts have been the reason that only three out of five observed locations have been fully studied.

The second step is to detect and track all vehicles and their positions over the time they were observed. Vehicles have been detected by finding their trajectories in combined longitudinal cross-sections. Trajectory lines have been detected using a very accurate method that had not been used before for this purpose, namely edge detection. This method detects possible vehicle movements by checking changes in colour intensities in adjacent pixels.

The starts and ends of each vehicle have been set by a in this research new developed program, which returns image indices of the location of the cursor registered by mouse clicks.

Tracking vehicles over their trajectory (from start to end) has been carried out by applying the Dijkstra shortest-path algorithm, which has been exclusively programmed as part of this study.

To finally convert vehicle movements over pixels to real life distances, pixel locations have been transformed to real life distances using known dimensions of pavement markings.

Analysed adaptation effects in driving behaviour

Because congested conditions have not been observed, observed accelerations were small. This resulted in problems in analysing adaptation effects in empirical driving behaviour:

- It has not been possible to determine the complete shape of the fundamental diagram using empirical data;
- It has not been possible to integrally estimate model parameters of the selected car-following model.

Differences were visible in observed headways, speeds at corresponding following distances and speed-following distance distributions at a range of 25 to 30 m following distance, which imply changes in configuration capacity.

Differences in driver heterogeneity between configurations have not been observed, but they have been between distinguished vehicle types. The heterogeneity of heavy vehicles was significantly lower than of passenger cars.

No significant differences in lane occupation distributions have been observed. Therefore, it was legitimate for this research to exclude lane changing behaviour.

Despite it was not possible to estimate the entire model parameters set of the Extended IDM, individual model parameters have been estimated to investigate macroscopic effects. By using an existing simulation tool, which combined the calibrated car-following model (the extended IDM) and a lane changing model (LMRS), macroscopic effects of differences in free flow speeds and desired time headways have been investigated, which resulted in:

- Reduced lane widths from 2x3.5 m to 3.25 and 3.0 m in combination with a barrier as channelizing device instead of normal guard rail resulted in a reduction in capacity of 1.5%;
- A small reverse curve is responsible for a relatively large additional decrease in capacity of 4.7%.

Practical recommendations

Recommendations have been presented towards data collection using an unmanned helicopter. It has been recommended to analyse possible locations in detail and consulting an unmanned helicopter specialist, before doing measurements.

To reduce problems during stabilizing frames, reference points could be manually placed and the stabilization program itself should be adjusted, so it can deal with stabilization errors itself.

For designing work zones, it has been recommended to avoid abrupt changes in the road layout, as the small reverse curve caused a relative large decrease in capacity. So, it has been advised to spread changes in layout over longer road stretches.

Recommendations for future research

For this research only three deterrent influences have been investigated. To determine adaptation effects and performances of more work zone configurations other determinants have to be investigated as well.

Other recommendations yield the development of methods that detects and tracks vehicles more easily:

- Vehicles have to be automatically detected from combined, edged, longitudinal cross-sections;
- A faster algorithm could be programmed to replace the relatively slow Dijkstra algorithm for connecting vehicle starts and ends.

This research showed that problems can occur when car-following models are calibrated to data which do not consist each traffic state. Therefore it has been recommended to analyse the relationship between differences in uncongested driving and differences in congested driving. When a relation is found, it could be possible to estimate changes in driving behaviour under congested conditions based on changed behaviour at uncongested driving only.

Samenvatting

Het is op dit moment niet mogelijk te bepalen hoe goed wegvakken met wegwerkzaamheden presteren op basis van de specifieke wegvakconfiguraties. De mate waarin individueel rijgedrag verandert bij wegwerkzaamheden is onbekend en kan dus niet gemodelleerd worden. Het doel van dit afstudeeronderzoek is dan ook: *"Inzicht krijgen in mogelijke adaptatie-effecten gerelateerd aan de wegvakconfiguratie bij wegwerkzaamheden, in empirisch individueel rijgedrag en daaruit voortvloeiende macroscopische effecten, inclusief het presenteren van de gebruikte methode"*.

Determinanten analyse en selectie

Eerst zijn factoren (determinanten) die rijgedrag mogelijk beïnvloeden door middel van een literatuurstudie onderzocht, waarna determinanten zijn geselecteerd voor dit onderzoek. De determinanten zijn onderverdeeld in twee categorieën, namelijk statische en dynamische determinanten, waarna ze verder onderverdeeld zijn in dwarsdoorsnede, alignement en bebakening voor statische determinanten en in verkeersafhankelijke en onafhankelijke determinanten voor dynamische determinanten. De selectie van onderzoeksdeterminanten is gebaseerd op twee criteria:

- Is de determinant specifiek is voor wegwerkzaamheden?
- Is de waarde van de determinant door wegbeheerders en aannemers te beïnvloeden?

Op basis van deze criteria, zijn strookbreedte, geldende snelheidsbeperking, type langsafzetting, en aanwezigheid van contra-flow (bijvoorbeeld een '4-0 systeem') en/of slingers geselecteerd.

Methoden voor analyseren van individueel rijgedrag en macroscopische effecten

Individueel rijgedrag wordt beschreven door voertuigbewegingen van elk afzonderlijk voertuig, welke mede beïnvloed worden door interactie met andere voertuigen. Het rijgedrag bij wegwerkzaamheden kan het best beschreven worden door middel van een microscopische analyse op een 'tactisch niveau', welke rijgedrag zoals snelheid en volgafstand bevat.

De methoden om individueel rijgedrag, en veranderingen daarin, te analyseren, beschouwen individuele variabelen, zoals volgtijden, snelheidsdistributies en de relatie snelheid - volgafstand. Macroscopische effecten worden geanalyseerd aan de hand van macroscopische variabelen, zoals intensiteiten en dichtheden. Deze variabelen kunnen geanalyseerd worden door gebruik te maken van empirische data en van resultaten van het simuleren van individueel rijgedrag.

Dus door modellen te gebruiken die het gekalibreerde individuele rijgedrag schatten voor simulatie, kunnen macroscopische effecten worden onderzocht.

Data verzameling

Voordat benodigde data verzameld kon worden, moet de verzamelmethode gekozen worden. Deze keuze is gebaseerd op basis van de benodigde data voor de genoemde analyse. Deze eisten dat voertuigen gedurende een langere tijd empirisch gevolgd konden worden. Om de kosten te beperken en meer data te kunnen verzamelen, is gekozen voor een innovatieve methode voor dit type onderzoek: De onbemande helikopter (in plaats van de bemande helikopter).

Voor de 3 volledig geanalyseerde configuraties, zijn de waarden van geselecteerde determinanten in onderstaande tabel weergegeven.

Configuratie		Locatie		
		2	4a	4b
Snelheidslimit (km/u)		90	90	90
Contra-flow		Nee	Nee	Nee
Langsafzetting	Links	Geleiderail	Barrier	Barrier
	Rechts	Geleiderail	Geleiderail	Geleiderail
Vluchtstrook		Ja	Ja	Ja
Rijstrookbreedte (m)		2x3.5	3.25-3.00	3.25-3.00
Slinger		Nee	Ja (klein)	Nee

Waarden van determinanten voor de onderzochte configuraties.

Data verwerking

Na het maken van ruwe HD videobeelden met de onbemande helikopter, zijn de beelden verwerkt tot individuele voertuigbewegingen. Deze verwerking bestond uit twee stappen:

- Het voorbereiden en stabiliseren van de beelden;
- Het detecteren en volgen van voertuigen.

De eerste stap zou de losse frames gestabiliseerd moeten hebben, maar bevatte helaas veel stabilisatiefouten. Deze kwamen tot uitdrukking in korte perioden van gestabiliseerde frames, welke los behandeld moesten worden. Dit is de reden dat slechts drie van de in totaal vijf geobserveerde configuraties volledig zijn uitgewerkt.

De tweede verwerkingsstap bestond uit detecteren en vervolgens volgen van voertuigen. De detectie vond plaats door het combineren van langsdorsneden tot trajectoriën. Deze trajectoriën zijn gevonden met een nog niet eerder gebruikte methode voor dit type onderzoek, namelijk 'rand detectie'. Deze methode detecteert mogelijke voertuigbewegingen door kleurverschillen in aangrenzende pixels.

Het start- en eindpunt van de voertuigen is aangegeven met een voor dit onderzoek nieuw ontwikkeld programma, welke locaties van de cursor opslaat. Daarna zijn deze verbonden met behulp van een kortste-pad algoritme: het Dijkstra algoritme. Dit algoritme is als onderdeel van dit onderzoek voor het eerst geïmplementeerd in Matlab.

Ten slotte zijn voertuiglocaties omgerekend van pixellocaties naar real-life locaties met behulp van aanwezige wegmarkering.

Geanalyseerde adaptatie effecten in rijgedrag

Doordat geen congestie waargenomen is, zijn de waargenomen acceleraties klein. Dit bracht problemen met zich mee voor het analyseren van effecten van de toegepaste configuratie:

- Een integrale schatting van modelparameters bleek niet mogelijk;
- Het empirisch bepalen van de vorm van het fundamenteel diagram was niet mogelijk.

Tussen configuraties zijn significante verschillen waargenomen in de volgtijden, de relatie snelheid – volgafstand en in de snelheid – volgafstand distributies bij de volgafstand 25 - 30 m, wat een daling in capaciteit van het wegvak impliceert.

Er zijn geen significante verschillen in heterogeniteit tussen bestuurders waargenomen bij de verschillende configuraties, maar wel tussen typen bestuurders. De standaardafwijking van zware voertuigen was aanzienlijk lager dan die van personenauto's.

Verschillen in rijstrookbezetting zijn niet waargenomen, wat het rechtvaardigt rijstrookwisselingen in dit onderzoek buiten beschouwing te laten.

Ondanks dat het integraal schatten van modelparameters niet mogelijk bleek, zijn modelparameters individueel geschat om macroscopische effecten te onderzoeken.

Met gebruik van een bestaande simulatietool, dat het geselecteerde volgmodel (Extended IDM) en een rijstrookwisselmodel (LRMS) combineert, zijn macroscopische effecten van verschillen in vrije snelheden en gewenste volgtijden onderzocht, wat de volgende resultaten opleverde:

- De versmalde rijstrook van 2x3.5 m tot 3.25 en 3.0 m in combinatie met een barrier als langsafzetting in plaats van een geleiderail heeft een daling in capaciteit van 1.5% tot gevolg;
- Een kleine slinger zorgt voor relatief een grote extra daling in capaciteit van 4.7%.

Praktische aanbevelingen

Er zijn aanbevelingen aangaande het observeren met behulp van de onbemande helikopter. Zo wordt aangeraden de locaties te bezoeken en gedetailleerd te bekijken, en een specialist op het gebied van onbemande helikoptervluchten te raadplegen voordat metingen uitgevoerd worden.

Om problemen tijdens het stabiliseren van de beelden te verkleinen, kunnen tijdens observaties eigen referentiepunten in het landschap aangebracht worden, bijvoorbeeld een gekleurd grondzeil.

Voor het ontwerpen van werkvakken, wordt aangeraden abrupte veranderingen in lay-out te vermijden. Zoals uit de resultaten blijkt, kan een kleine verandering in de lay-out relatief grote gevolgen hebben voor de capaciteit van het werkvak. Daarom wordt aanbevolen om noodzakelijke veranderingen geleidelijk over een lange afstand toe te passen.

Aanbevelingen voor toekomstig onderzoek

Voor dit onderzoek is de invloed van slechts drie determinanten onderzocht, maar om adaptatie-effecten en prestatie van meer configuraties te bepalen, is meer onderzoek noodzakelijk naar andere determinanten.

Aanbevelingen aangaande de ontwikkeling van voertuigdetectie- en voertuigvolgmethoden zijn:

- Het automatisch detecteren van voertuigen uit gecombineerde, rand gedetecteerde langsdoorsneden;
- Het implementeren van een sneller kortste-pad-algoritme dan het huidig geïmplementeerde Dijkstra algoritme.

Uit dit onderzoek bleek dat problemen op kunnen treden bij het integraal schatten van volgmodellen, door het ontbreken van observaties tijdens congestie. Door de relatie te onderzoeken tussen veranderingen in rijgedrag die optreden zonder en met congestie, kunnen mogelijk veranderingen tijdens congestie geschat worden op basis van geobserveerde veranderingen, waarbij geen sprake was van congestie.

1 Introduction

In the ensuing the problem description is presented, after which the research objective and questions are given.

1.1 Background

Road users often encounter hindrance from facilities and other measures while driving in work zones. Work zones are areas alongside, or on the freeway where road works take place (for an example see figure 1.1). It is necessary to apply work zones on freeways to safely carry out maintenance and other construction activities (e.g. construction of an extra lane or new onramp) without closing of one or both directions of the freeway section. Components of work zones are illustrated in figure 1.2.



Figure 1.1: Example of a freeway work zone.

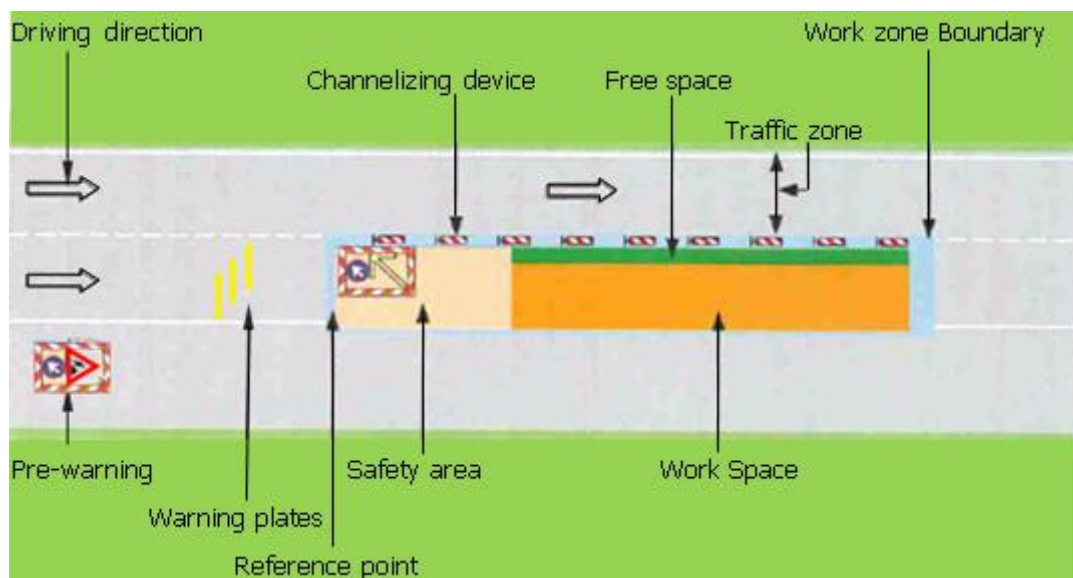


Figure 1.2: Work zone layout (CROW (2005)).

Hindrance causes delay for road users that leads to economic losses, so it is an important societal aspect to limit hindrance for road users and environment. Freeway authorities, who prescribe where activities have to be carried out, therefore aim more at limiting this hindrance for road users. Rijkswaterstaat, as freeway authority in the Netherlands, selects contractors who carry out roadwork activities, often through intensive tender procedures. To limit disutility during realization as much as possible, the disutility aspect is an important criterion for selecting contractors. During realization, authorities try to reduce hindrance by using payments for performance, which depend on measured disutility during realisation.

Hindrance experienced by road users, are divided into a number of categories (Rijkswaterstaat (2010)):

- An increase in travel time;
- A higher volume to capacity ratio;
- Annoyance caused by:
 - Poor information service in advance (e.g. announcements are missing);
 - Incomplete or missing of alternate routes;
 - Absence of construction activities while passing the work zone.

A way of measuring hindrance due to presence of work zones, is measuring increased travel time. The increase depends on the layout and length of the work zone and on traffic intensity. An increase in travel time (i.e. delay) can appear in different locations with respect to the work zone location:

- Over the full length of work zones (e.g. in case of a decreased speed limit);
- Upstream of the work zone (e.g. in case of a lane drop, which causes a bottleneck).

The influence of work zones on traffic flow operations can be analysed on two scales, namely microscopic and macroscopic scale. Characteristics of these scales are described in the next sections.

1.1.1 Microscopic scale

From a microscopic perspective, the traffic system contains individual behaviour of individual road users in relationship with the road network, road layout, and interaction of individual road users with other road users. This individual behaviour, describing the so-called 'driving task' is hierarchically divided by Michon (1985) into three levels:

- Strategic level;
- Tactical level;
- Operational level.

Strategic level

This level involves general trip planning before and during travelling, including route goals and mode choice (e.g. car, bicycle or public transport). This level is influenced by (expected) costs, risks, traffic states and mood of the traveller.

Tactical level

Drivers have to manoeuvre over road system and interact with other traffic during the trip. The level describing this behaviour is called the tactical level and consists of longitudinal and lateral behaviour. Longitudinal driving behaviour and overtaking manoeuvres can be observed using trajectories. A vehicles' trajectory consists of its position during the period it is observed and when trajectories of all vehicles are determined, their interaction can be investigated. Such a set of trajectories is illustrated in figure 1.3.

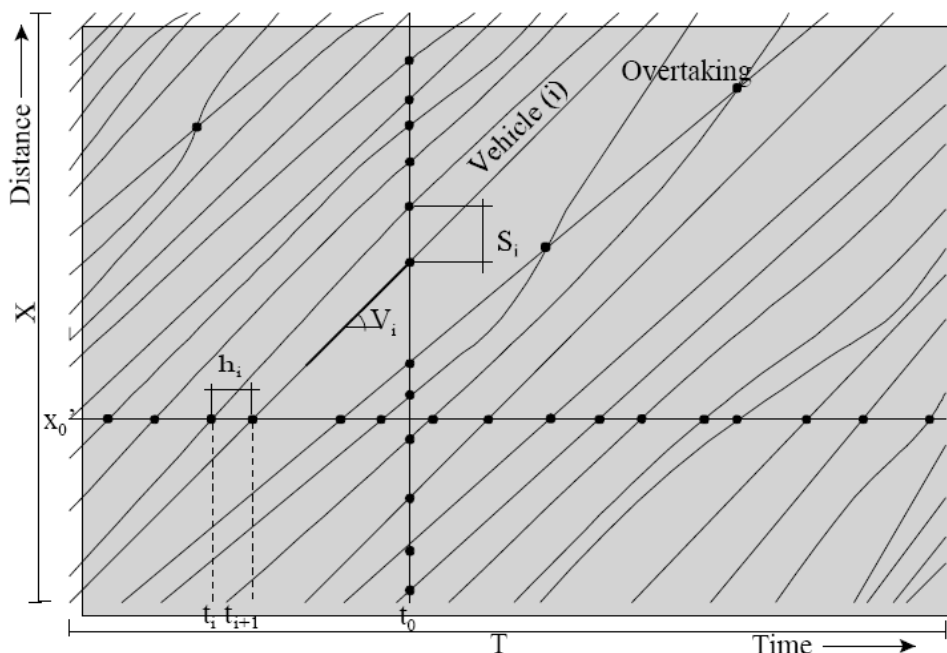


Figure 1.3: Example of vehicle trajectories (Hoogendoorn et al. (2004)).

From trajectories, individual driving behaviour variables as speed, acceleration, deceleration and following distances can be observed. Specific lateral driving behaviour that can be observed from trajectories are overtaking manoeuvres.

Lateral driving behaviour can be described by movements between lanes (lane changing) and movements within lanes (with respect to a lanes' middle axis).

Lane changing behaviour that is required for reaching the destination (e.g. for reaching an exit) is described as Mandatory lane changing behaviour. Discrete lane changes describe lane changes that are performed to achieve speed/acceleration advantages (e.g. overtaking).

Operational level

The operational level includes primary tasks that have to be performed in order to operate a vehicle. Examples are using pedals to accelerate, using the steering wheel to turn and changing gears. The workload for this level based on road geometry has been researched by Green et al. (1993) for factors as sight distance, curves, and distance towards obstacles from the edge of carriageway.

Task level integration

Workload distributed over the aforementioned three levels interact in both directions, as described by Schaap (2012), and illustrated in figure 1.4. Actions and level of attention required for one of the three levels influence behaviour on other levels. For example, due to presence of fog, visibility is reduced, which increases the difficulty of the driving task on operational level as well as tactical level (e.g. lane keeping becomes more difficult). Workloads on individual levels have been proven to have a strong influence on macroscopic traffic flow dynamics (Ossen (2008) and Tampère et al. (2005)).

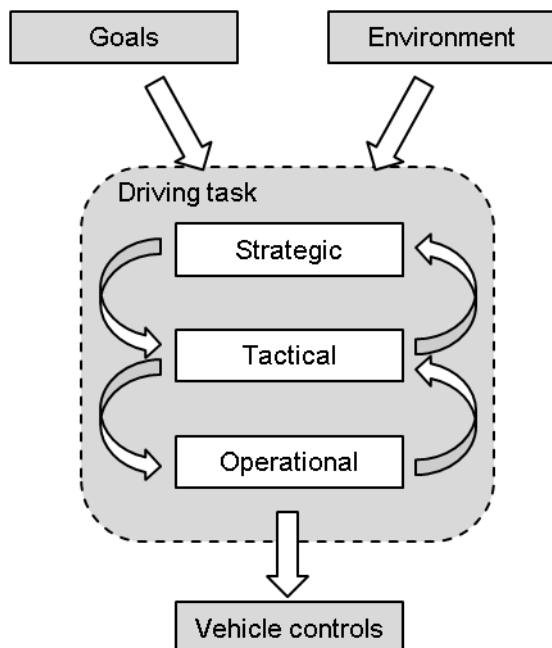


Figure 1.4: Classification of driving tasks of Michon (1985), adapted by and copied from Schaap (2012).

Microscopic models

With observed individual driving behaviour, microscopic driving models can be calibrated. These models predict behaviour of a driver (e.g. speeds, accelerations, lane changes), based on drivers' experienced circumstances. By calibrating model parameters, effects of specific circumstances can be examined.

1.1.2 Macroscopic scale

Macroscopic analysis do not take individual driving behaviour into account, but consider average traffic flow variables, such as average speeds, intensities (number of vehicles over time) and densities (number of vehicles over distance).

These variables can be observed from induction loop data, as well as from simulation results of individual driving behaviour models.

With these averages the flow – density relationship can be found, called the Fundamental diagram (figure 1.5). In this diagram, the traffic states can be distinguished and mean speeds can be derived. Lateral driving behaviour and driver heterogeneity are not explicitly described, but flow, capacity and jam density can easily be derived.

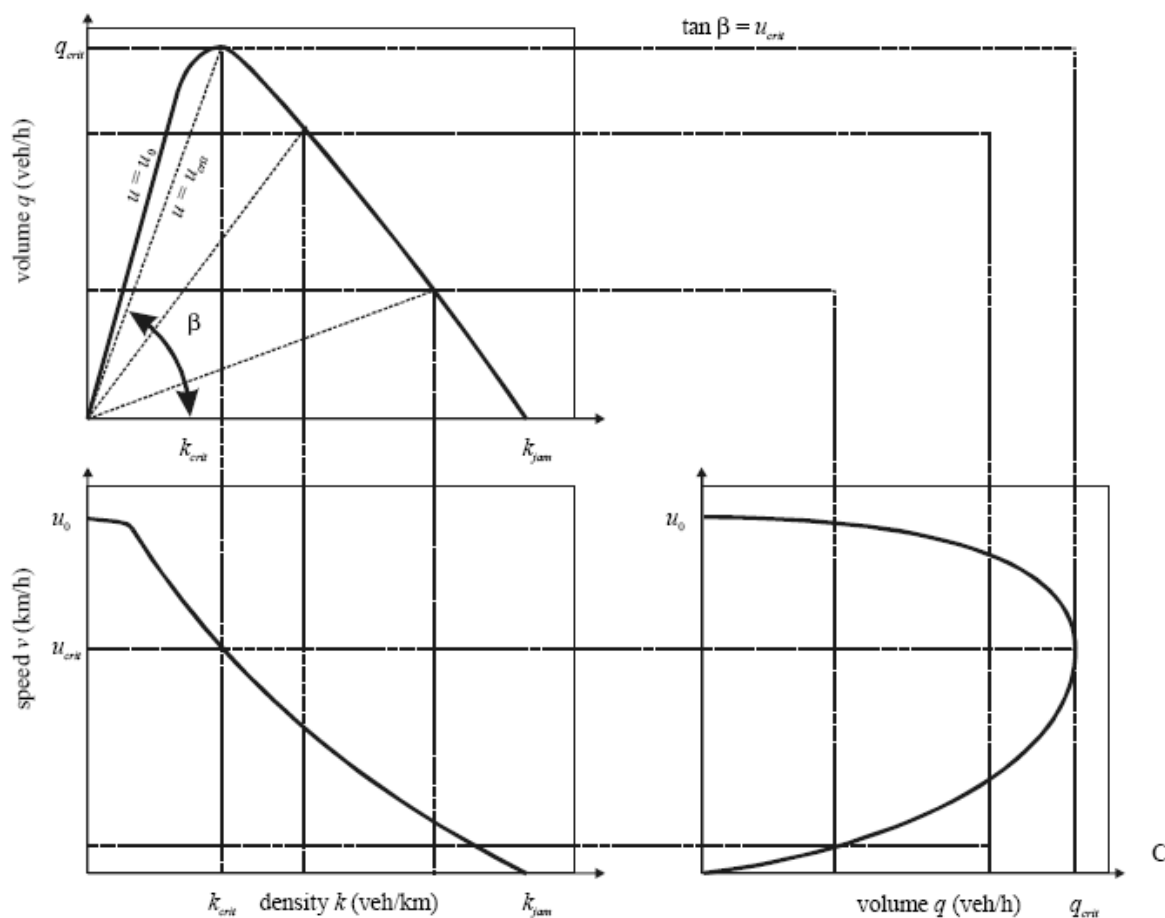


Figure 1.5: Fundamental diagram (Hoogendoorn et al. (2004)).

However, collected flow – density values are presented by a cloud of data points, which do not precisely follow the line of the fundamental diagram. Differences can be observed for each location and time instance, due to variation in driving behaviour (heterogeneity in driver characteristics) and external circumstances (e.g. weather conditions). An example of such a data cloud (collected by induction loops) is given in figure 1.6.

Capacity values can be estimated by analysing the data cloud, as illustrated in figure 1.7. In this figure, the so-called capacity drop is shown as well, which entails the phenomenon that capacity suddenly decreases when traffic state transfers from uncongested (green line) to congested (red line).

Macroscopic models

Against microscopic models, also macroscopic models exist. These models predict macroscopic variables as average travel time (e.g. BPR-function, presented in Traffic Assignment Manual (1964)).

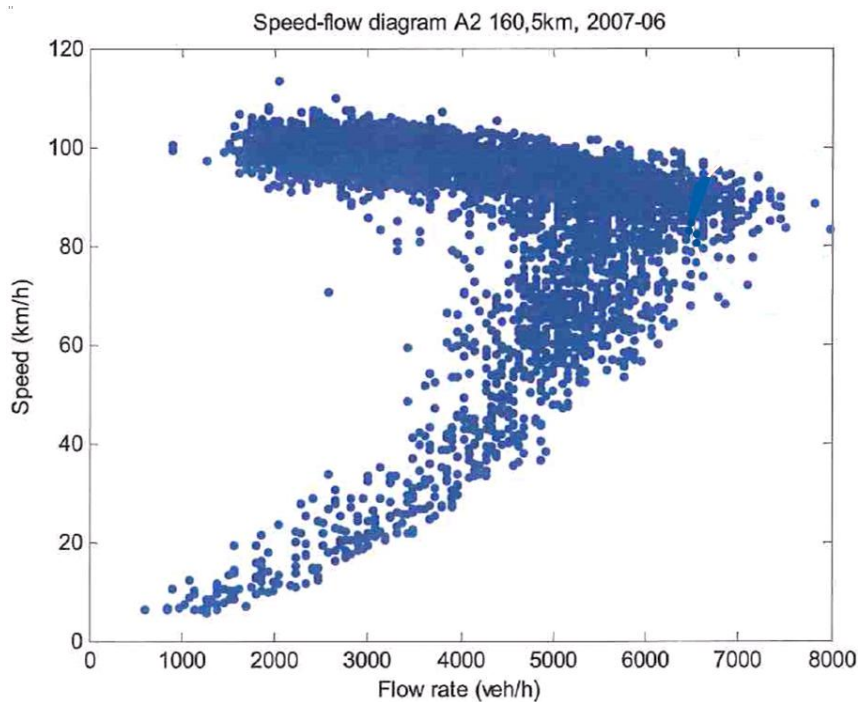


Figure 1.6: Data points collected by induction loops (Zheng (2009)).

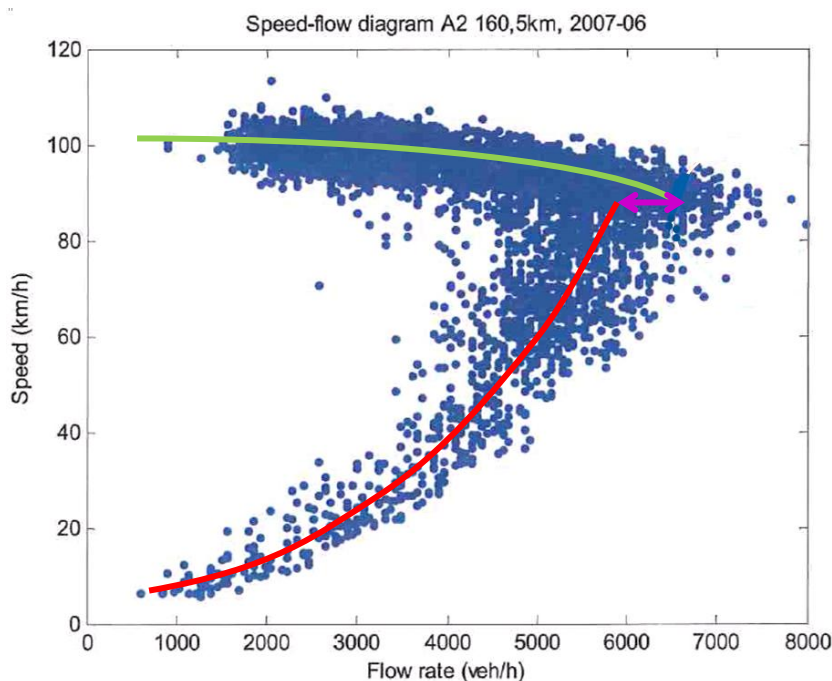


Figure 1.7: Data points with sketched fundamental diagram and capacity drop in pink (Zheng (2009)).

1.2 Problem definition

The influence of road layouts on macroscopic flow variables were researched by Van Begin (2002), Ter Kuile (2006) and HCM (2000), but not all factors that could influence macroscopic traffic flow characteristics were incorporated. From a microscopic perspective, even fewer factors (i.e. determinants) were examined, especially researches using empirical observations.

The consequence is that traffic flow operations in work zones cannot accurately be modelled and the relationship between microscopic and macroscopic effects is not clear. Difficulties in modelling individual driving behaviour appear when model parameters have to be adjusted to let the model represent the driving behaviour at the specific work zone layout.

These restrictions limit authorities and contractors in their possibilities in comparing possible work zone configurations and therefore it is not possible to accurately determine hindrance and delay of a specific freeway work zone.

1.3 Research objective

Gain insight into possible adaptation effects related to the layout of work zones, in empirical individual driving behaviour and subsequent in macroscopic effects, by presenting the applied method.

1.4 Research questions

To achieve the research objective, the following research questions have to be answered:

1. What are determinants of individual driving behaviour and which are going to be examined?
2. How is empirical individual driving behaviour described and related to macroscopic traffic flow operations?
3. Which data have to be collected to analyse individual driving behaviour best, and which collection and processing methods can be used best to do these analyses?
4. Which adaptation effects in empirical driving behaviour can be observed related to research determinants?
5. How are adaptation effects of the individual driving behaviour related to macroscopic effects?

1.5 Research approach and report outline

This section describes the research approach based on the aforementioned research questions. This process is illustrated by a flow diagram (figure 1.8).

In Chapter 2, determinants of individual driving behaviour are investigated and the examined determinants are selected.

Chapter 3 presents methods to analyse empirical driving behaviour and how this behaviour is related to macroscopic traffic flow operations.

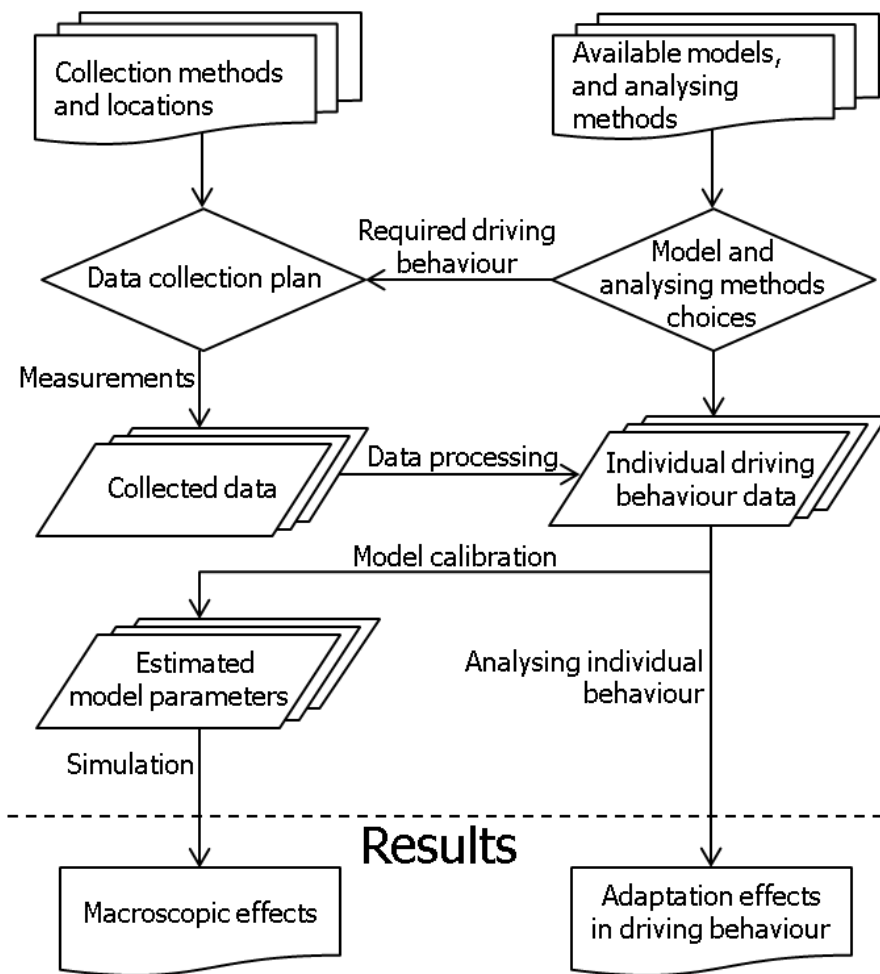


Figure 1.8: Flow diagram research plan.

Logically, to perform data analysis, data have to be collected first. The process of data collection is described in Chapter 4, after which the data processing is presented in Chapter 5.

In Chapter 6 the analysis and results are presented and simulations are run, after which conclusions and recommendations are presented in Chapter 7.

To avoid confusion between terms, names and definitions are provided for five important terms, which are used unambiguously throughout the report. Terms and processing order are illustrated in figure 1.9 and explained below.

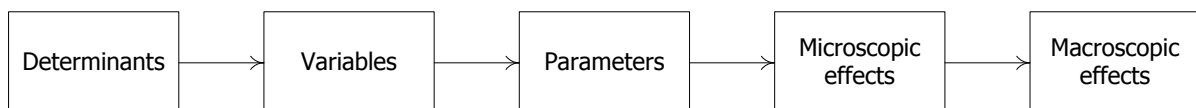


Figure 1.9: Data types from determinant to macroscopic effects.

- **Determinants:** This term describes external influences that could influence individual driving behaviour (e.g. lane width and type of channelizing device);
- **Variables:** Variables are measured data, such as speed and following distance;

- Parameters: Parameters are constants in models. By calibrating parameters to the collected data, the model can simulate specific configurations (e.g. desired speed and desired headway time);
- Microscopic effects: Microscopic effects are differences in empirical driving behaviour resulting from changes in determinant values (e.g. differences in headway time distributions);
- Macroscopic effects: Macroscopic effects are differences in simulation results between configurations (e.g. differences in the shape of fundamental diagram).

2 Determinants of driving behaviour

This Chapter describes determinants of individual driving behaviour and presents selected determinants that are examined in this research.

2.1 Determinant analysis

This state-of-the-art presents a list of determinants of individual driving behaviour, after which corresponding references are elaborated in detail (see section 2.1.2).

Determinants are divided into static and dynamic determinants, which are divided into cross-section, alignment and signage (signs, lightening) groups for static determinants and dynamic determinants are divided into traffic dependency groups.

2.1.1 Determinant overview

Static determinants:

- Cross-section:
 - Lane width, researched by Benekohal et al. (2003), Cohen (2004) and HCM (2000);
 - Number of lanes available and closed, researched by HCM (2000) and Zheng (2009);
 - Presence of contra-flow, studied by Zheng (2009) and Van Begin (2002);
 - Availability of hard shoulder or emergency lane (Benekohal et al. (2003) and HCM (2000));
 - Type of channelizing device between work zone and through going traffic and distance towards edge of the carriageway (barrier, traffic cones, narrow barricades), investigated by Benekohal et al. (2003).
- Alignment:
 - Change in horizontal alignment (e.g. presence of a reverse curve);
 - Road gradient, researched by Kim et al. (2001).
- Signage:
 - Type of marking: Continued or discontinued;
 - Speed limit, investigated by Benekohal et al. (2003).

Dynamic determinants:

- Traffic independent:
 - Weather conditions (temperature, precipitation, darkness, visibility);
 - Time of measurements (e.g. peak or off-peak hours), investigated by (HCM (2000);
 - Intensity of construction activities (Benekohal et al. (2003)).

- Traffic dependent:
 - Proportion of heavy vehicles, studied by Van Begin (2002);
 - Occurrence of incidents or other distractions and adverse conditions (Hoogendoorn (2011));
 - Traffic state, researched by Benekohal et al. (2003), HCM (2000) and Treiber et al. (2000);
 - Driver state and driver variability, including preparedness (Benekohal et al. (2003)).

2.1.2 State-of-the-art

In this section, researches mentioned in the previous section are elaborated in detail.

Benekohal: Evaluation of Construction Work Zone

Benekohal et al. (2003) collected data at 14 work zones (9 long-term and 5 short-term) in Illinois (USA) using a camera on ground level, which collected traffic flow data (headways, speeds, traffic volume and queue length). Other information about layout of, and work intensity at work zones was manually reported as well. Investigated determinants were preparedness, intensity of construction activities, lane width and availability (and width) of right and left hard shoulder. These determinants were related to the maximum flow and speed as described in the Highway Capacity Manual (HCM (2000)).

The defined relationship was linear, except for intensity of construction activities, for which speed reduction was used. This reduction was based on the number of workers (one to ten) and the number of construction equipment (one to five) divided by the distance between the active work area and the open lane (one to nine feet)). The natural logarithm of the so-called work intensity ratio (WI_r) plus the constant speed reduction, defined the total speed reduction for work zones.

For short term work zones, data were collected from surveys conducted among drivers at rest areas, where data for long term work zones were collected from actual field data. The differences in results between these observation methods was very large (more than 9 mph), which seems unrealistic. Also rather unrealistic is that the speed reduction was not influenced by the speed limit.

Cohen: Using the Hard Shoulder and Narrowing Lanes to Reduce Traffic Congestion

Cohen (2004) investigated effects for total capacity and occurrence of congestion by using hard shoulders and narrowed lanes for accommodating an extra lane. The effects were investigated using induction loop data, providing flow rate, speeds and occupancy rate. The results showed a mean increase of 16% in capacity when an extra lane was accommodated.

Van Begin: Towards a Better Planning of Road Works

Van Begin (2002) started a method to improve the planning of road works, and described differences in capacity dependent work zone layouts and separating opposites traffic streams. The capacity values and reductions were based on a state-of-the-art, in which Van Begin described that capacity increased with 5 to 10% when the proportion of heavy vehicles is 5% and that capacity decreased with 10 to

15% when the proportion of heavy vehicles is 30 to 40%. Also the intensity of construction activities was investigated, but only in case of a lane closure on a two lane freeway, which led to capacity values of 1500, 1250 and 1100 vehicles per hour per lane for respectively light, medium heavy and heavy construction activities. The influence on capacity of lane width, preparedness and speed limits was studied in a similar way.

An aspect mentioned was the stochastic nature of traffic and that therefore congestion could occur when intensity is lower than the calculated capacity.

Zheng: Freeway Work Zone Capacity Prediction

In the thesis report of Zheng (2009), he referred to the CIA manual, in which capacities for different work zone layouts were presented (see appendix 2). He compared results of data collected with induction loops at 2x2 and 2x3 lane freeways with the CIA manual, with varying speed limits and lane widths. Results showed a reduction in capacity when lane width increases and an increase in capacity when speed limits increased (from 70 to 80 and 90 km/h).

Kim: A New Methodology to Estimate Capacity for Freeway Work Zones

Kim et al. (2001) developed a multiple regression model to estimate work zone capacity. The values of coefficients and corresponding parameters however, seem very limited and specific applicable, for example because of the linear relation with the work zone length and the small decrease in capacity when a lane closure was applied.

El-Kaisy: Guidelines for Estimating Capacity at Freeway Reconstruction Zones

Al-Kaisy & Hall (2003) presented another example of estimating capacity of work zones. In this research, guidelines for capacity estimation at freeway reconstruction zones were created by using the HCM (HCM (2000)) and observations by induction loops with lane or shoulder closures. The format of the proposed model estimated work zone capacities by multiplying original capacities with correction factors (e.g. peak or off-peak periods, and ratio of heavy vehicles). Unfortunately, many often used varying circumstances factors were not implemented in the model.

Maze: Capacity of Freeway Work Zone Lane Closures

Maze et al. (2000) researched variation in maximum free flow volumes with data collected by camera (on a telescopic mast). Variations in capacity values and a decreased flow were found.

Godley: Perceptual Lane Width

Godley et al. (2004) investigated influences of narrower and perceptual narrower lanes in relation to changes in driving speeds. Although the focus of this research was to limit driving speeds and data were collected from only 28 participants using a driving simulator, it is concluded that a perceptual narrower lane should lead to lower driving speeds.

Gunay and Hoogendoorn & Daamen: Lateral variation

From data collected from straight sections of multilane highways, Gunay (2007) investigated the relationship of lateral distance between the lead vehicle and its follower and time headways.

Subsequently, Hoogendoorn & Daamen (2007) found that variation in lateral position of drivers decreased as lane width decreased.

Sun: Impact of Pavement Edge Line on Vehicular Lateral Position

Sun et al. (2006) showed from data collected at curved/tangent sections rural two-lane highways, that edge lines tend to move vehicles away from the road edge and prevent vehicles to cross the centreline at night.

2.2 Selection of research determinants

To select research determinants, they have been compared and scores are presented in table 2.1. The comparison is based on two criteria:

1. How specific is the determinant for work zones?

To investigate the influence of work zone configurations, research determinants have to be specific for work zones. Based on the state-of-the-art of the previous section, where studies about determinants in work zones are presented, it is determined if determinants are work zone specific and could influence individual driving behaviour.

2. Can authorities and contractors influence the determinant value?

If a determinant can be influenced, it is possible to adjust work zone performances by changing that determinant value.

Determinant	Work zone specific?	Influence rate?	Total
Lane Width	+	+	+
Markings	0	0	0
Speed Limit	+	+	+
Lanes available/closed	+	0	0/+
Contra flow/Reverse curve	+	+	+
Traffic state (congested or not)	-	-	-
Presence of hard shoulder	0	0	0
Channelizing device	+	+	+
Road gradient	-	-	-
Preparedness	+	-	0
Intensity of constructions activities	+	0	0/+
Weather condition	-	-	-
Peak or off-peak, week or weekend	-	-	-
Ratio heavy vehicles	-	-	-
Incidents	-	-	-

Table 2.1: Determinant trade-off (+: matches criterion, 0: partly matches criterion, -: not matching criterion).

With scores out of table 2.1, scores of selected -all static- determinants are marked green:

- Lane width;
- Speed limit;
- Contra flow/Reverse curve;
- Channelizing device.

Variation in these determinants between locations will be investigated, so other determinants are desired to stay equal.

2.2.1 Description of selected determinants

Interdependence of selected determinants

Values of determinants depend on each other. Dutch safety standards, published by the CROW (2005), prescribe speed limits based on differing lane widths, channelizing devices kind of activities and duration.

To choose a configuration with the best performance/cost ratio, possible configurations should be compared. An example with two possible configurations: In configuration 1, lanes are narrowed so a speed limit of 70 km/h during 2 weeks has to be applied. Configuration 2 has no narrowed lanes, with a speed limit of 90 km/h during 3 weeks including an extra phasing. To choose the optimal configuration, the total performance and costs of both configurations should be known.

Types of channelizing devices

Three types of channelizing devices are available for freeway work zones:

- Barrier;
- Narrow barricades;
- Traffic cones.

Figure 2.1 shows a barrier, which are usually located close to the carriageway, where behind construction activities can be carried out directly.

The narrow barricades (see figure 2.2) are placed at fixed intervals and require a safety distance from which construction activities can be carried out. Traffic cones require a safety distance as well and are often used for short-term work zones or setting up a long term work zone (see figure 2.3).



Figure 2.1: Concrete barrier as channelizing device.



Figure 2.2: Narrow barricades as channelizing device.



Figure 2.3: Traffic cones as channelizing device.

Presence of contra flow and reverse curves

Traffic streams are often guided through work zones by installed contra-flow and reverse curves. In case of contra-flow, traffic drives on the carriageway that is normally used for opposite traffic, reverse curves are required to guide traffic from their original carriageway to the contra-flow side (see figure 2.4) . Spatial properties of reverse curves are prescribed by speed limits.



Figure 2.4: Example of reverse curve (Wegenforum (2010)).

2.3 Conclusions

In this Chapter, determinants of driving behaviour have been investigated by a state-of-the-art, after which research determinants are selected. Determinants are divided into static and dynamic determinants, which are subdivided into cross-section, alignment, signage and traffic dependency groups.

The selection of research determinants is based on two criteria:

- Is the determinant work zone specific?
- Can authorities and contractors influence the determinant value?

Based on a trade-off, the next determinants have been selected as research determinants, for which effects in variation on individual driving behaviour and macroscopic traffic flow operations will be investigated:

- Lane width;
- Speed Limit;
- Type of channelizing device;
- Presence of contra flow and reverse curve.

In the next Chapter methods to analyse driving behaviour and traffic flow operations are presented and compared.

3 Analysing methods

This Chapter describes how empirical individual driving behaviour at work zones can be analysed and how it is related to macroscopic traffic flow operations.

3.1 Adaptation effect on different driving task levels

Microscopic adaptation effects can occur as well at strategic, tactical and operational level. For example, travellers could adjust their route to avoid work zones, adjust their speed when they choose to travel via work zones, and also increase attention towards lane keeping.

At which driving tasks levels adaptation effects will be investigated in this study is described below.

3.1.1 Driving task level selection: Tactical level

To investigate adaptation effects in empirical driving behaviour at work zones, investigating the driving task at a strategic level is not sufficient, because driving behaviour at work zones is not observed if travellers decide not to travel via work zones.

Investigating adaptation effects at the tactical driving task level, presents changed behaviour regarding interaction between driver and road system and between driver and other traffic (e.g. speed, following distance and time headways). Using that information, effects of varying work zone configurations on individual driving behaviour can be investigated and related to macroscopic effects by performing simulations using driving behaviour models with individual varying parameters.

The differences at the tactical level are caused by differences in operational level. For example, a driver decides to brake, causing its speed to decrease, and headways to increase. Therefore, it is sufficient to investigate adaptation effects in the tactical level of the driving task.

3.2 Analysing adaptation effects in driving behaviour

Two main analysing methods can be distinguished to analyse individual driving behaviour. These methods are given below and further explained afterwards:

- Analysing empirical variables, to analyse effects at macroscopic and macroscopic scale;
- Estimate parameter values of microscopic driving behaviour models based on empirical driving behaviour and run simulations to analyse effects of situations that are not empirically observed.

3.2.1 Analysing empirical variables of the tactical driving task level

Variables from manoeuvring a vehicle are presented, such that adaptation effects in observed configurations can be investigated (Knoop et al. (2009)).

Headway distributions

With headway distributions, investigated by Luttinen (1996), differences in desired headways between configurations can be investigated. When desired headways at corresponding following distances decrease, capacity increases.

Speed distributions

For time headway distributions, speeds of vehicles have to be known. When all vehicles' speeds are collected, speed distributions can be made, as presented by Berry & Belmont (1951). By looking at median speeds and variances of distributions, processed data can be compared and checked for consistency against visual observations (e.g. are processed speeds at observed congestion lower than when no congestion is observed).

Speed (differences) - following distance

When speeds and locations of all vehicles are collected, following distances (i.e. distance headways) can be calculated. A restriction to calculate the following distance of a vehicle is of course, that the location of the leader has been defined. With these data the desired driving speeds and minimal distance headways can be estimated.

For accelerations, time step sizes between instances determine the amplitude of accelerations (by larger time steps accelerations will be lower). Therefore, instead of accelerations, speed differences (i.e. relative speeds) between leader and follower are investigated. Accelerations are used for investigating macroscopic effects, which is further elaborated upon in section 3.2.2.

Speed distributions at specific following distances

By plotting speed distributions at specific ranges of following distances, influences of specific work zone configurations on speed and speed variance can be investigated, not influenced by varying following distances, which can also be used for estimating desired headway times, and driver heterogeneity.

Lane occupation distributions and lane changing behaviour

By looking at flows on different lanes at same time instances, lane-flow distributions can be determined (see figure 3.1), and differences analysed (Knoop et al. (2010)). For this research lane changing behaviour will not be explicitly investigated, because no large differences in lane changing behaviour are expected. To legitimate this exclusion, the significance between differences in lane occupancy distributions are checked.

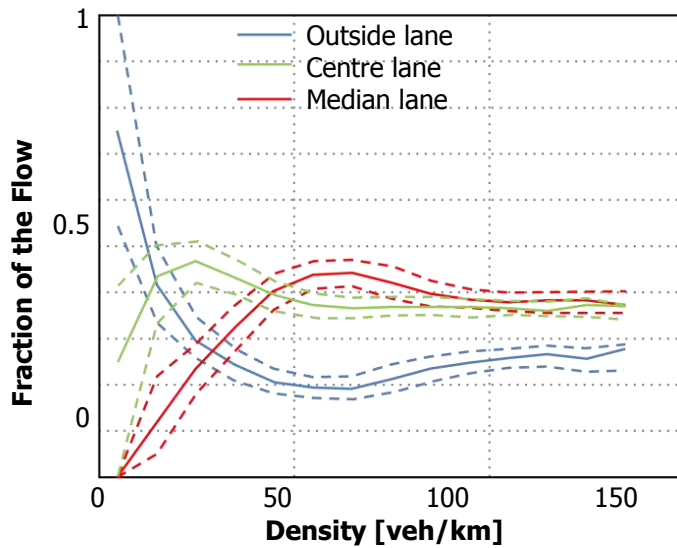


Figure 3.1: Lane occupancy distributions (Knoop et al. (2010)).

3.2.2 Using empirical variables for analysing macroscopic effects

The Speed-Density relation and Fundamental diagram

Knowing vehicles' speeds and locations for the whole range of densities, the speed-density relation and corresponding fundamental diagram can be determined by applying the fundamental relationship: $q = k \cdot u$. Except for looking at median values of speeds at corresponding following distances, variance in observations can be analysed as well.

3.2.3 Simulate calibrated driving behaviour models to analyse macroscopic effects

When not the whole range of densities are empirically observed, it is possible to determine macroscopic effects by simulating microscopic behaviour. By running simulations with differences in model parameters of microscopic driving behaviour models, macroscopic effects can be measured and compared. Through a state-of-the-art of various models, specifications of existing microscopic driving models are provided in the next section.

Microscopic driving behaviour models can be separated into three categories, namely car-following models, lane change models and integrated models which both deal with car-following as lane changing behaviour. Models are presented (Hoogendoorn (2011)) in the next part, after which for car-following and lane changing behaviour models are selected which are used for this research. Although observed lane changing behaviour will not be explicitly investigated, lane changing models are researched and compared, because lane changes are to be incorporated during simulations.

Car-following models

Car-following models try to predict behaviour of a vehicle following its leader. Therefore, it uses data of the leader and of the following vehicle (e.g. their location).

The models are categorized in four types by Brackstone & McDonald (1999), after which three are elaborated in detail:

- Stimulus response models;
- Safety distance models;
- Psycho-spacing models;
- Fuzzy logic-based models.

- **Stimulus-response models:**

Stimulus-response models predict the current behaviour of the following vehicle (eventually by taken reaction time into account) by the behaviour of its leader. Five well-known models are discussed:

- **The CHM model and GHP model (Gazis et al. (1959));**

This model is proposed by Chandler et al. (1958) and elaborated by Van Hinsbergen et al. (2009). It predicts the acceleration of the follower at a time instance $t + R_0$ (time plus reaction time) by the speed difference at t between the leading vehicle and its follower. To calculate the acceleration, the observed speed difference is multiplied with the model parameter λ . This leads to the formula: $a_{i+1}(t + R_0) = \lambda(v_i(t) - v_{i+1}(t))$.

- **Optimal Velocity Model (Bando et al. (1995));**

This model states that acceleration is influenced by its velocity and its following distance. With two model parameters α and constant h the acceleration is estimated: $a_i = \alpha(V(s_i) - v_i)$, where $V(s_i) = \tanh(s_i - h) + \tanh(h)$.

- **Tampère Model (Tampère (2004));**

This model distinguishes two regimes; constrained driving and free driving. The two regimes are described by one parameter for each regime, the so-called sensitivity parameters c_1, c_2 (which have to be calibrated): $a_i(t + T_r) = c_1 \Delta v_i + c_2 (s_i - s_0(v_i))$.

- **Helly model (Helly (1959));**

In this model acceleration depends on speed differences, desired distance and actual distance between the driver and its leader: $a_i(t + R_0) = \alpha \Delta v_i(t) + \beta (s(t) - (s_0 + h_{min} v_i(t)))$.

- **IDM (Treiber et al. (2000));**

The 'Intelligent Driving Model' (IDM) is a single lane car-following model that uses four empirical traffic states. These states are:

1. Equilibrium traffic: Traffic drives at their preferred speed, with a preferred following distance to their leader;
2. Acceleration to desired velocity: Traffic density is that low, that there is no significant interaction with other road users, and road users accelerate with their free-road acceleration to their desired velocity (restricted by the speed limit);
3. Braking as reaction to high approaching rates: A driver approaches a slower driving vehicle;

4. Braking in response to small gaps: This second braking state applies when there are no large speed differences, but the following distance is much smaller than the preferred following distance for that speed.

The four states are merged into a continuous formula, predicting the followers' acceleration:

$$a_i = a_0 \left[1 - \left(\frac{v_i}{v_0} \right)^\delta - \left(\frac{\tilde{s}(v)}{s_i} \right)^2 \right], \text{ in which } \tilde{s}(v) = s_0 + v_i T + \frac{v_i \Delta v_i}{2\sqrt{a_0 b_0}}.$$

- **Safety distance models with two driving regimes:**

The safety distance models are based on the basic Newtonian equations of motion. These models describe the safe following distance of a driver, that if the following distance becomes shorter, a collision may be unavoidable. The safety distance model that is incorporated in the selection process is presented below:

- **Gipps (Gipps (1981))** developed a safety distance model, where he distinguished two regimes, for which drivers select the minimum speed of two predicted speeds. For notational convenience the formulas are not fully expressed, but noted with function f :

1. Free flow regime: Driver wants to drive a desired speed based on a given acceleration;

$$v_i(t + R_0) = v_i + R_0 a_i \cdot f(v_i / v_0).$$

2. Car-following regime: Speed of the driver depends on a maximum deceleration rate which prevents a rear-end collisions;

$$v_i(t + R_0) = b_i R_0 + f(b_i, R_0, s_i, v_{i,i-1}).$$

- **Multi-anticipative car-following models:**

These models work as stimulus response models, but do incorporate following distances, speeds and speed differences of more vehicles in front of the driver.

- Lenz et al. (1999) extended the model of Bando et al. (1995), so following distances of vehicles further downstream of the leader are incorporated as well. This leads to an adjusted formula, where r is the number of downstream vehicles taken into consideration:

$$a_i = \sum_{p=1}^r \alpha_j (V(x_{i+p} / p - x_i / p) - v_i), \text{ with the condition } \alpha_j / \alpha_1 \leq 1, \text{ indicating that the closest vehicle is always more important than vehicles further downstream.}$$

- **GT model (Generalized Tampère model);**

The GT model as proposed in Hoogendoorn et al. (2006) and Hoogendoorn et al. (2007) extends the model of Tampère (referred in Ossen (2008)) using a method similar to the way Lenz et al. (1999) extended the Optimal Velocity Model:

$$a_i(t + T_r) = \sum_{j=1}^{m_1} c_{1,j} \Delta v_{i,j} + \sum_{j=1}^{m_2} c_{2,j} (s_{i,j} - s_0(v_{i,j})).$$

- **Extended IDM;**

Schakel et al. (2010) extended the IDM by incorporating reaction time, anticipation of multiple vehicles and distinguishing the driver being in the car-following or non car-following state.

- **Psycho spacing (i.e. action point) models:**

These models state that drivers do not react on every change in following distance or acceleration of the lead vehicle, but only when it crosses set boundaries of following distances and.

- This method was proposed by Wiedemann (1974), which uses the desired following distance, which depends on the speed. Although, a driver only reacts on its leader when the following distance and corresponding speed difference crosses a perception threshold. The perception threshold principle (Dijker & Knoppers (2004)) and a typical following pattern (Higgs et al. (2010)) are illustrated in figure 3.2.

An elaborated method using four thresholds is proposed by Wiedemann & Leutzbach (1986). For accelerating and braking there are two different perception thresholds, and for the small negative and positive closing speeds another two thresholds are introduced.

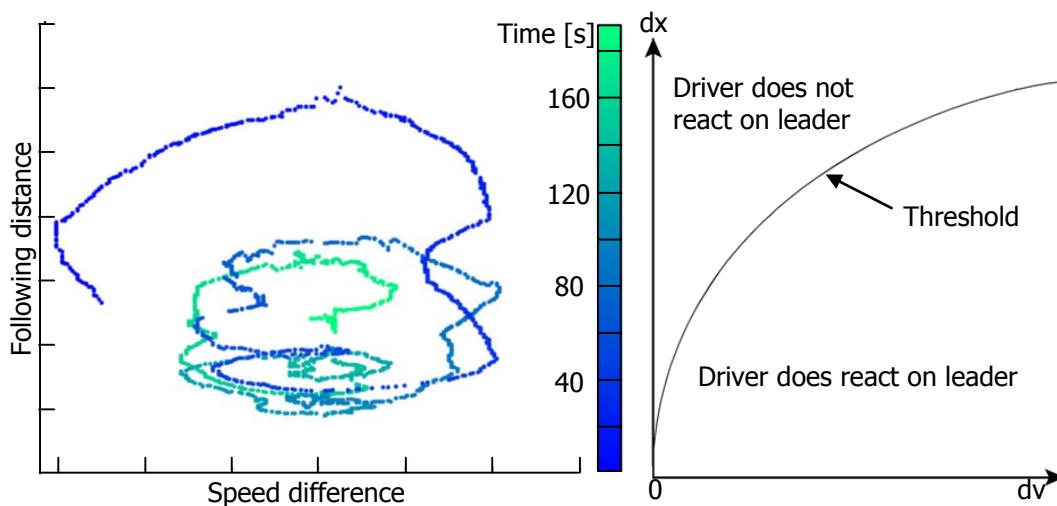


Figure 3.2: Typical following pattern (left) and the Wiedemann threshold principle (right).

Lane changing models and integrated models

Lane changing models predict lateral (lane changing) behaviour. Two different behaviour pattern are distinguished: mandatory lane changes (which have to be performed to complete their trip over the (pre)defined route), and discretionary lane changes (lane changes due to interacting with other vehicles). A limited selection of seven lane changing models are presented:

- **Gipps model (Gipps (1986));**

The Gipps model predicts mandatory lane changes only and divides lane change behaviour in three patterns, dependent of the distance to the intended turn. When the driver is far away he does not influence discretionary lane changing behaviour only tries to attain his desired speed. When he comes closer to the intended turn, he starts increasingly to ignore opportunities to change lanes in the other direction of the intended turn in order to keep his desired speed. When the driver is in the area close to his intended turn, he is only interested in his position to be in the lane closest to the lane of the intended turn.

An important advantage of using this model is that it can be used in combination with the car-following model developed by Gipps.

- **Yang & Koutsopoulos model (Yang & Koutsopoulos (1996));**

This model both deals with mandatory and discretionary lane changes. When the driver has decided to change lanes, he checks the lead and lag gap. If both are acceptable, it changes lanes immediately. In case of a mandatory lane change, the acceptable gap time decreases when the driver approaches the intended turn until it reaches a minimum acceptable gap time.

- **Ahmed model (Ahmed et al. (1996));**

This model deals with lane changing when coming from an onramp. It is assumed that the driver has already decided to merge into the through going stream, causing that only gap acceptance is considered. This decision process is considered to be log-normal distributed over the distance.

- **Hidas model (Hidas (2002));**

In this model the desired lane selection is combined with the necessity of lane changing. This is done by implementing the intended turn, incidents, transit lanes, speed advantages and queue advantages.

- **Toledo model (Toledo et al. (2009));**

This model is an integrated model that incorporates both car-following and lane change behaviour. This is done by assuming that a driver has short term plans to accomplish, including short time goals and is determined by the target lane. This target lane is one of the three lanes that are close to the current position, namely the left, current and right lane. When the target lane has to be reached by lane changing, the driver has to consider if there is an acceptable gap. The difficulty in calibrating the model is that the target lane and target gaps cannot be observed, only the actions of the drivers can be observed.

- **MOBIL model, described by Kesting et al. (2007);**

The MOBIL model is a general lane changing model for car-following models and is named as an abbreviation of a Minimizing Overall Braking Induced by Lane change.

A new parameter is introduced, called the politeness parameter. This parameter determines an incentive criterion that takes into account the advantages and disadvantages of the other drivers when the driver considers a lane change. It can therefore distinguish differences towards egoistic and cooperative driving behaviour. In particular, a driver makes a trade-off between his own advantage of changing a lane and the disadvantage for the follower in the target lane.

The model is designed in a way that it can be combined with all car-following models calculating the new acceleration.

- **LMRS (Schakel et al. (2011));**

This model is like the MOBIL model, but includes relaxation and synchronisation as well. Relaxation tackles the relatively large (predicted) deceleration after a small gap is accepted. With

relaxation included, the driver accepts temporary a small headway (with a small deceleration over a longer period).

Synchronisation is behaviour where drivers adapt their speed towards the speed of the target lane, before performing the lane change (i.e. lane change preparation).

3.2.4 Model assessment and selection

In this section the trade-off between models is presented, so the model can be selected that has to be used for simulation.

Model assessment

This assessment consists out of criteria towards theoretical background (for 50%) and suitability (also 50%) for this study. The criterion towards theoretical background checks which components of individual driving behaviour are implemented in the model, and how accurate these implementations are. The suitability criterion checks the usability of the model for this research (if it is not applicable, the model is useless for this study). These main criteria are divided into sub criteria, which are presented next.

The criteria describing the theoretical criterion are:

- **Car-following:** How accurate are car-following model types incorporated (e.g. is following distance included)?
 1. Car-following and unconstrained driving regimes (30%)?
 2. Multi-anticipative behaviour (10%)?
 3. Psycho spacing (10%)?
- **Lane changing:** How is lane changing behaviour incorporated, or how easy can it be incorporated in the model?
 1. Discretionary lane change behaviour (25%)?
 2. Mandatory lane change behaviour (5%)?
 3. Compatible with lane changing models (20%)?

The suitability is divided into two criteria (used for both model types):

4. **Parameter calibration:** What is the complexity level to implement and adjust the model, parameters and determinants (20%)?
5. **Simulation:** Are there any programs available to use this model for simulation (30%)?

The trade-off matrix of car-following models is presented in table 3.1 and of lane changing behaviour in table 3.2.

Car following model	Criterion (+weighting)					Total
	1 (30%)	2 (10%)	3 (10%)	4 (20%)	5 (30%)	
GHP/CHR/CHM	-	-	-	0	-	-
Bando et al.	-/0	-/0	-	-/0	-	-
Tampère	0/+	-/0	-	-/0	-	-/0
IDM	0/+	-	-	0/+	0	0
Helly	+	-	-	0/+	0	0
Gipps	0	-	-	0	-	-/0
Lenz et al.	-/0	+	-	0	-	-/0
Generalized Tampère	-/0	+	-	0	-	-/0
Extended IDM	+	+	-	0	+	0/+
Leutzbach & Wiedemann	0	-	+	0	-	-/0

Table 3.1: Car following model comparison (performance scale: + high; 0:neutral; -: low).

Lane changing model	Criterion (+weighting)					Total
	1 (25%)	2 (5%)	3 (20%)	4 (20%)	5 (30%)	
Gipps	-	+	+	-/0	-	-/0
Yang & Koutsopoulos	+	+	0	-/0	-	0
Ahmed	-	+	0	-	-	-
Hidas	+	+	-	-/0	-	0
Toledo	+	+	+	-/0	-	0
MOBIL	+	+	+/0	-/0	0/+	0/+
LMRS	+	+	+/0	-/0	+	+

Table 3.2: Lane changing model comparison (performance scale: + high; 0:neutral; -: low).

Model selection

Table 3.1 shows that out of nine reviewed car following models, the extended IDM has a high score compared to the other models. To estimate the model parameters for the IDM a Matlab program already exists, and a simulation program is available for an extended version of the IDM as well. The trade-off of lane changing models shows for this research that LMRS has a high score.

Description of the selected individual car-following model

For the selected car-following model, symbols and units are explained. The calibration method of parameter estimations is described in section 6.2.1.

- **Extended IDM:**

The Extended Intelligent Driver Model uses the next equation:

$$a(t + T_r) = a_0 \cdot \min \left[1 - \left(\frac{v(t)}{v_0} \right)^\delta, \min_{i=1}^{n(t)} \left(1 - \left(\frac{\tilde{s}_i(t)}{s_i(t)} \right)^2 \right) \right], \text{ in which}$$

$$\tilde{s}_i(t) = i \cdot (s_0 + v(t) \cdot T_{des}) + \frac{v(t) \cdot \Delta v(t)}{2\sqrt{a_0 b_0}}, \text{ and}$$

$$s_i(t) = \sum_{j=1}^i s_j(t), \text{ where:}$$

$a =$	The predicted acceleration for a vehicle [m s^{-2}];
$v =$	Vehicle speed [m s^{-1}];
$s =$	Headway distance [m];
$\Delta v =$	Difference in speed of following vehicle and leading vehicle [m s^{-1}];
$T_{des} =$	Desired headway [s];
$\delta =$	Exponent, set to 4 [-];
$T_r =$	Reaction time [s];
$a_0, b_0 =$	To be calibrated model parameters 'maximum acceleration and deceleration' [m s^{-2}];
$v_0 =$	To be calibrated model parameter 'desired speed' [m s^{-1}];
$s_0 =$	To be calibrated model parameter called 'stopping distance' [m];
$n =$	Maximum number of anticipated vehicles;
$i =$	Possible number of anticipated vehicles;
$j =$	Process number for determining number of anticipated vehicles.

3.3 Conclusions

To analyse adaptation effects in empirical driving behaviour at work zones, variables of the tactical level of the driving task will be analysed. Differences in variables values and their distributions will be investigated for the following variables:

- Headway distributions;
- Speed distributions;
- Speed (differences) against corresponding following distances;
- Speed distributions at specific following distances;
- Lane occupation distributions.

Macroscopic effects can be investigated using empirical variables and by simulating calibrated driving behaviour models. With empirical data of all vehicles, macroscopic variables (e.g. density) can be computed and analysed as well. To analyse non-observed parts of macroscopic variables the Extended IDM as car-following model is selected for simulating longitudinal individual driving behaviour and analysing macroscopic variables. The LRMS is selected to simulate the lane changing part of individual driving behaviour.

In Chapter 4, methods for collecting required data for performing these analyses are presented. The analysis of driving behaviour and adaptation effects are presented in Chapter 6.

4 Data collection

To analyse variables as described in the previous Chapter, in this Chapter (section 4.1) data that are required for further analyses and configuration comparisons, are collected. In section 4.2, collection methods are inventoried and compared, after which the most appropriate method to collect these data is chosen. The locations where data are collected with the selected method are described in section 4.3.

4.1 Required data for analysing individual driving behaviour

In table 4.1, for each variable of individual driving behaviour, the required data that have to be collected to perform analysis as described in the previous Chapter is given.

Individual required data	Required source/raw data
Headways	Speeds and following distances
Speeds	Longitudinal vehicle positions at corresponding times
Following distances	Longitudinal position of vehicles and their leading vehicles
Accelerations	Speed changes
Lane occupation distributions	At corresponding times: Flows at corresponding lanes
Flows	At corresponding times: Densities and average speeds
Average speeds	Mean speeds of a number of vehicles over a time span
Densities	Length of road stretch and number of vehicles present or flow and speeds
General required information	Method
Layout and properties of work zone	Inventories work zones when doing measurements
Other: Date, weather conditions, ect.	Report when doing measurements

Table 4.1: Required data for each parameter.

4.2 Data collection methods

In this section, possible methods for measuring individual road user behaviour are described. For each method, expected output is checked against the requirements out table 4.1, after which the final collection method is selected and elaborated in detail.

4.2.1 Overview of Collecting Methods

To collect data that are required to do further analysis, different measuring methods are presented:

- Helicopter video (remote sensing) used by Knoop et al. (2009);
- Induction loops, used by Zheng (2009);
- Fixed location video, used by Maze et al. (2000);
- Driving simulator, used by Hoogendoorn (2012).

Helicopter data

A way of observing traffic is by helicopter, which records aerial imagery with an on board (video) camera. By this method, the road, vehicles and their locations are recorded by the recording frequency over a road stretch (Van Loon et al. (2006) and Hoogendoorn et al. (2003)).

- **Available helicopter data;**

Ter Kuile (2006) collected data with a helicopter, which is available for this research as well. He researched driving behaviour at work zone configurations with two barriers, narrower lanes and a reduced speed limit from 120 to 70 km/h.

- **Manned helicopter;**

The method to collect data with a manned helicopter is the most used method of collecting aerial imagery. Recordings cost about € 5000,- per hour and take place at about a height of 300 m. The camera can be controlled on board to record the desired locations.

- **Unmanned helicopter;**

This method is to collect data using an unmanned helicopter (see figure 4.1, (Aerial Group (2012))). This recording method is not used for this purpose yet at Delft Technical University (indeed at other Universities (Coifman et al. (2006))) and costs about € 1000,- per hour with an observation height of 200 m.

Induction loop data

The second method is collecting data by induction loops. Induction loop detectors are the most utilized sensor in traffic management systems. Induction loops are wires in pavement, which behave as an electrical circuit: when a vehicle passes the loop, the inductance is reduced. The control unit noticed this as a decreased frequency and stores this event as a passed vehicle (Research Development and Technology (2012)). An example of induction loops on a multilane freeway is shown in figure 4.2 (Rijkswaterstaat (2000)). The induction loops detect vehicles' speeds and stores the number of vehicles passing the detector (i.e. intensities).



Figure 4.1: Unmanned helicopter.

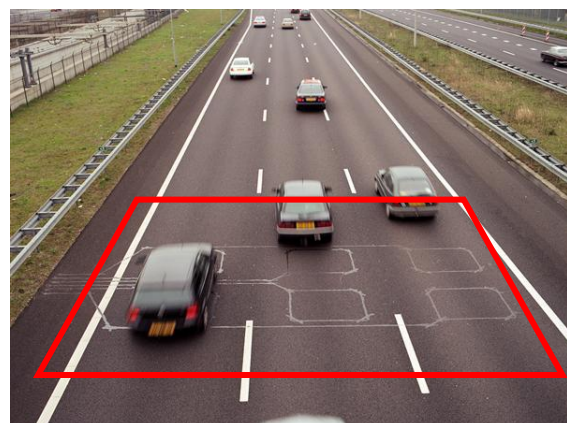


Figure 4.2: Induction loops in pavement on a freeway.

Video camera on fixed location around the freeway

Here, three methods based on a fixed location around the freeway are reviewed:

- **Fixed High Location;**

To record freeways from a fixed high location, the condition that highly limits possibilities to make these recordings is that such a high location should exist near a freeway with applied work zones. Also, often the owner/authority has to agree in making these recordings.

- **Telescopic mast;**

Another method to collect data is using a van including a telescopic mast of approximately 30 m at maximal height. An advantage of this method is that locations are much less limited than when selecting a fixed high location. A picture taken with the telescopic mast and the van with the mast tripod are displayed in figure 4.3 and figure 4.4.

- **Video camera on ground level;**

The third method of collecting data from a fixed location is to simply record from ground level.



Figure 4.3: Picture taken from the telescope mast.



Figure 4.4: Van with tripod of mast.

Driving simulator data

The last proposed method is collecting data by a driving simulator. Here, specific configurations can be programmed.

4.2.2 Collection method assessment

Now collection methods have been described, in this section the methods are judged if they meet the requirements (from table 4.1).

When meeting the requirements, other criteria are taken into consideration as well (see figure 4.5):

- Amount of data;
- Expected data validity and quality;
- Measurement possibilities;

- Analysing simplicity;
- Costs.

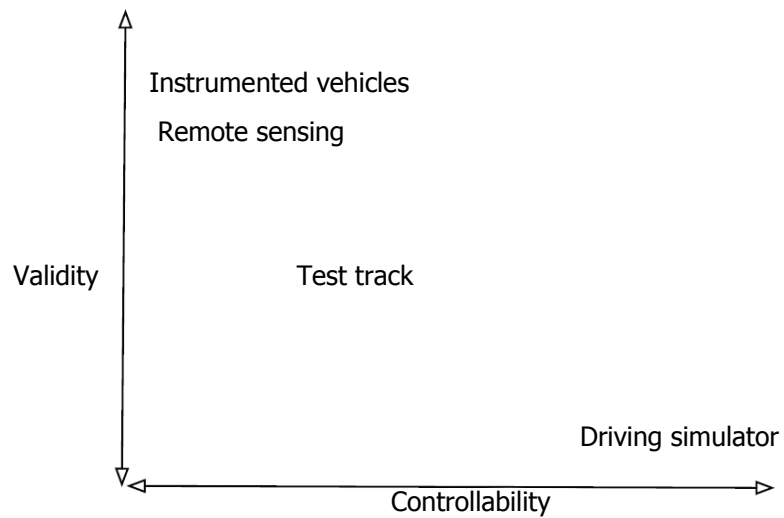


Figure 4.5: Data validity against controllability for different collection methods (Hoogendoorn (2012)).

Evaluation of the methods is summarised in table 4.3. The quantification judgement symbols used are explained in table 4.2.

Symbol	Explanation
Y	Yes
N	No / Not
n/a	Not applicable
++	Very positive
+	Positive
o	Neutral
-	Negative
--	Very negative

Table 4.2: Explanation and quantification judgement symbols.

Method	Speeds	Car-Following	Flows	Densities	Lane Distributions	Accelerations	Vehicle types	Meets criteria	Amount of data	Validity/quality	Analysing Simplicity	Collecting possibilities	Costs
Induction loops	Y	N	Y	Y	Y	N	Y	N	n/a	n/a	n/a	n/a	n/a
Helicopter imagery: Available data	Y	Y	Y	Y	Y	Y	Y	Y	o	+	o	++	++
Helicopter imagery: Manned helicopter	Y	Y	Y	Y	Y	Y	Y	Y	-	++	o	-	--
Helicopter imagery: Unmanned helicopter	Y	Y	Y	Y	Y	Y	Y	Y	+	++	o	+	+
Fixed location: High existing location	Y	Y	Y	Y	Y	Y	Y	Y	++	+	+	--	++
Fixed location: High telescopic mast	Y	Y	Y	Y	Y	Y	Y	Y	++	+	+	-	+
Fixed location: Ground level	N	N	N	N	N	Y	Y	N	n/a	n/a	n/a	n/a	n/a
Driving simulator	Y	Y	N	Y	Y	Y	N	N	n/a	n/a	n/a	n/a	n/a

Table 4.3: Comparison of data collection methods.

When looking at table 4.3, it is clear that if there is a fixed high location near a freeway with applied work zone, that location will be investigated first:

- **High fixed locations;**

The first location which is considered to be a suitable location to do measurements is at the project Hooggelegen near Utrecht on the A2. Next to a work zone an office building of approximately six levels is located, which has a perfect view over the work zone (see figure 4.6).



Figure 4.6: Facet building.

To make video images out of the building of the freeway work zone, permission of the owner/renter is necessary. The building is owned by a German real estate company and therefore the renter was directly contacted, but unfortunately the company has a policy that is not allowed to make video images from or out of the office building.

The second location is a location on the other side of the freeway. An advertisement mast stands about 50 m of the freeway, and this company allows that measurements using a camera take place, but there is uncertainty about the usefulness of the data that can be collected. Especially when the camera only has a line of sight of 40°, which leads to a maximum stretch of the freeway that can be observed of 60 m. This is too small with regard to observable interaction between vehicles, and the small time of a vehicle remaining in the system.

Another company has not been requested, because the same uncertainty yields for this location, as well as for the telescopic mast: Do the observations lead to useful imagery? Also with the telescopic mast there is large uncertainty, so no further investigation has been done towards this method.

4.2.3 Method selection: Unmanned helicopter

Collecting data by helicopter provides required empirical individual data. To observe actual driving behaviour, the method usually applied is using a manned helicopter. The duration of an observation period of this method is approximately a half an hour. This small observation period, together with the high costs and the innovative much cheaper method of the unmanned helicopter, is the reason that the unmanned helicopter is selected. Unmanned helicopters (i.e. drones) flights and recordings are performed by a selected company, Aerialtake.

Measurement registration form

To prevent the outcome to be restricted, measurements should not be taken during adverse conditions, such as conditions influenced by incidents (e.g. accidents) or extreme weather conditions. To check none of these conditions occurred, circumstances during the measurement period are monitored (see appendix 3).

Observation devices

The unmanned helicopter is controlled from ground level using a remote control. When the remote control sends no signal, because for example it reached its desired location, it holds its position and rate of rotation using GPS and a barometric altimeter. The remote control with altimeter is shown in figure 4.7 and the used unmanned helicopters can be seen in figure 4.8 and figure 4.10.

The type of camera which is used is the Canon 5DMII, which records full HD images, with a resolution of 1920 x 1080 pixels and a frequency of 25 frames per second. Low resolution of the imagery can be viewed live at ground level during the flight to check the recorded view.

During a flight, the camera settings can be adjusted: It can be vertically rotated and brightness can be adjusted. Camera rotation can be done by rotating the helicopter itself.

During collecting useful imagery, the helicopter was at a height of about 200 m and therefore barely visible (see figure 4.9). For each location, a measurement period of 2 hours resulting in 40 minutes of useful data.

Safety first

Unfortunately, there is always a small chance that the unmanned helicopter crashes during a flight. To prevent serious damage to persons or objects if a crash would happen, precautionary measures are taken:

- **Weather conditions:**

To minimize the risk that a crash happens, the weather forecast and conditions are precisely analysed. If the wind-force (forecast) is larger than 4 Beaufort, there are heavy gusts or precipitation occurs, the flight period is cancelled or interrupted.

- **Position of helicopter:**

The helicopters' position was never directly above the freeway, but always above non-built-up areas, to prevent that a crash causes serious damage.



Figure 4.7: Remote control.



Figure 4.8: Used helicopter for location 3 and 4.



Figure 4.9: Visual helicopter size at 200 m.



Figure 4.10: Used helicopter for location 1 and 2.

4.3 Configurations of observed locations

For collecting data, possible observation locations have been investigated for having different research determinant values and constant other determinant values. Searching within work zones set up by Mourik, finally four locations did match this criterion. At July 17th and September 15th 2011, in total four locations of urban freeways are observed by unmanned helicopter. By visiting possible measurement locations, landing places for the unmanned helicopter were considered and checked for appropriateness (e.g. is there enough space present, could through going traffic get distracted).

Geographical location of the measurement locations

At the time of data collection, as a participant of the combination 'De Utrechtse Tulp', Mourik carried out road works at the A28 freeway between Utrecht and Amersfoort. At different locations and time instances, different work zone configurations were applied, which led to interesting and comparable measurement locations. Numbering and exact geographical measurement locations are shown in figure 4.11. Location 1 and 2 were observed at July 17th 2011, location 3 and 4 were observed at September 15th 2011. During measurements, only at location 4 congested traffic has been visually observed.



Figure 4.11: Measurement locations on the A28 (Google (2011)).

Equal determinants applied for all locations

To find adaptation effects of certain differences in work zone configurations, most circumstances should be equal. Only in that case, influence of individual measures can be determined. In the next list, determinant values that do not (significantly) change over locations are given:

- Speed limit: For all locations a speed limit of 90 km/h is set;
- Number of lanes available/closed: No lanes are closed and any location, there are always two lanes are available for through going traffic, no onramps or exits were present;

- Road Gradient: No significant road gradient is present at any location;
- Weather conditions: Differences in weather conditions are relatively small:
 - Temperature: 12-18 °C;
 - No precipitation;
 - During daylight;
 - Wind force <5 Beaufort.
- Time of measurements do not differ much:
 - No holiday period;
 - Weekday.
- Occurrence of construction activities, incidents or other adverse conditions: None of these determinants differ between locations;
- Preparedness: All work zones were at least a couple of weeks set up already.

Differences in determinant values between locations

At the four measurement locations, five configurations have been observed. Differences in determinant values over these configurations are listed in table 4.4, in which configuration 2 is the control condition. A picture of each location is shown in figure 4.12 to figure 4.17. Separate top views of the locations are attached in appendix 5.

		Configuration				
Configuration		1	2	3a	4a	4b
Marking		White	White	White	Yellow	Yellow
Contra Flow		No	No	Yes	No	No
Channelizing Device	Left	Guard rail	Guard rail	Barrier	Barrier	Barrier
	Right	Narrow Barricades	Guard rail	Barrier	Guard Rail	Guard Rail
Hard Shoulder		Yes	Yes	No	Yes	Yes
Lane width (m)		2x3.5	2x3.5	3.25-3.00	3.25-3.00	3.25-3.00
Reverse Curve		No	No	No	Yes (small)	No

Table 4.4: Determinant values of all locations.



Figure 4.12: Configuration 1, direction West-East.



Figure 4.13: Configuration 2, direction West-East.

**Figure 4.14: Configuration 2, direction East-West.****Figure 4.15: Configuration 3, direction West-East.****Figure 4.16: Configuration 3, direction East-West.****Figure 4.17: Configuration 4a, direction East-West.****Figure 4.18: Configuration 4b, direction West-East.**

4.4 Conclusions

In this Chapter, data collection methods have been compared towards requirements of to be collected data and observation locations have been chosen. Based on required data and costs for doing measurements, in total five configurations have been observed by an innovative method, the unmanned helicopter.

Road works carried out by 'De Utrechtse Tulp' turned out to have interesting and comparable work zone configurations. A control condition, where no road works were set up, and four configurations with applied work zones, with varying research determinants (lane widths, channelizing devices and presence of reverse curves) have been observed.

In the next Chapter, the process from raw collected imagery to individual trajectories is described.

5 Data processing

To analyse collected video imagery, empirical variables and calibrate parameters of the driving behaviour model video recordings have to be converted into individual vehicle trajectories and corresponding individual required data. This process consists out of two main steps, also described by Hoogendoorn et al. (2003): 'Image pre-processing' and 'Vehicle detection & tracking'.

5.1 Step 1: Image pre-processing

Step 2, 'Vehicles detect & Tracking', deals with stable images as isolated frames from continuous imagery. Before detecting and tracking vehicles, next steps have to be performed first:

- Extract frames from raw imagery;
- Deinterlace;
- Useful period selection;
- Lens correction;
- Stabilization.

Raw imagery properties

The raw imagery, 'Interlaced High Definition video files', were recorded with unmanned helicopter. In total 28 useful movies containing 8 minutes of useful data have been collected (200 Gb). The movies were quite stationary already, which meant about three large or abrupt movements per recorded movie.

The resolution of raw imagery was 1920 x 1080 pixels, collected at a height of circa 200 m. The camera was fully zoomed out for all recording periods (same optic angle) and recorded road stretches of 200 – 280 m, which was dependent on the perpendicular distance of the camera towards the freeway and of the camera angle towards the longitudinal direction of the freeway (illustrated by figure 5.1). As mentioned before, the frequency of the recorded video was 25 frames per second.

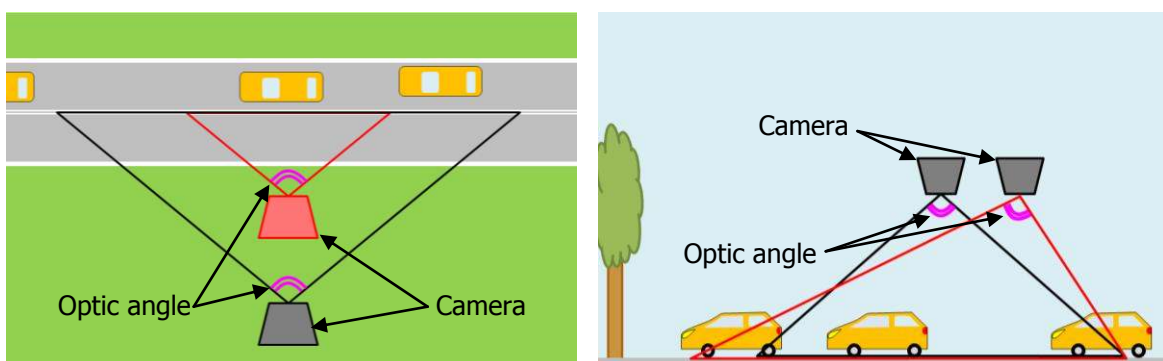


Figure 5.1: Different observed stretches with same optic angles (left: top view, right: longitudinal view).

5.1.1 **Extract and deinterlace frames from raw imagery**

The first step of image pre-processing is to isolate single frames from the movies. This led to a total number of frames, equal to the duration of the movies multiplied by the frequency.

The process of extracting frames has been done by an existing open source program 'M-Player'. The program and manual can be freely downloaded at <http://www.mplayerhq.hu/>. The method how to extract frames with this program is explained later.

A complicating property of the recorded movies is that they were interlaced. Interlaced recordings create a frame by combining two frames of half the height. Firstly, odd pixel rows are recorded and saved, after which even rows are recorded and saved. Unfortunately there is a time gap between odd and rows, which is clearly visible when focussing on moving objects (e.g. vehicles). An example of (a part of) an interlaced frame is shown in figure 5.2.

Because stabilization of interlaced frames has turned out to be difficult (the stabilization program was not well able to stabilize the interlaced frames), frames have been deinterlaced. This has been done by replacing even rows, by averages of the next and previous odd row, which were recorded at the same time instance. This led to images as the example shows in figure 5.3. Fortunately, 'M-Player' can deinterlace images simultaneously with extracting them from the raw imagery.



Figure 5.2: Example of interlaced frame



Figure 5.3: Corresponding deinterlaced frame

M-Player command line

To extract and deinterlace imagery, one has to browse to the desired output folder using a command line interface first (e.g. Microsoft Windows uses Command Prompt). When browsed to the destination folder, an example of a command line is:

```
"C:\Programs\Mplayer\mplayer.exe -vf framestep=1, pp=li -vo png:z=0  
D:\Data\0000.mts"
```

In this command first the path of the application is given, `-vf` stands for isolating frames, `framestep` determines the frequency of frames which have to be extracted, `pp=li` represents the deinterlacing method (in this case linear) and `-vo` determines output properties, like compression level and type of

output images. Finally the path of the source movie is given. To execute one of the other available commands, search for the M-Player manual.

Period selection

The frame extraction process resulted in a large amount of data (1.5 Tb of isolated frames). To continue the next image pre-processing step, useless periods have been deleted (when the helicopter was not at the desired height (± 0.5 Tb)).

5.1.2 Lens correction and stabilization

The image pre-processing steps lens correction and stabilization of using isolated frames is described in detail by Hoogendoorn et al. (2003) and explains how frames are corrected from raw images to stable, corrected images. A brief overview of this process is presented in the sections below, which describe the phenomena and corrections for 'pincushion distortion' and 'perspective distortion'.

An existing Java application 'ImageTracker' (developed at the Delft University) has been used to perform these pre-processing steps, of which an manual is attached in appendix 4.

Pincushion distortion correction

This step towards individual vehicle trajectories corrected imagery for lens convexity, which especially occurred at the edges of imagery, causing stretched images.

To correct the imagery, the extent of this phenomenon for the used camera device has been inventoried. This has been done by shooting a frame of a chess-board pattern under the important condition that same zoom settings were applied here, as during measurement periods. A chess-board pattern per definition, consists of equal, perpendicular squares, but due to lens convexity, the recorded frame did not show exact squares (see figure 5.4). By adjusting the frame, exact same sized squares have been reproduced (see figure 5.5). By applying this same correction for all frames, they have been corrected for pincushion distortion.

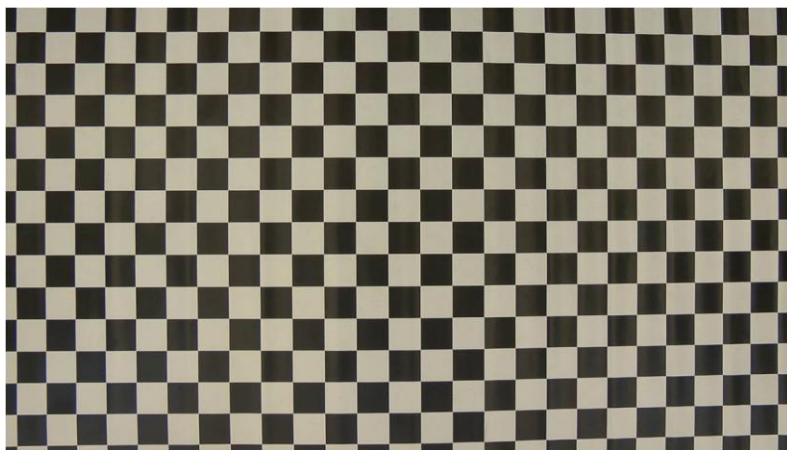


Figure 5.4: Chess board pattern, calibration picture of camera Aerialtake.

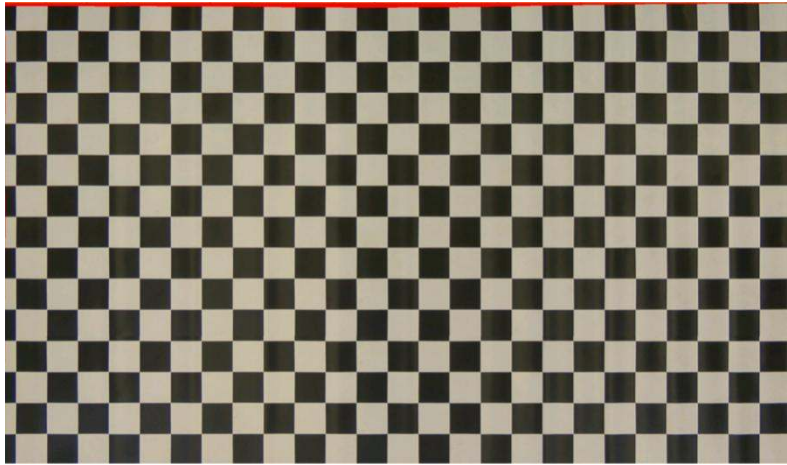


Figure 5.5: Chess board pattern after calibrating.

Perspective distortion

The second correction corrected perspective distortion. This distortion occurred, because the observed location was not exactly located under the camera (see figure 5.6 for a schematic sketch of this phenomenon), so a pixel at the back of the frame (far away) describes a larger distance than a pixel at the front of the frame (nearby).

This distortion has been set manually for each movie, illustrated in figure 5.7.

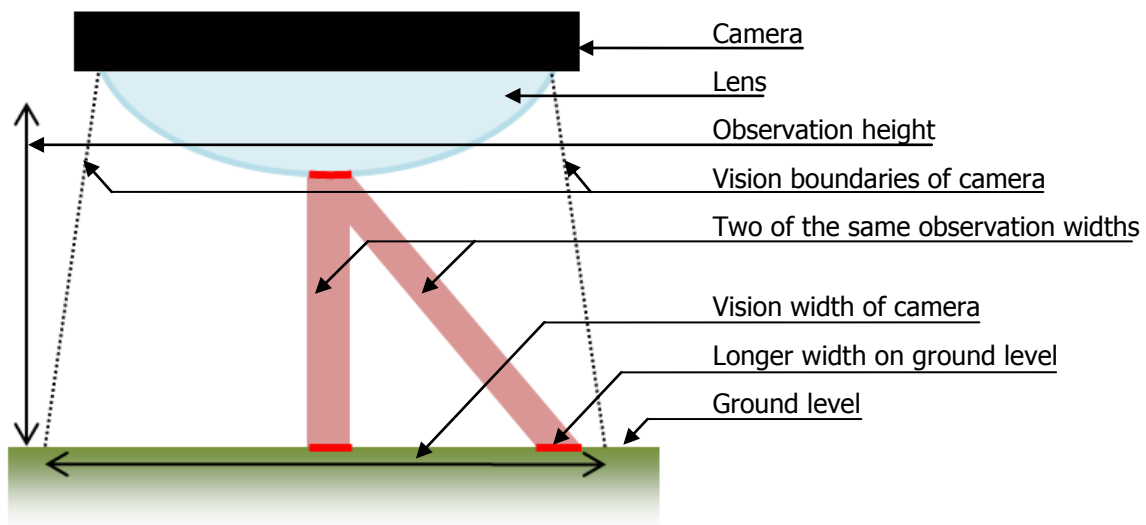


Figure 5.6: Schematic sketch of the distortion introduced by the perspective vision.

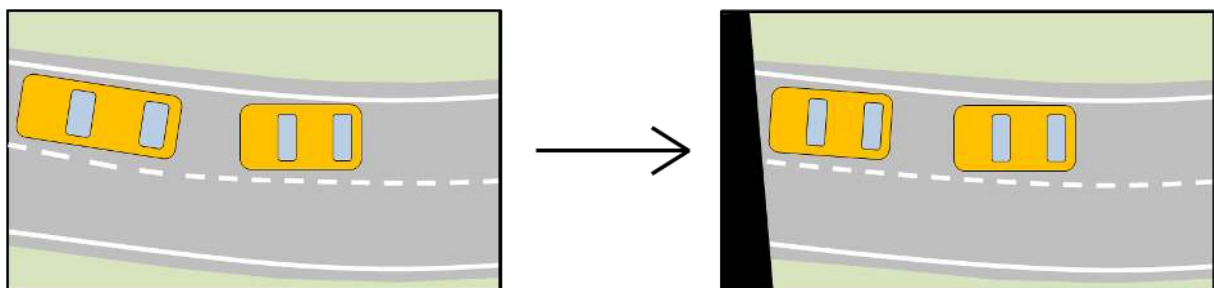


Figure 5.7: Illustration of a lens convexity correction for an isolated frame.

Stabilisation method

After correcting errors of lens convexity and perspective distortion, frames have to be stabilised. This operation has to be performed because it is not possible to keep the helicopter at the exact same location, so imagery are moving and vibrating. Because vehicles have to be detected by changes between isolated frames, these frames have to show the same background, except moving vehicles.

By performing lens correction for all frames, they can be used for frame stabilisation. The stabilisation program tries to fit every frame on first frame by minimizing the differences between the two frames. Because the only objects moving over the frames are vehicles, the program stabilises the frames on other visible elements. For an illustration of the stabilisation process, see figure 5.8 to figure 5.13. For illustration convenience, the illustration compares and fits frame 2 to contours of frame 1 instead of the complete image, as 'ImageTracker' does.

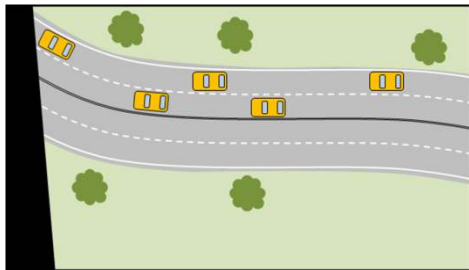


Figure 5.8: Frame 1, corrected for lens convexity.

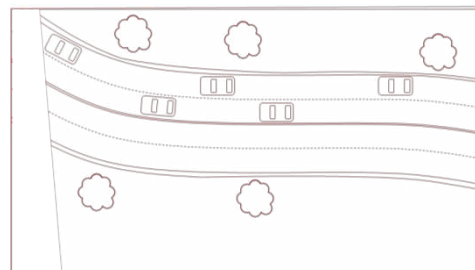


Figure 5.9: Object contours of frame 1.

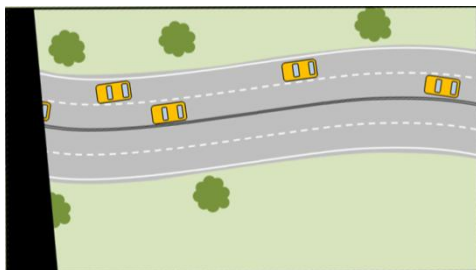


Figure 5.10: Frame 2, ready for stabilisation.

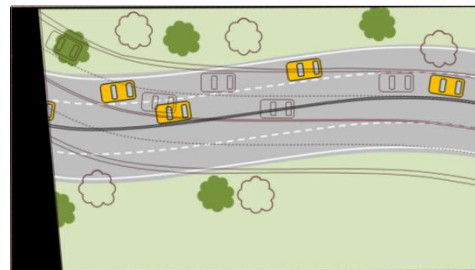


Figure 5.11: Frame 2, with contours of frame 1 in red.

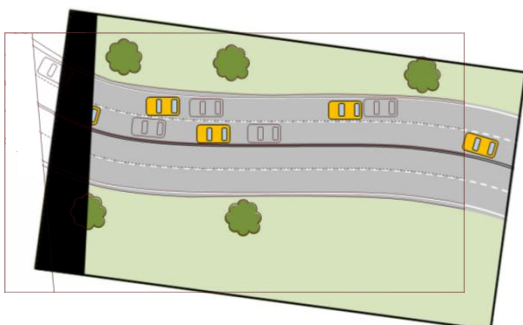


Figure 5.12: Frame 2 fitted best on frame 1.

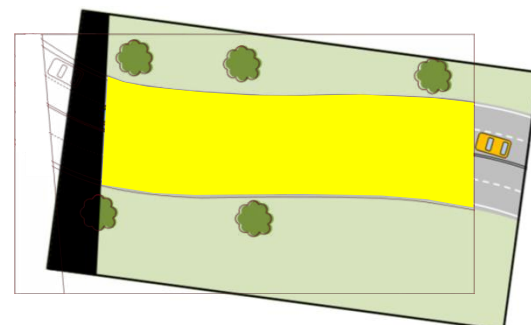


Figure 5.13: Useful part in yellow.

Stabilization problems

The process of stabilizing these images for all 28 movies has been done by parallel runs of 'ImageTracker' using 90 computers (quad core) during one weekend.

The movies were judged quite stable by the developer of the stabilization program on beforehand and therefore no large stabilisation difficulties were expected, but unfortunately stabilization resulted in approximately 350 parts with 85 different backgrounds. These parts were results of unexpected 'jumps' which occurred during stabilization using 'ImageTracker'.

Here, the stabilisation program could not fit all images correctly and found wrong optima (not the smallest error). As a result, output images did not have the same backgrounds and cannot be directly used.

Jump detection and removal

By trying to remove these unexpected and undesired 'jumps', a Matlab program has been created. This program calculated the difference between a stabilized image and the initial stabilized image. By comparing differences of two successive frames, jumps have easily been detected (see figure 5.14). The basis of source code for this program is given in appendix 5.

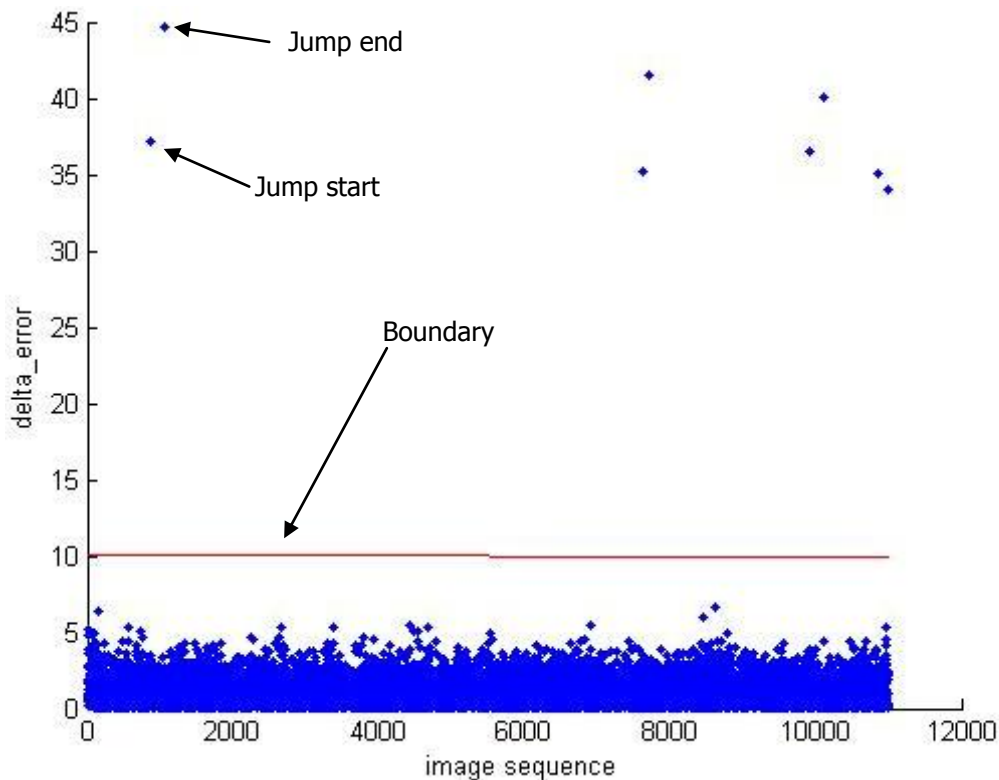


Figure 5.14: Detecting jumps in stabilized frames.

A jump has been removed by setting another image as reference image and continue the process with last correct stabilized image stabilization parameters, which are stored in an output file of the stabilization program.

This method has been tried, but despite large manual effort, new jumps appeared. Therefore, the process is continued with 85 different backgrounds.

From figure 5.14, it is clear that jumps can easily be detected by the presented method, and therefore it is recommended that this method is implemented in the stabilization program. By implementing this method, the now manual required actions can be automated.

For all 85 parts (called 'zones' in the remainder) different detect and tracking settings should be configured. This process yields a huge amount of manual editing, and therefore it has been chosen to continue with only two of the four measurement locations (location 2 and 4).

After completing lens convexity correction and stabilisation (see figure 5.15 for an output example), the process for detecting and tracking of vehicles can be started.



Figure 5.15: Example of stabilized frame.

5.2 Step 2: Detecting and tracking vehicles

With the frames corrected and stabilised, vehicles can be detected and tracked over isolated frames. The detecting and tracking method differs from the method published by Hoogendoorn et al. (2003). The use of the hereafter presented method instead of continuing the previous process, is because the method presented by Hoogendoorn usually takes much more manual and computational effort.

The method applied here is published by Knoop et al. (2009), for which an illustrated description is presented below and consists of:

- Creating longitudinal cross-sections;
- Selecting pixels of possible trajectories;
- Removing stabilization edges and useless areas;
- Detecting and tracking vehicles;
- Translating pixel distances to real distances;
- Selecting vehicle types;
- Converting individual to car-following data.

5.2.1 Longitudinal cross-sections

The detection and tracking of vehicles have been done for each lane successively and here described for one lane. Pictures have been created of longitudinal cross-sections for each time step in a selected lane. The lanes have been selected by setting points in the middle of the lane over the length of the frame, after which a curve has been automatically drawn through the points (illustrated in figure 5.17 and figure 5.16).

To select points through which the curve has been fitted, the Python program has been used. This program has been developed for another step in this graduation study (see section 5.2.4), and has been very useful selecting these points. This open source program ('Highway Traffic Flow Analysis'), consisting out of a settings file, 3 different applications, a manual and some support files (Github (2012)). In the settings file, preferences (e.g. source path and number of start image) can be changed. The 3 applications load images and register the cursors' pixel location with a mouse click. These (zero-based) locations are saved in one text file per image. A brief overview of the Matlab code to create the curves (i.e. longitudinal cross-sections) based on saved pixel locations is given in appendix 5.

After determining longitudinal cross-sections, a picture with a height of 1 pixel has been taken along this section. The stabilized frame with defined curve is presented in figure 5.16, illustrations are presented in figure 5.17 and figure 5.18.

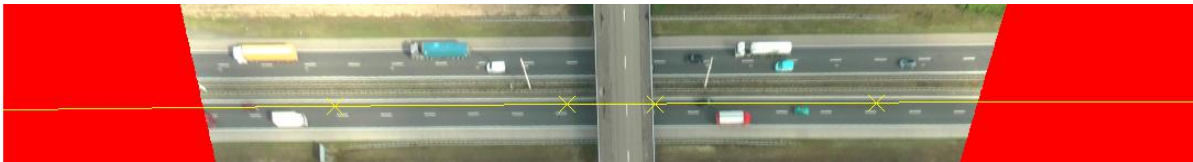


Figure 5.16: Curve in real stabilized image.

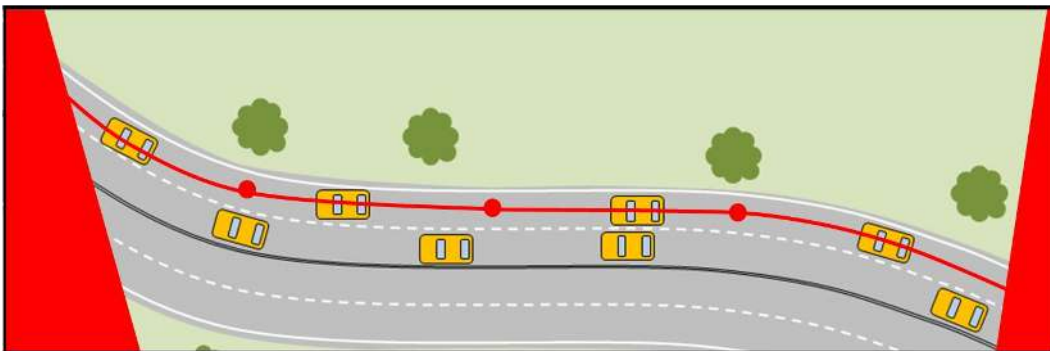


Figure 5.17: Corrected and stabilised frames with connected points on right lane.

Figure 5.18: Picture of one longitudinal cross-section.

This one pixel high picture has been taken for each time step and combined downwards to images as illustrated in figure 5.19. Here, trajectories of vehicles are already visible.

This process resulted in 372 images (0.8 Gb) and took a computational time of circa 48 hours using a double core processor.



Figure 5.19: Pictures of a number of time steps of a longitudinal cross-section.

5.2.2 Edge detection for vehicle detection

Knoop et al. (2009) proposed a method of finding and tracking vehicles by comparing pixel intensities along the road. This method calculates the average pixel intensity for every position over a limited distance during a short period of time (see figure 5.20). By comparing current with average pixel intensities and a boundary for the difference, vehicles were detected by a Boolean check (if the boundary was crossed or not).

Figure 5.20: Average colour along the longitudinal section.

Unfortunately, the results of combined cross-section images were noisy, therefore averages have turned out being not useful for detecting vehicles.

To overcome this problem, a method called 'edge detection' has been applied to find vehicles. This method, which was never used before for detecting trajectories, checks for intensity changes (first and second derivative) instead of differences towards an average value. This method is explained by Trucco & Alessandro (1998) and Jain et al. (1995) and is programmed in Matlab using a built-in function (see appendix 5), and turned out to be much faster than the method presented by Knoop et al. (2009).

This Matlab function has a number of built-in methods for detecting edges. Based on online documentation and best-practice, the 'Canny' algorithm has been chosen to be used for detecting the edges in the images. The boundaries for detecting edges are set automatically by default, based on the input image values. Because automatically determined boundaries, compared to manually set boundaries led to good results, automatically boundaries were used.

The whole edge detection process took only about 90 minutes (resulting in a total file size of 20 Mb). An example of combined cross-sections and a result after edge detection are presented in figure 5.21.

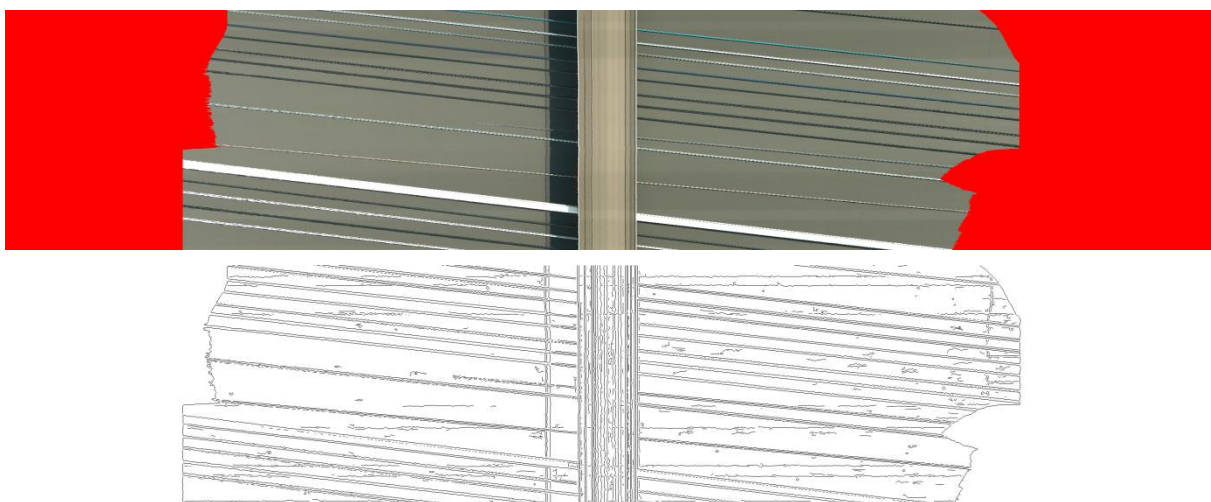


Figure 5.21: Example of combined cross-sections (top) and found corresponding (negative) edges (bottom).

5.2.3 Remove stabilization edges and viaduct

To track vehicles over edges, as much of possible connections between separate vehicles have to be removed. These connections mostly exist at stabilization edges and at the present viaduct. Stabilization edges are per definition determined by the colour shift of only red to not-only red from both sides of the image, and therefore easy to remove. To remove the viaduct edges, the location of the viaduct has to be determined, which has been done manually for every separate zone with the program also used for selecting curve indices ('Highway Traffic Flow Analysis', 10 minutes of processing time). The Matlab code that dealt with removing edges for these regions, is given in appendix 5. The example with removed stabilization edges and edges at the viaduct location is given in figure 5.22.

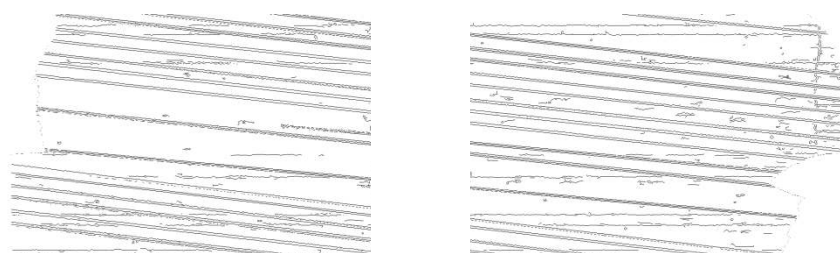


Figure 5.22: Example of removed edges.

5.2.4 Track vehicles: Dijkstra algorithm

Set start and ends of vehicles

Before trajectories of vehicles can be tracked, vehicles have to be selected from non-removed edges. For this research, starts and ends of the vehicles have been manually selected using the Python indices program, which has been quite time consuming (30 hours). For future research it is recommended that a Matlab program performs a raw selection, which is manually checked and corrected afterwards (using the indices program).

Connect start and ends

To connect the starts and ends of selected vehicles, a program with a shortest path algorithm has been developed. The algorithm that has been used, is the Dijkstra algorithm (Dijkstra (1959)), which is not the fastest shortest-path algorithm, but a very straight forward method, which always results in the shortest path. For future research, a faster algorithm could be developed or implemented to limit the required computational time.

The computational time highly depends on the traffic intensity (causing correct edges in the images), noisiness of the image (causing faulty edges), and distance between the end and start pixels and the completeness of found edges (number of disruptions per trajectory).

Now, it took about 5 days to process the Dijkstra algorithm (described below) to connect all trajectories:

- Start: A image with edge and non-edge pixels;
- Resistance (i.e. distance) for travelling over an edge pixel (1 in general), and for travelling over a non-edge pixel (e.g. 50). A non-edge pixel has to have such a low value that small interrupted edges can be passed;
- Start and end points of vehicles;
From the starting point, connected pixels are set 'active' and minus 1 to their resistance. If the pixel resistance is now zero, set connected not yet visited pixels 'active' and the current pixel 'visited'. By setting a pixel 'active', save also the direction from where it is set active. Continue this loop until the destination pixel is set active, and find the way back using the saved directions.
- Correcting wrong trajectories;
Unfortunately, not all trajectories have been selected correctly, because paths over other vehicle trajectories have a shorter path to the destination. To correct trajectories which contain errors, intermediate nodes are selected (using 'Traffic Flow Analysis'), after which the Dijkstra algorithm has been performed successively.

The previous process led to complete trajectories of all observed vehicles, with deviations for sometimes tracking fronts of vehicles and sometimes tracking rears of vehicles. Attempts to removing this deviations, have been unrewarded.

A start of an automatic selecting program, the complete checking and correcting program and the complete programmed algorithm to find the path from a vehicles' start to its end, is presented in appendix 5. An example of a result is given in figure 5.23.

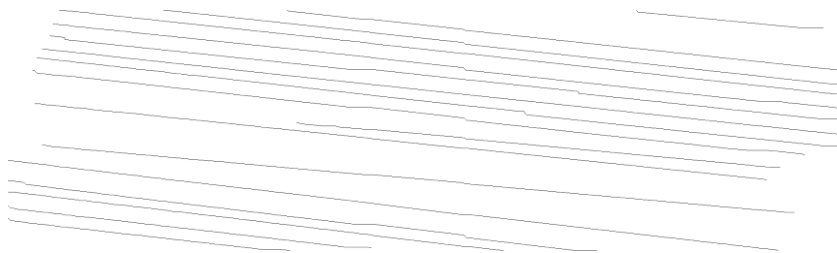


Figure 5.23: Result of connected trajectories.

5.2.5 Select vehicle types

The ratio of heavy vehicles influences the traffic state and therefore the heavy vehicles have to be distinguished. This has been done by a Matlab program, which has to be manually corrected afterwards. The method is based on vehicle lengths, using median distances of a second edge towards the selected edge. If the vehicle exceeds a pre-set boundary, the vehicle is indicated to be a heavy vehicle. In other cases, the vehicle is indicated as a passenger car.

5.2.6 Translate pixel distances to real distances

Now, pixel locations of observed vehicles are known at all time instances. To analyse vehicle movements, real locations have to be known. This has been done by setting known distances in stabilized frames for all zones (see figure 5.15), using the indices program. For this research, pavement markings are used for setting positions, after which the rest of the positions have been inter- and extrapolated.

By knowing the position of each vehicle at specific time instances, speeds and accelerations at these instances can be calculated.

5.2.7 From individual to car-following data

Now, positions of all vehicles have been defined. To smooth observations, all even time instances have been removed from the dataset. By selecting all present vehicles at each left time instance, car-following data has been determined. This program is given in appendix 5. Speeds used for analysis are in meters per second (m/s).

5.3 Conclusions

The steps from raw imagery to individual trajectories and car-following data have been broadly elaborated in this Chapter.

The step of stabilizing images and correcting them for pincushion and perspective distortion led to large difficulties, so it was unavoidable to use only two of original of four locations in the ensuing of this research (configuration 2, 4a and 4b).

Detecting and tracking individual vehicles have been done by using mostly innovative methods (edge detection and the Dijkstra algorithm) and self-developed programs (Python indices program) and resulted in 8355 useful trajectories of individual vehicles of approximately 8 seconds (100 separate observations) per vehicle:

- Configuration 2 included 4827 vehicles, of which 611 were heavy vehicles (13%);
- Configuration 4a included 1707 vehicles, of which 264 were heavy vehicles (15%);
- Configuration 4b included 2051 vehicles, of which 347 were heavy vehicles (17%).

The trajectories and car-following data that are extracted from raw imagery are used in Chapter 6 to investigate microscopic and macroscopic effects of changed determinants.

6 Analysis Results

The process to analyse adaptation effects of changes in research determinants is presented in this Chapter by:

- Analysing empirical car-following behaviour;
- Estimating car-following model parameters;
- Simulating configurations using estimated parameters;
- Presenting results.

6.1 Analysing empirical car following behaviour

As described in section 3.2, following empirical variables are analysed:

- Headway distributions;
- Speed distributions;
- Speeds against Following distances;
- Speed distributions for following distances in a specific range of 25 - 30 m;
- Lane occupation distributions.

For all analysed variables yield that data to draw the distributions consist of each individual vehicle at each time instance (approximately 100 observations per vehicle).

6.1.1 Carriageway layout and consistency analysis

Variables are analysed for each work zone configuration and if applicable, for each lane. Lane numbering that is used throughout the analysing process are indicated in figure 6.1.

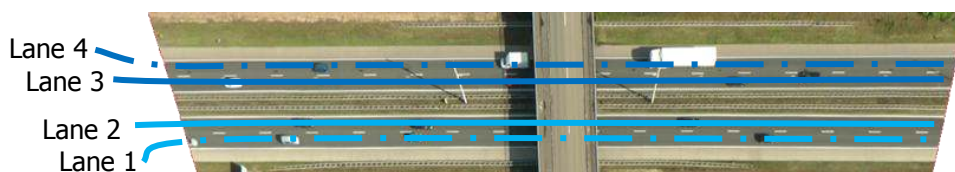


Figure 6.1: Lane numbering.

Before analysing empirical variables in detail, two consistency checks are performed, to check the presence of strange values (especially near the observation boundaries). For these checks hypotheses are defined:

- Compare speed distributions of configurations with and without applied work zone;
- Compare speed distributions over distances.

Hypotheses for consistency checks:

- Shapes of speed distributions do not differ much between configurations;
- Speed distributions do not differ much over the distance of the observed road stretch;

- Speeds are lower at configurations with applied work zone than without applied work zone;
- Speeds are lower on right lanes than on left lanes;
- Speeds of heavy vehicles are lower than speeds of passenger cars.

In figure 6.2, speed distributions are drawn of the control situation (configuration 2), and the situation with applied work zone (configuration 4). It can be seen that the speed distribution with applied work zone shifted to a lower speed compared to the control condition and that shapes of both distributions differ, specifically at low speeds.

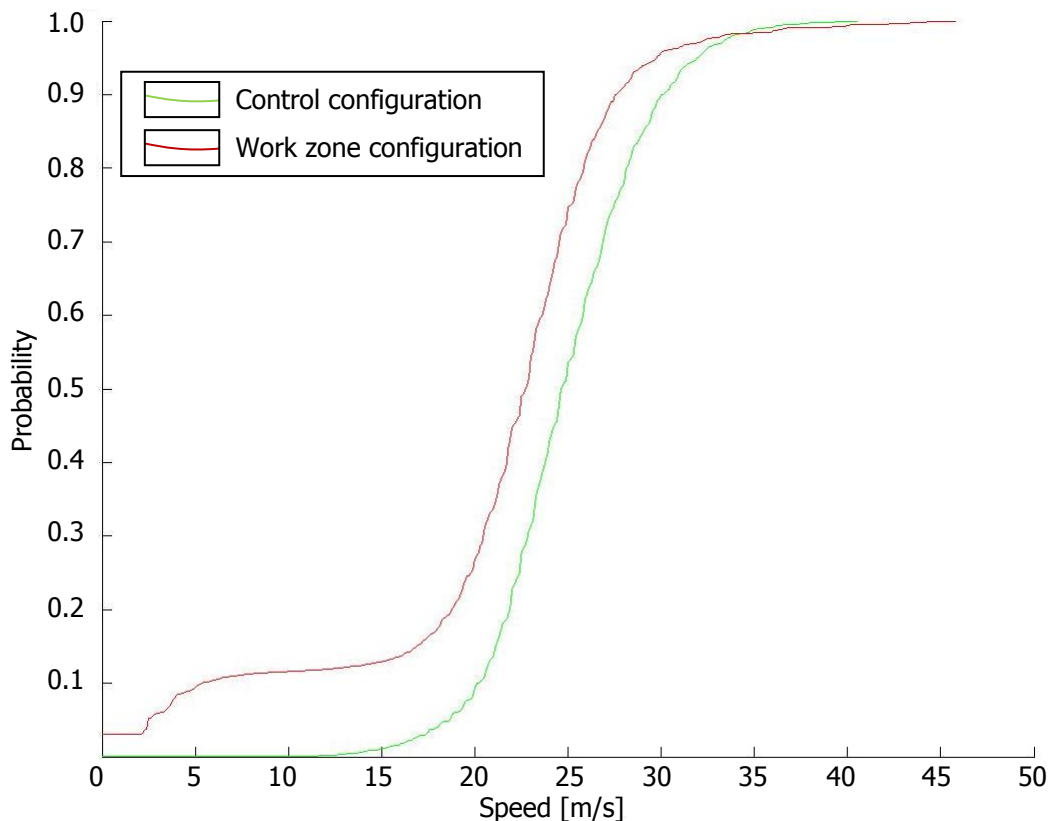


Figure 6.2: Cumulative speed distributions for each observed location.

The speed distributions for separate lanes are plotted in figure 6.3, showing generally that speeds at left lanes are higher than at right lanes.

Speed distributions per vehicle type are also considered (see figure 6.4). In these distributions it is clear that in general, passenger cars drive at higher speeds compared to heavy vehicles, and that speed differences among heavy vehicles are less than among passenger cars.

To check if distances have been set correctly and vehicles have been correctly tracked over the distance, mean speeds (and 95% confidence intervals) were plotted for each location, lane and configuration. A characteristic plot is given in figure 6.5, which shows high deviations in mean speeds at low and high distances.

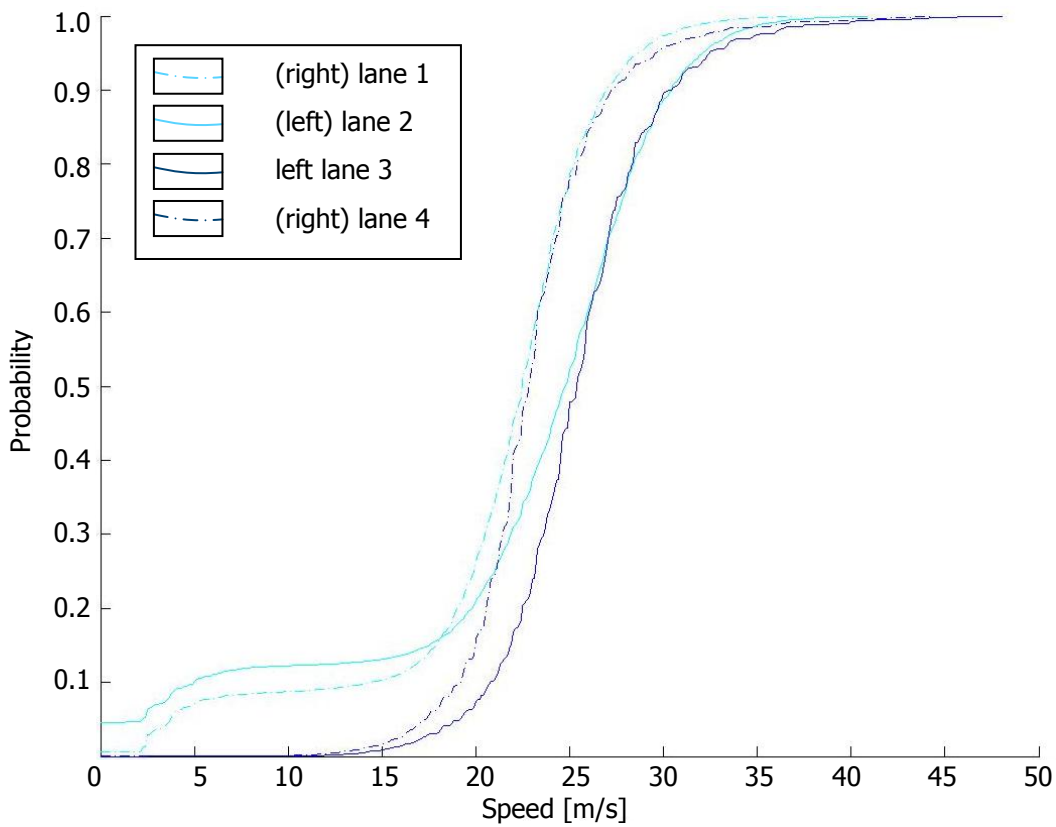


Figure 6.3: Cumulative speed distributions per lane.

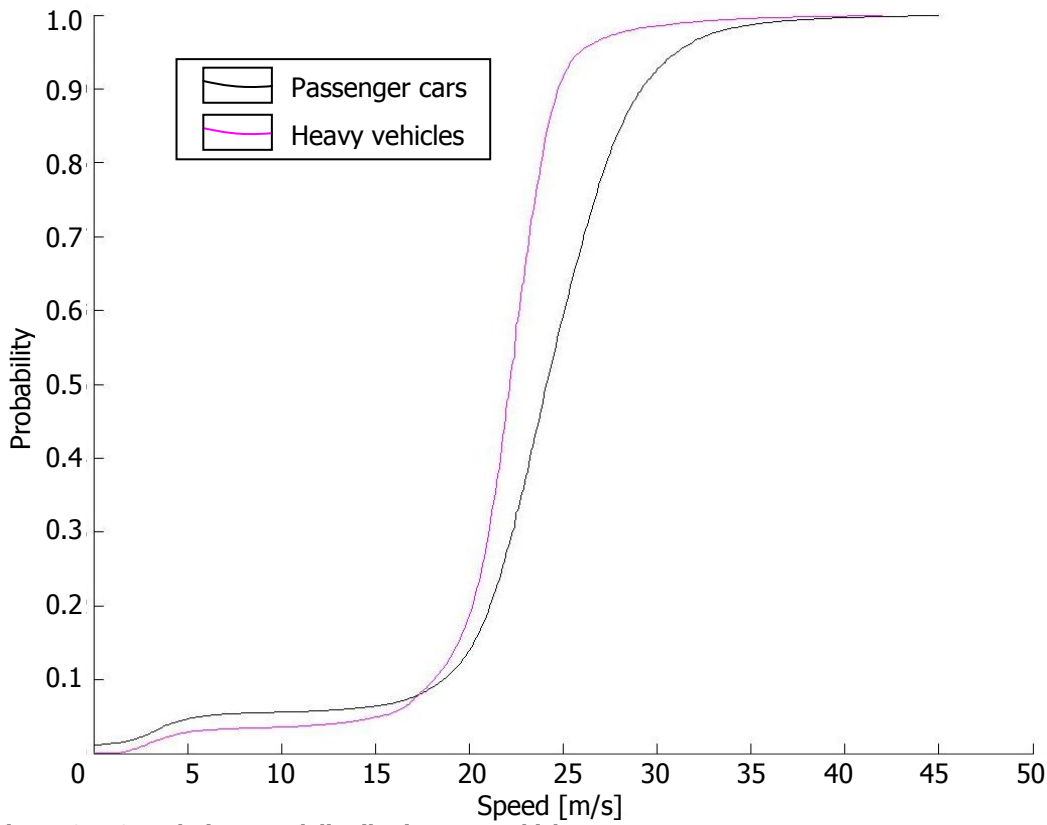


Figure 6.4: Cumulative speed distributions per vehicle type.

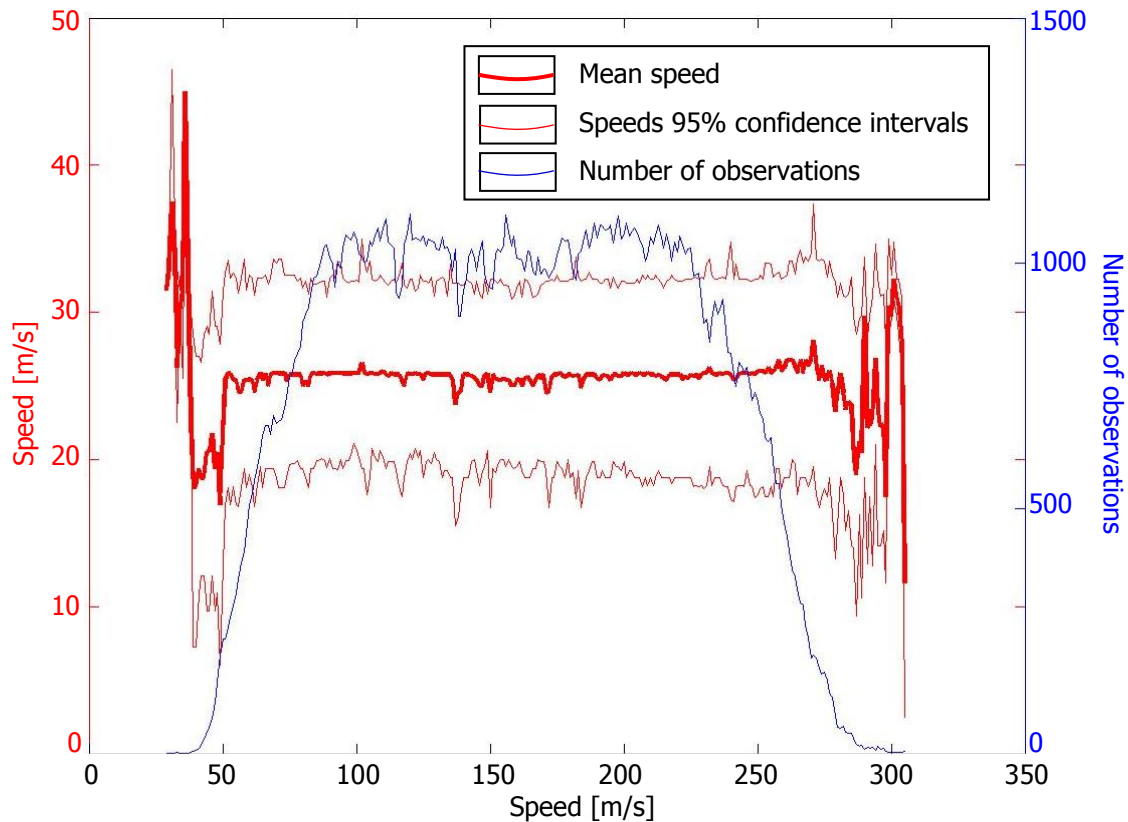


Figure 6.5: Speed over distance plots for configuration 2, lane 3.

The results show that three out of five hypotheses were met:

- Speeds were lower at configurations with applied work zone than without applied work zone;
- Speeds were lower on right lanes than on left lanes;
- Speeds of heavy vehicles were lower than speeds of passenger cars.

Two hypothesis were not met:

- Shapes of speed distribution differ much between configurations:
 - A relatively high fraction of low speeds were observed at work zone configurations.
- Speed distributions differ much over the distance of the observed road stretch:
 - At small and large distances, large differences were observed in mean speed values.

Discarding observed congestion, small and large distances

By analysing the flow density relation (see section 3.2.2), it turned out that the relatively high fraction of low speeds occurred at high density values (congestion). Therefore, observations involving the congested traffic state, have been discarded, to be able to compare the control situation with the work zone situations.

The disproportional differences at high and low distances are caused by observing a very long freeway stretch under an angle (see figure 5.1), which caused perspective problems. Individual pixels covered large longitudinal distances, which involved problems setting reference distances and tracking vehicles. Therefore, observations at distances outside the 50 to 250 m range have been discarded.

To show that data, after discarding congestion and large and small distances, meet the hypotheses, the speed distribution for the control situation and the work zone situation is presented below. Speed distributions cannot be directly compared, because the intensity of configurations were different. Therefore, graphs are not quantitatively investigated.

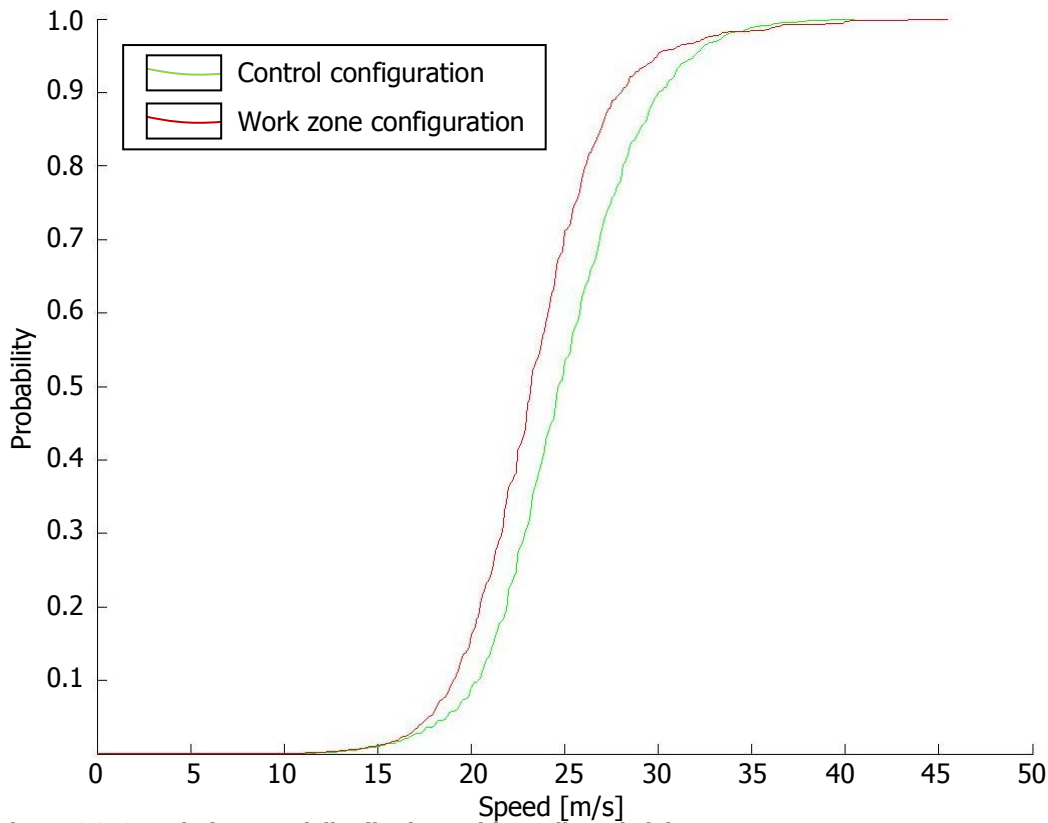


Figure 6.6: Cumulative speed distributions without discarded data.

6.1.2 Headway distributions

It is expected that headway time distributions shift towards longer headways when work zones are applied. Because most of observed headways are relatively small, the log-normal distribution has been used to fit the time headways (Luttinen (1996)). The empirical and fitted headway distributions are presented in figure 6.7 to figure 6.12. Expected values of fitted log-normal distributions for each configuration, for each vehicle type are presented in table 6.1.

	Passenger Cars			Heavy vehicles		
	Config 2	Config 4a	Config 4b	Config 2	Config 4a	Config 4b
$E(T)$	1.51 s	1.65 s	1.53 s	2.45 s	2.42 s	2.37 s

Table 6.1: Expected headway times for different configurations and vehicle types.

The expected value of passenger cars presented consistent results compared towards the hypothesis, the headway times increased when a work zone is applied (it even increases more when a reverse curve is installed). Heavy vehicles show inconsistent results towards the hypothesis, probably because they were not car-following (observed time headways are relatively large).

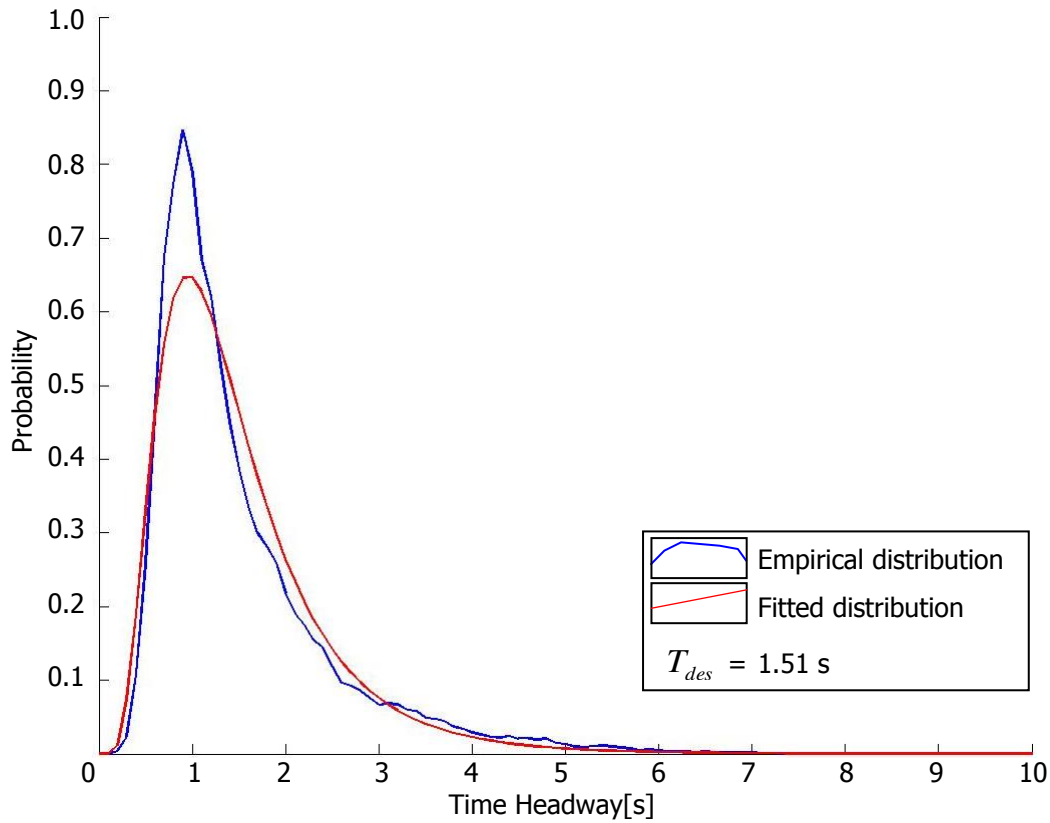


Figure 6.7: Fitted and empirical time headway distribution, configuration 2, passenger cars.

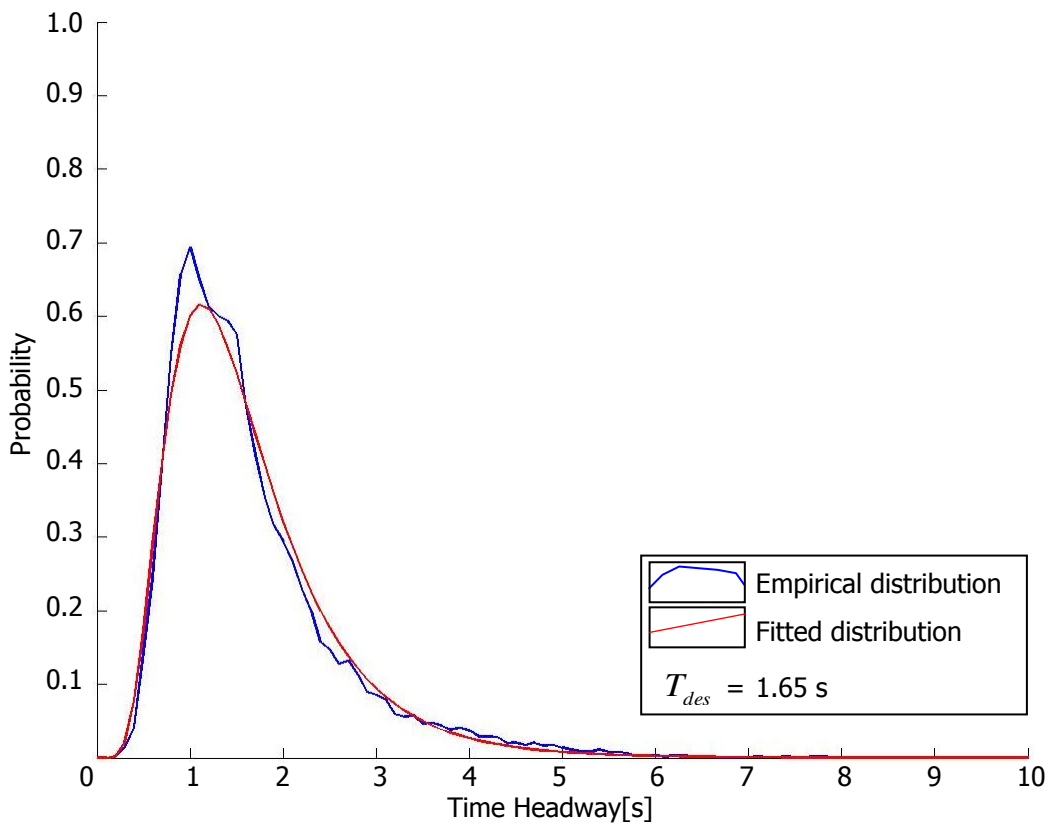


Figure 6.8: Fitted and empirical time headway distribution, configuration 4a, passenger cars.

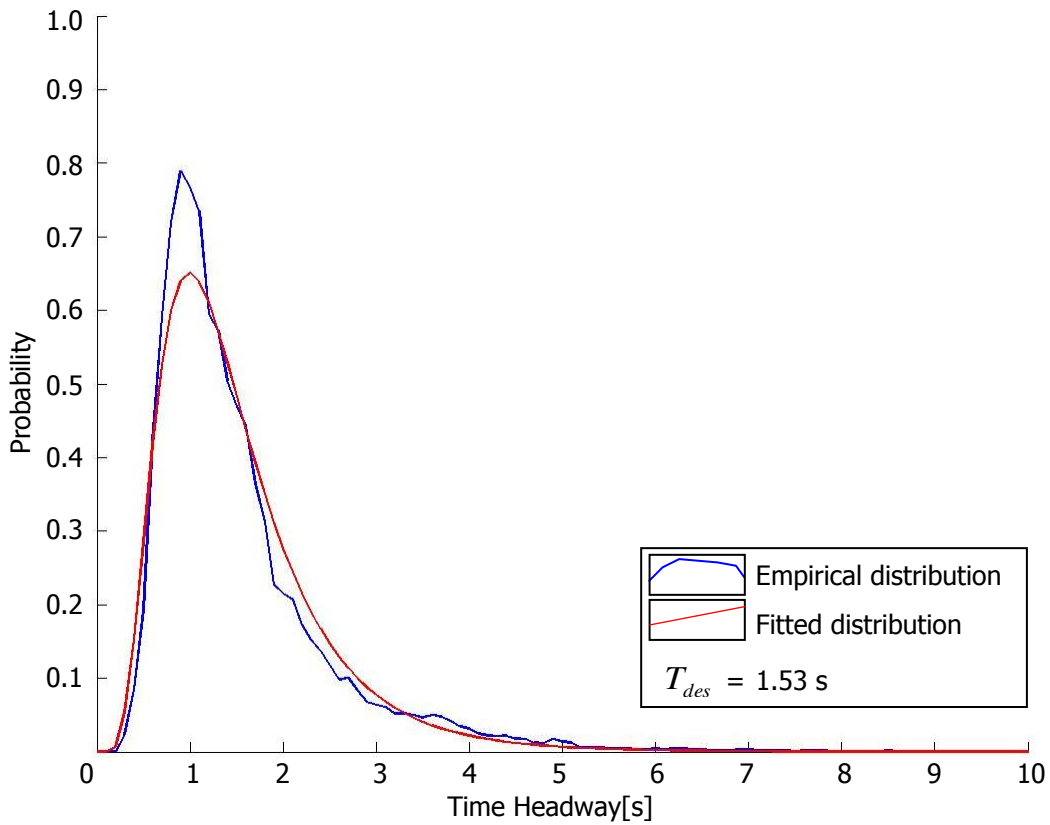


Figure 6.9: Fitted and empirical time headway distribution, configuration 4b, passenger cars.

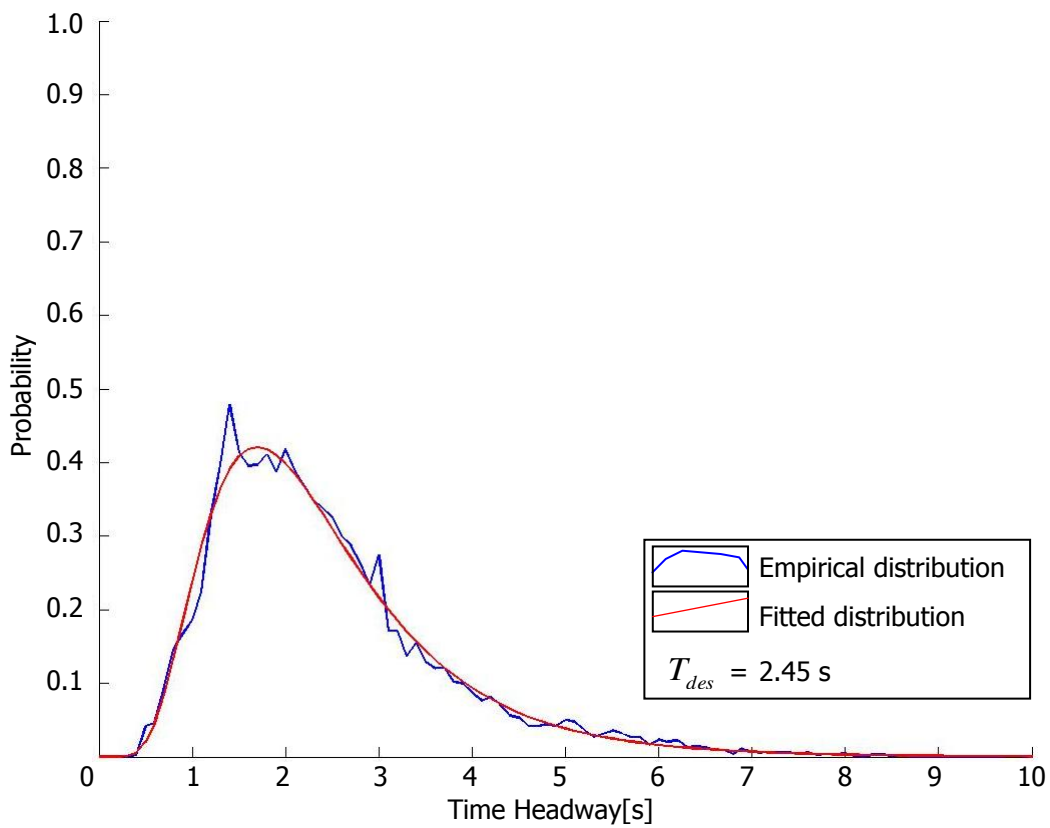


Figure 6.10: Fitted and empirical time headway distribution, configuration 2, heavy vehicles.

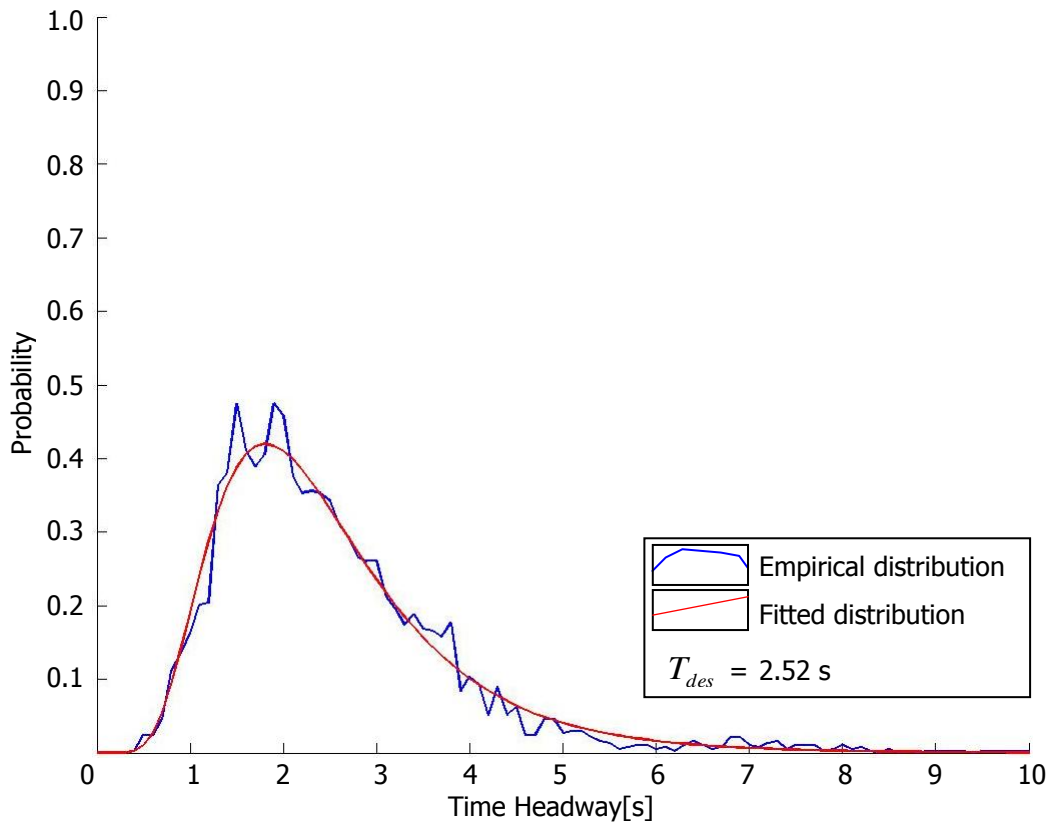


Figure 6.11: Fitted and empirical time headway distribution, configuration 4a, heavy vehicles.

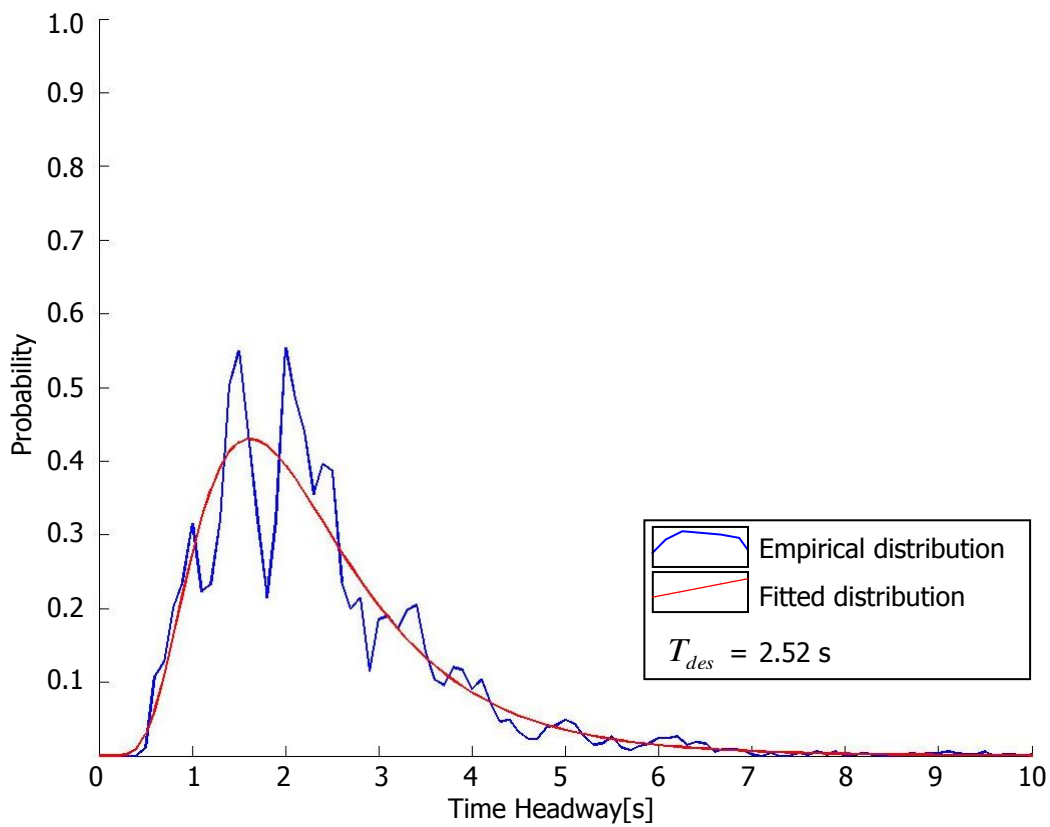


Figure 6.12: Fitted and empirical time headway distribution, configuration 4b, heavy vehicles.

6.1.3 Speed-following distance

In this section, speeds and corresponding following distances for all vehicles are analysed. Speed differences at corresponding following distances and speeds, influence the capacity, because with the following distance, the traffic state can be explicitly described:

- Mean following distance (front vehicle to front leading vehicle) = density⁻¹.

Hypotheses for relation speed – following distance

- By increasing following distances, speeds increase as well;
- When work zones are applied, speeds are lower at corresponding following distances.

In figure 6.13 to figure 6.21, for each configuration and vehicle types, following distances are plotted against corresponding median speeds and the amount of observations. For speeds, also the 5 and 95 percentiles have been plotted.

It is ensured that no measurement errors were incorporated for 5 and 95 percentiles, because by increased time steps (which should flatter measurement errors), deviations of percentiles towards median values did not significantly decrease.

Results of median speeds at different following distances are presented in table 6.2.

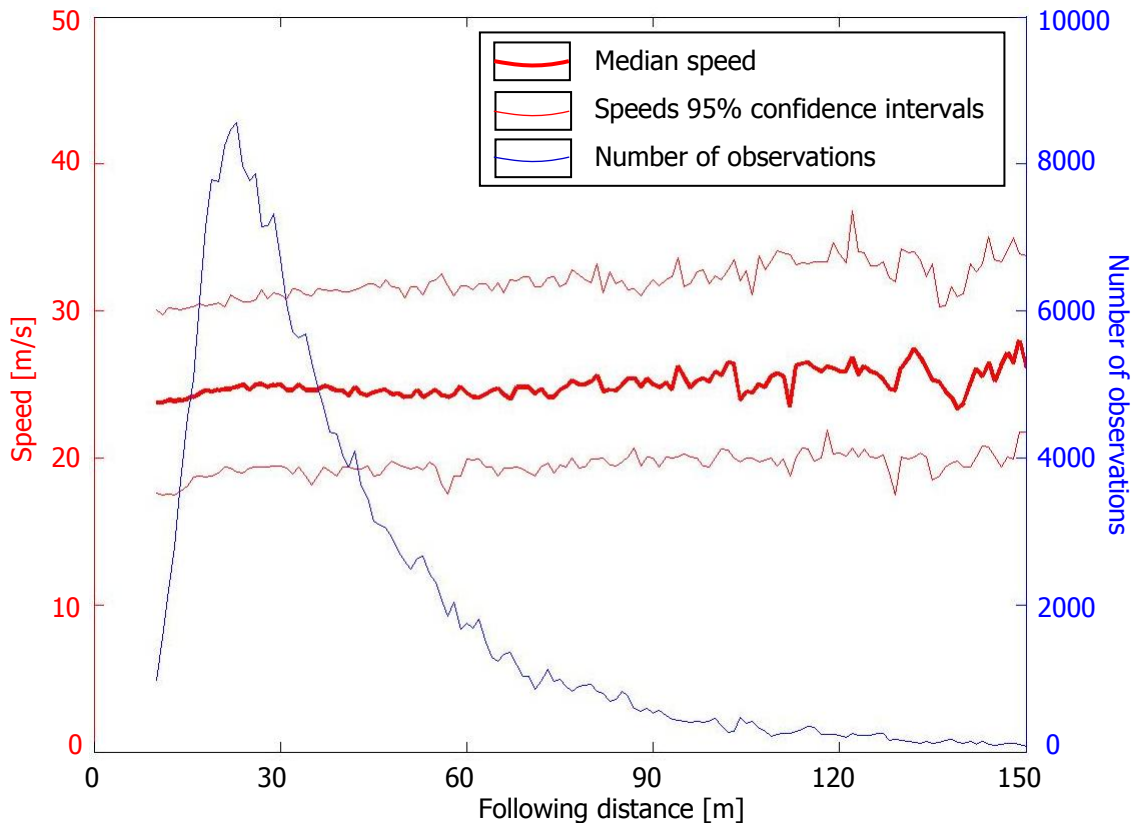


Figure 6.13: Relation Speed - Following distance for configuration 2.

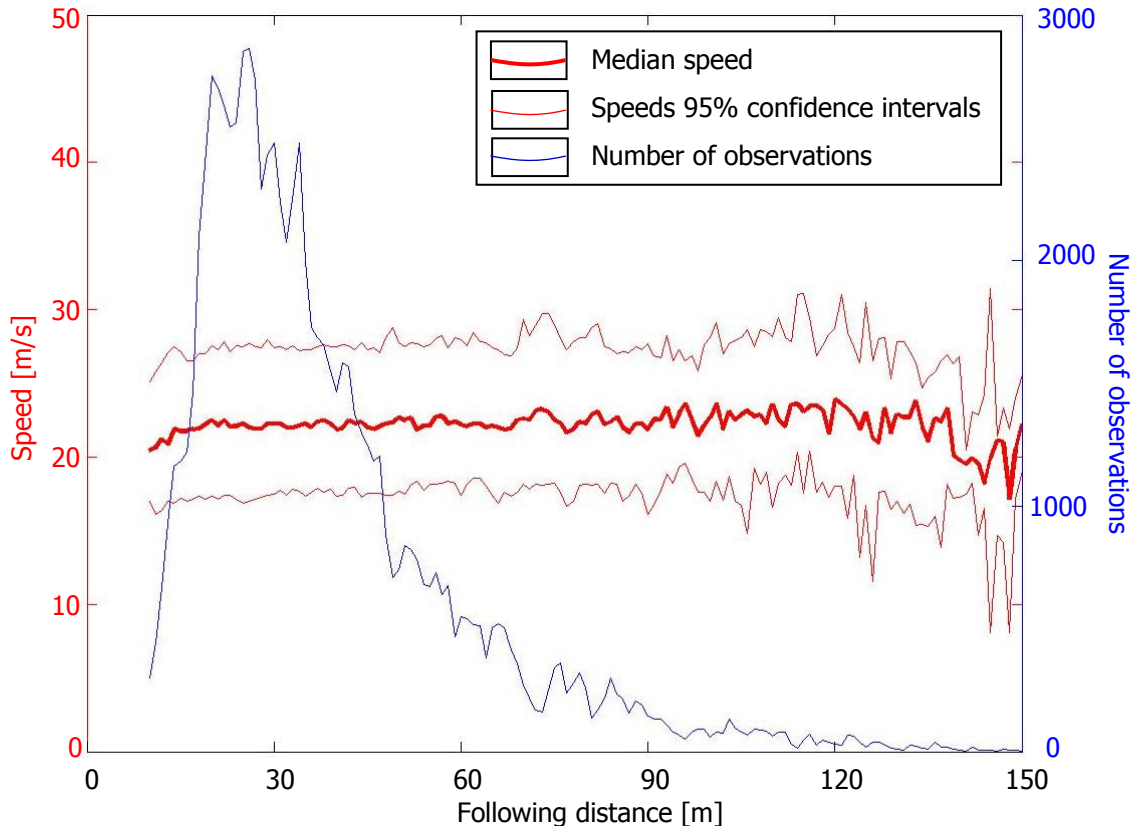


Figure 6.14: Relation Speed - Following distance for configuration 4a.

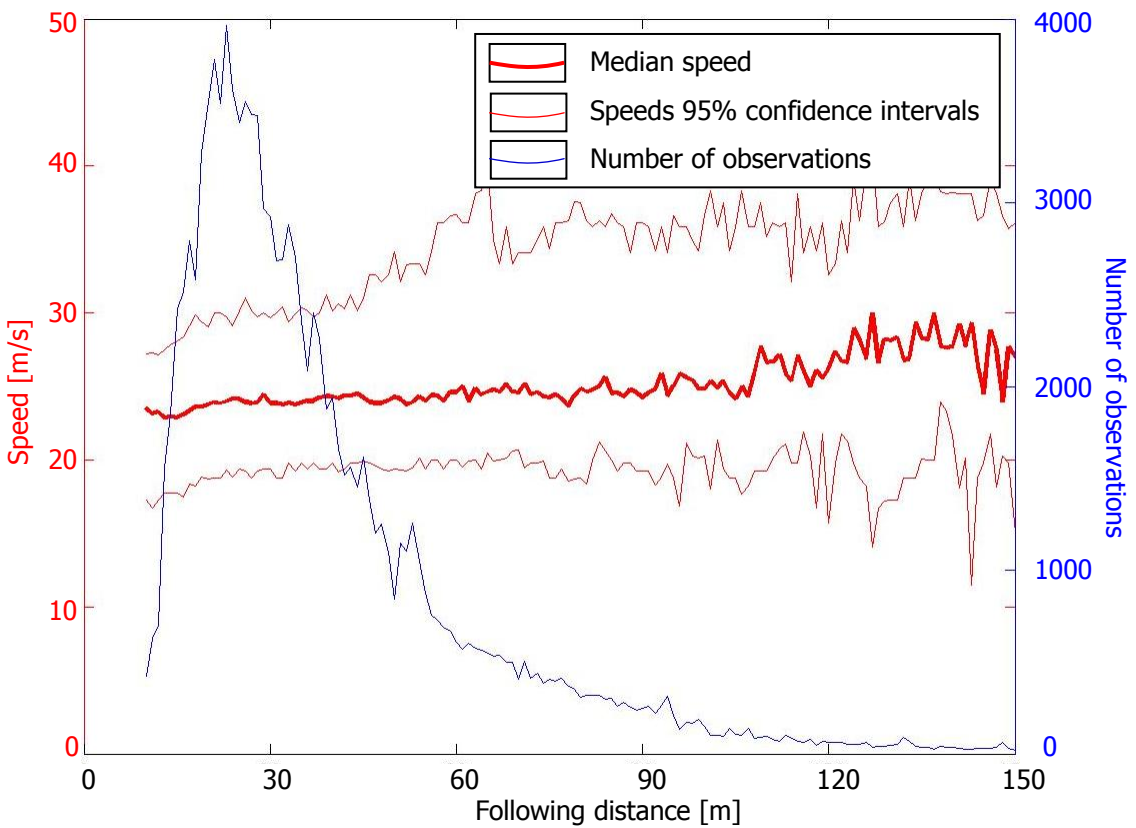


Figure 6.15: Relation Speed - Following distance for configuration 4b.

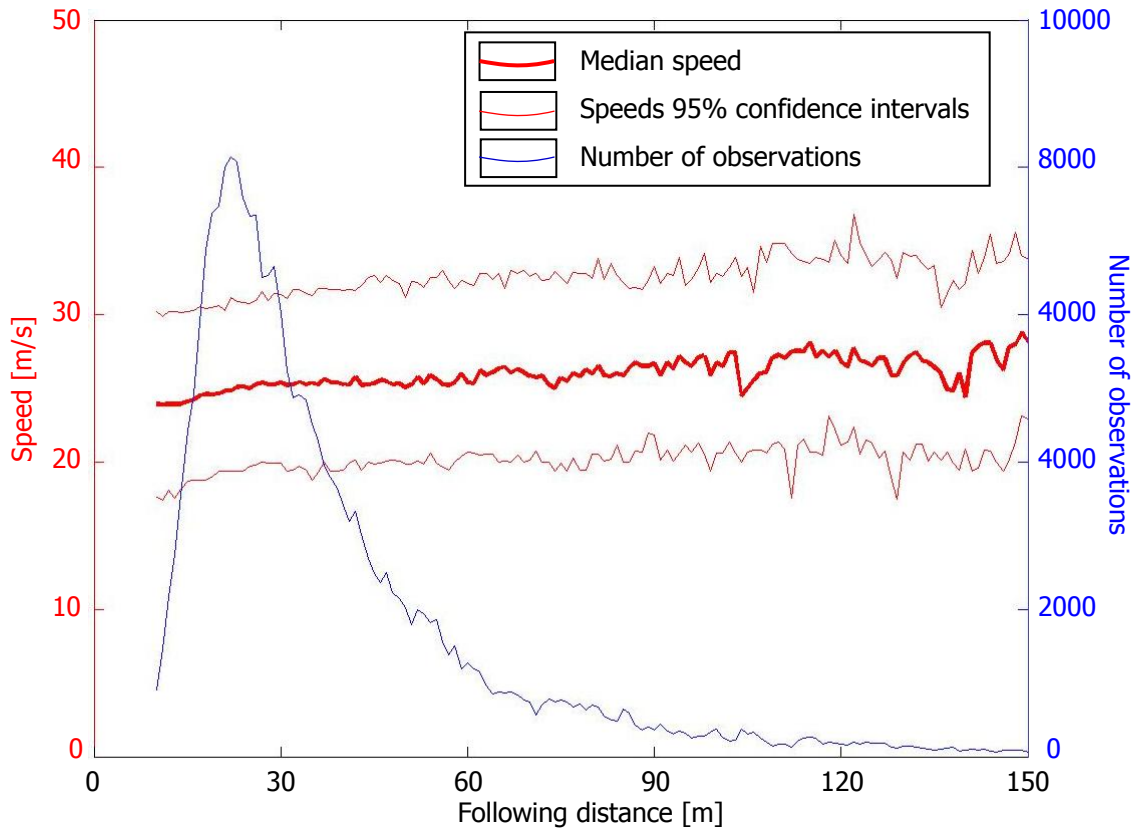


Figure 6.16: Relation Speed - Following distance for configuration 2 and passenger cars.

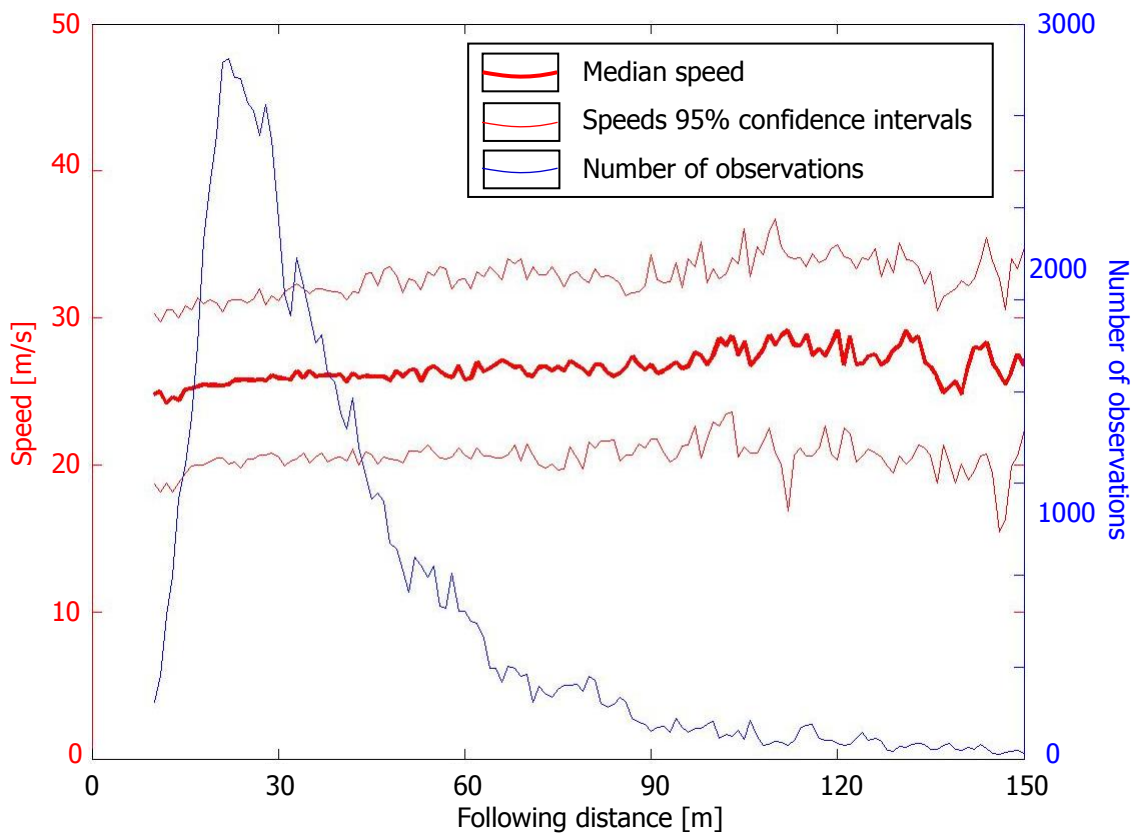


Figure 6.17: Relation Speed - Following distance for configuration 4a and passenger cars.

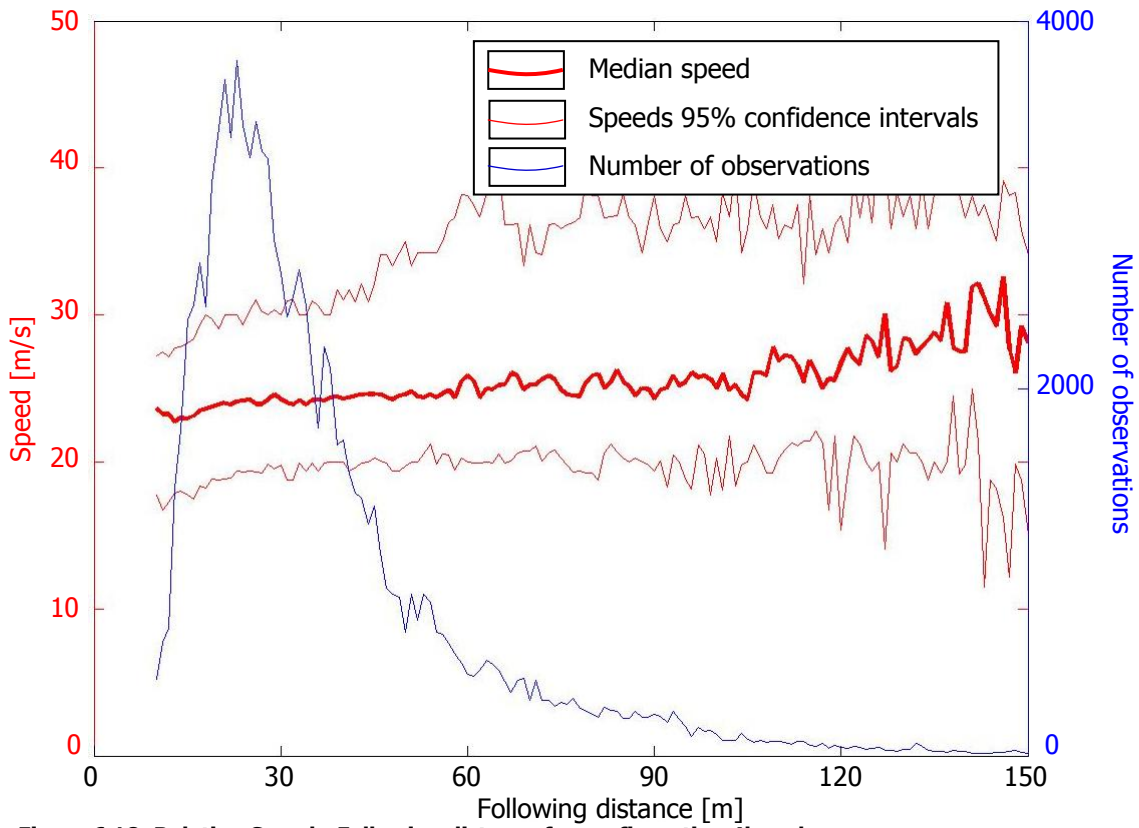


Figure 6.18: Relation Speed - Following distance for configuration 4b and passenger cars.

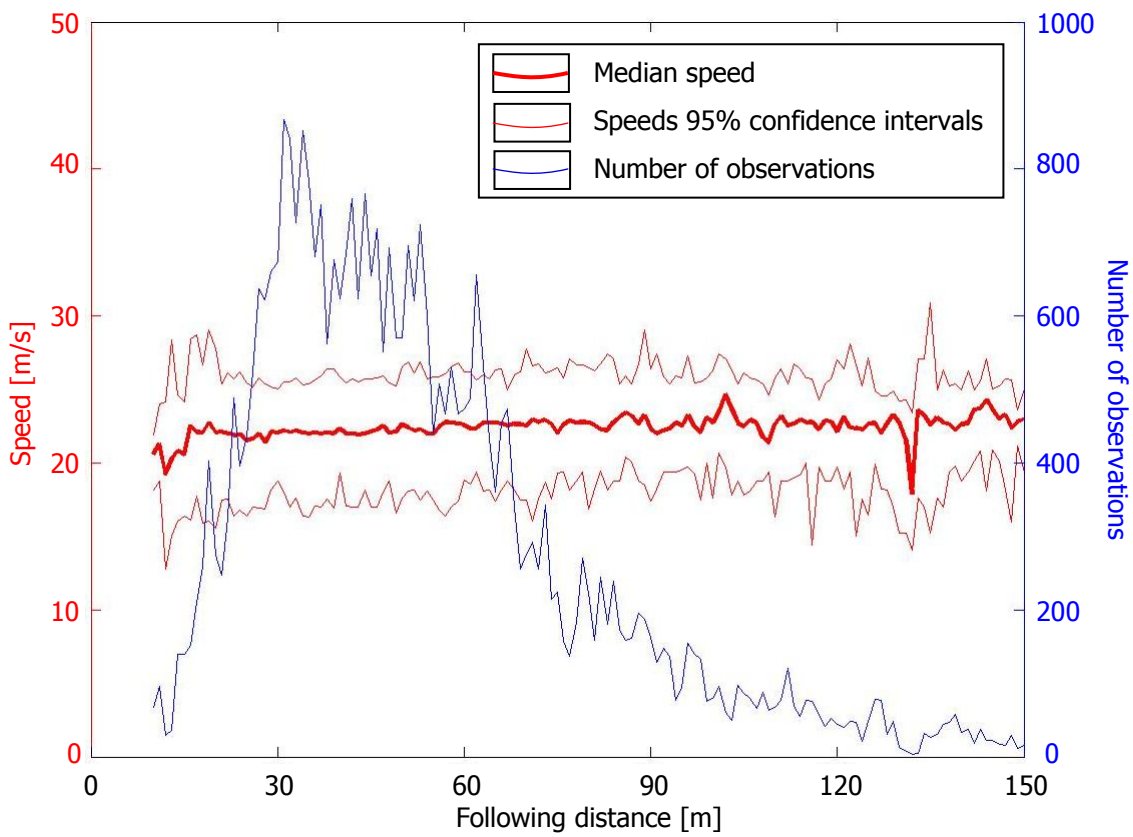


Figure 6.19: Relation Speed - Following distance for configuration 2 and heavy vehicles.

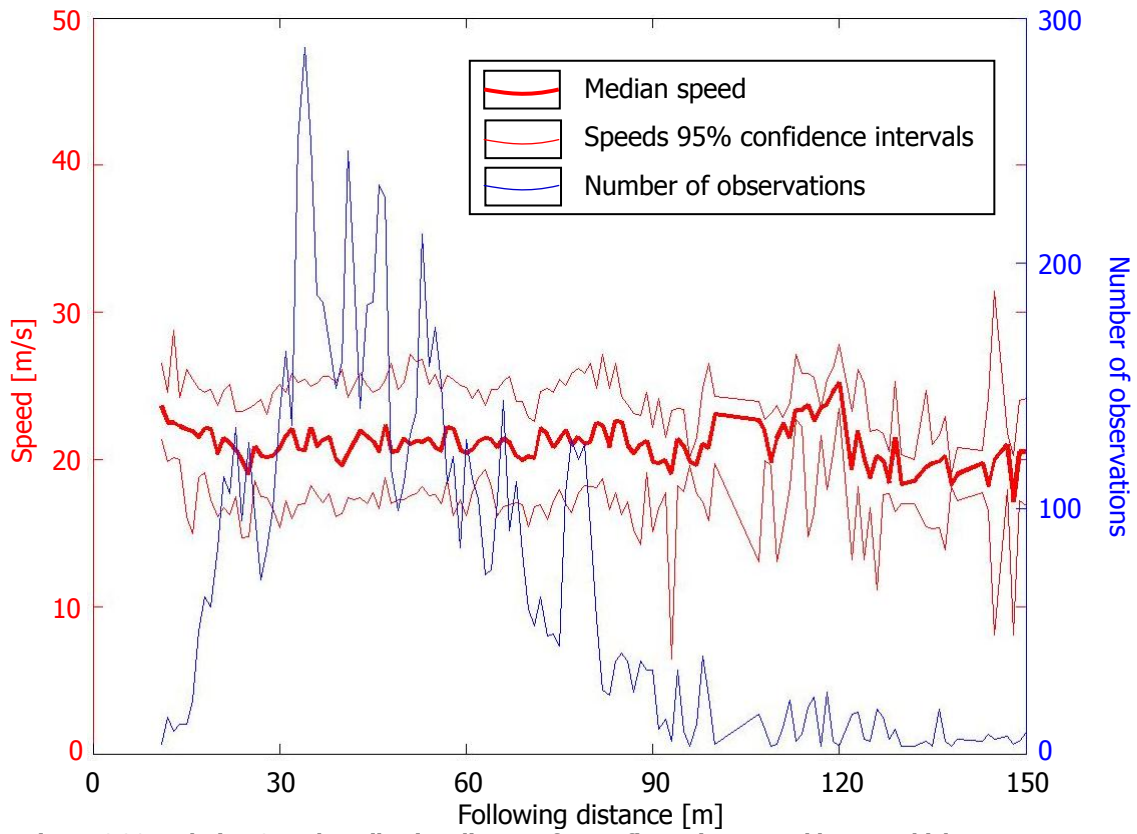


Figure 6.20: Relation Speed - Following distance for configuration 4a and heavy vehicles.

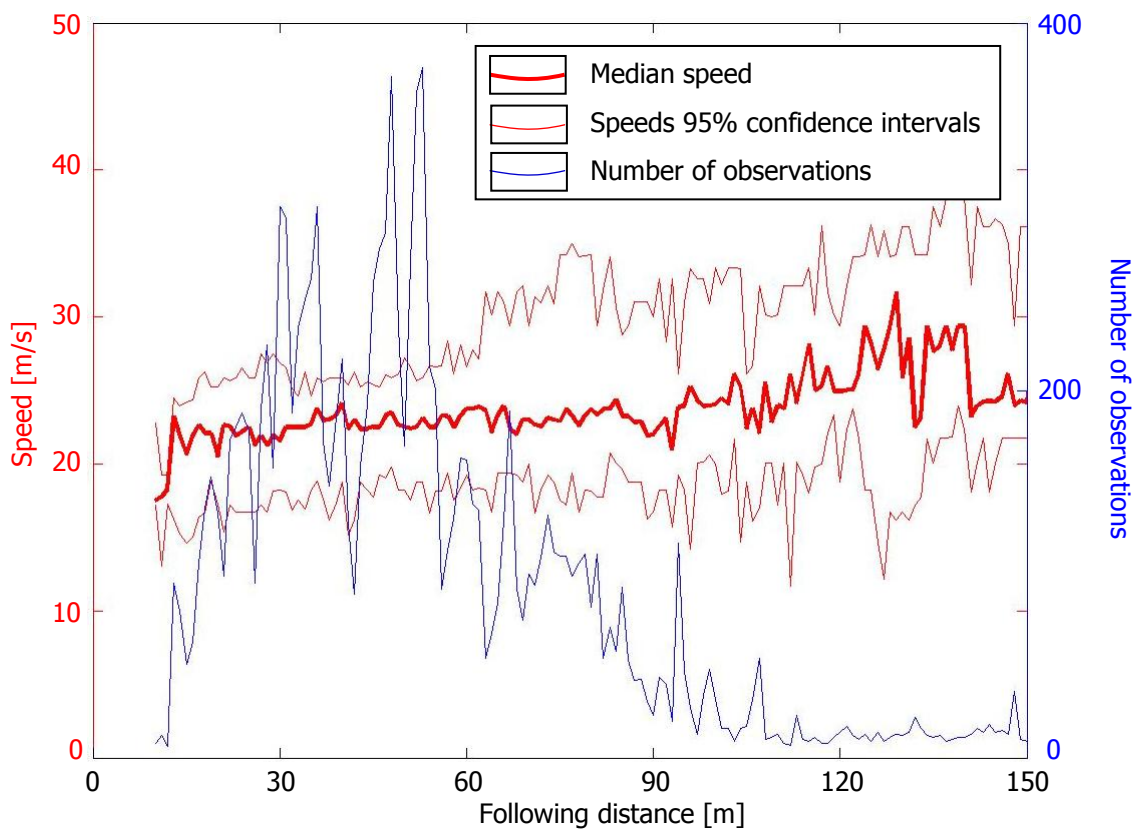


Figure 6.21: Relation Speed - Following distance for configuration 4b and heavy vehicles.

Configuration	Following distance (m)		
	30	60	90
2	24.9	24.9	25.1
4a	22.1	22.1	22.4
4b	24.1	24.3	24.6
2: Passenger cars	25.1	25.6	26.1
4a: Passenger cars	22.1	22.4	22.4
4b: Passenger cars	23.9	24.6	24.6
2: Heavy vehicles	21.9	22.4	22.4
4a: Heavy vehicles	20.7	20.9	20.9
4b: Heavy vehicles	21.9	23.0	23.0

Table 6.2: Speeds at specific following distances at each configuration for each vehicle type.

The results in table 6.2 meet the hypotheses. They show that for both vehicle types, speeds increase when following distances increase and speeds are lower at corresponding following distances if a work zone is applied. Between the two applied work zone configurations, speed differences are also consistent (except for heavy vehicles): At configuration 4a, where a small reverse curve is applied, speeds are lower than at configuration 4b.

From the graphs, it can be concluded that the observed headways are relatively small compared to the observed speeds, because a median speed of approximately 23 m/s is observed at a following distance of 20 m, yielding time headways of about 0.85 second (see figure 6.13). This is possible, because no low speeds have been observed. The relatively small amount of observations that incorporate small headways, correspond logically to high speeds as well.

Relative speeds against following distance

By investigating relative speeds, the extent of reactions at corresponding following distances have been investigated, and results are plotted in figure 6.22 to figure 6.24.

Hypotheses for relative speeds (based on Hoogendoorn (2012)):

- Median values of reactions are around 0 m/s for all following distances;
- Reactions are larger when a work zone is applied at corresponding following distances.

The figures show that the first hypothesis is valid, the median value in ranges with many observations is approximately 0 m/s. The second hypothesis is not valid. Configurations with applied work zones show smaller relative speeds than the control condition. A possible reason is, that drivers in work zones apply relaxation to increase their following distance instead of braking, which leads overall to lower speed differences.

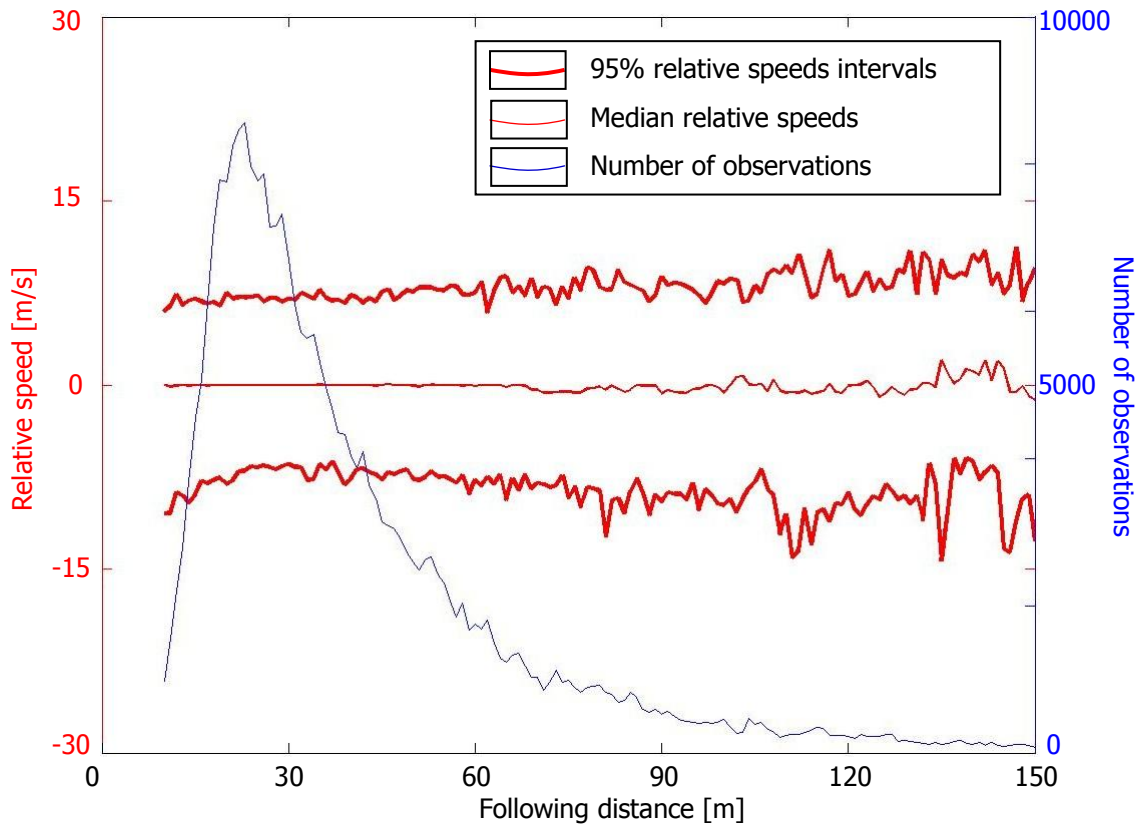


Figure 6.22: Relative speeds – following distance, configuration 2.

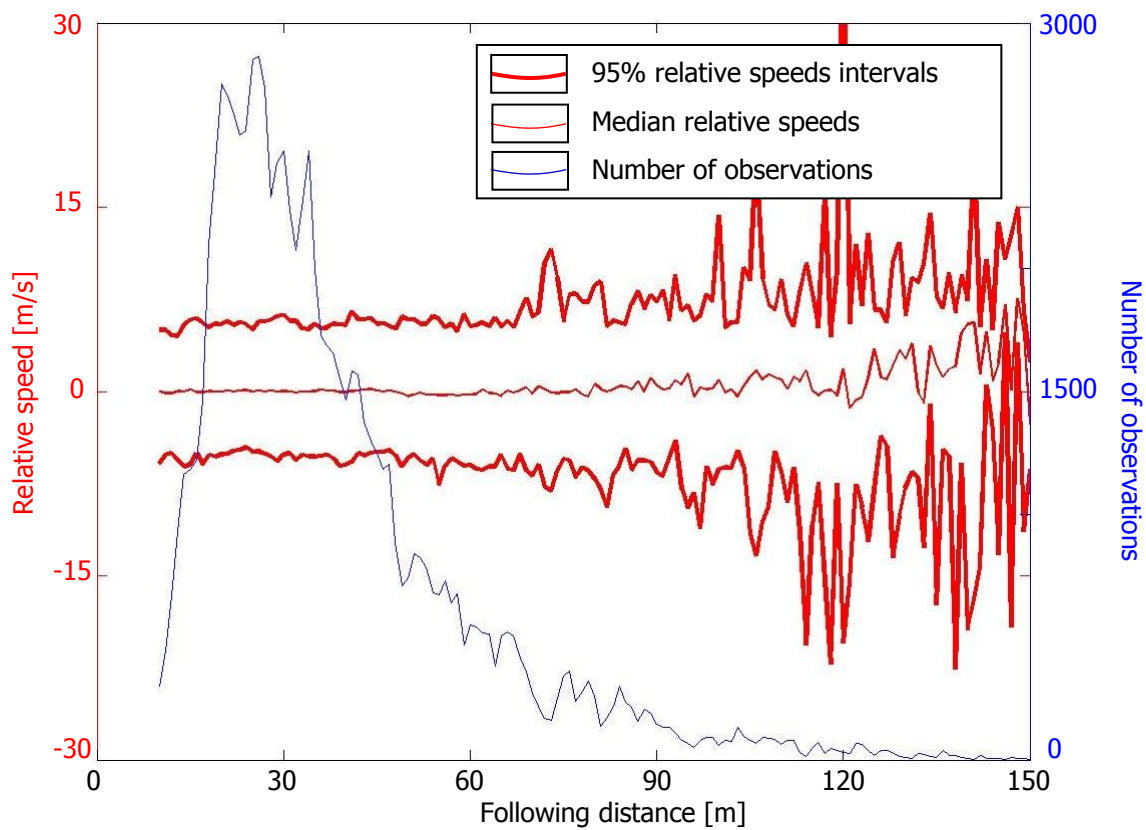


Figure 6.23: Relative speeds – following distance, configuration 4a.

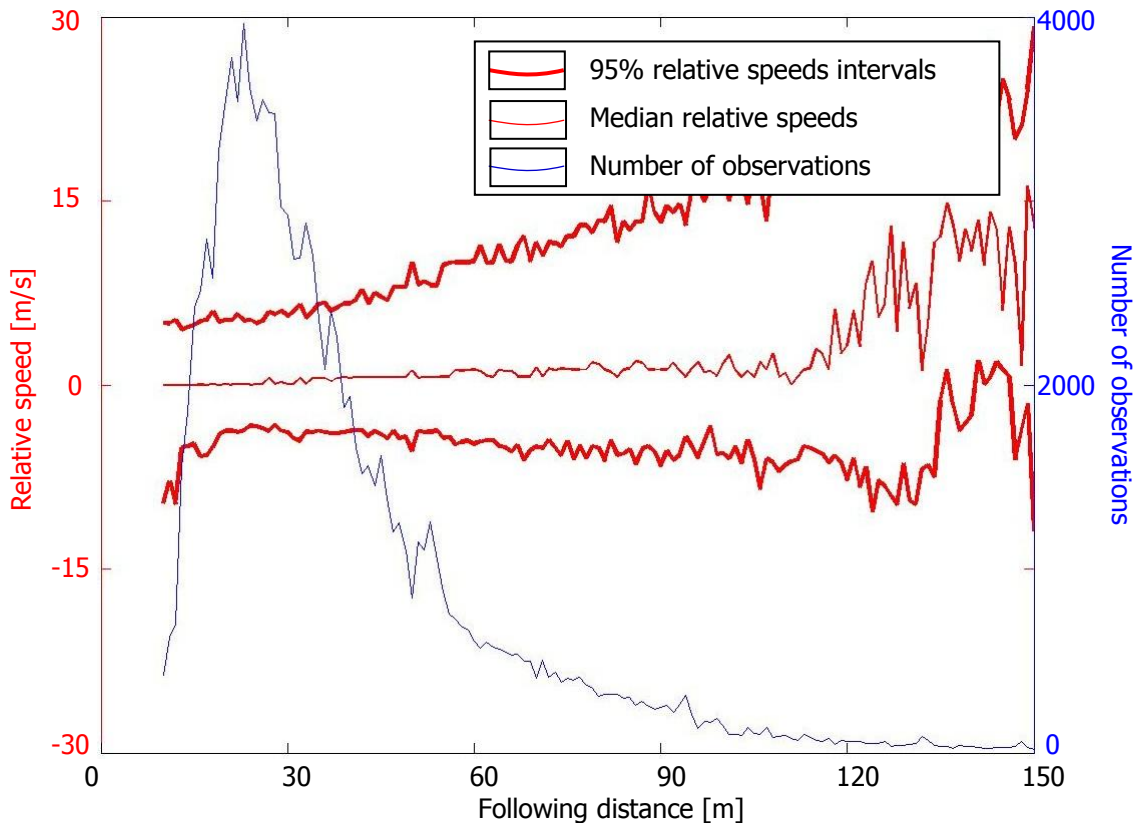


Figure 6.24: Relative speeds – following distance, configuration 4b.

6.1.4 Speed distributions at specific range of following distance

To analyse differences in speed changes between observed configurations and car-following heterogeneity, cumulative speed distributions have been drawn for a specific range of following distances. The selection of this range is based on the number of observations at corresponding following distances. Most observations are at a following distance of 25 - 30 m (see figure 6.13 to figure 6.21), so that range is selected.

Hypothesis for specific following distance speed distributions and heterogeneity

- Speeds are lower at corresponding following distances when work zones are applied;
- Heterogeneity between drivers reduces when work zones are applied.

By fitting a normal distribution through cumulative data, the variance (squared standard deviation) as a measure for heterogeneity and median speeds can be determined for comparing configurations. The cumulative distributions and fitted normal distributions are presented in figure 6.25 to figure 6.33, after which results are summarized in table 6.3.

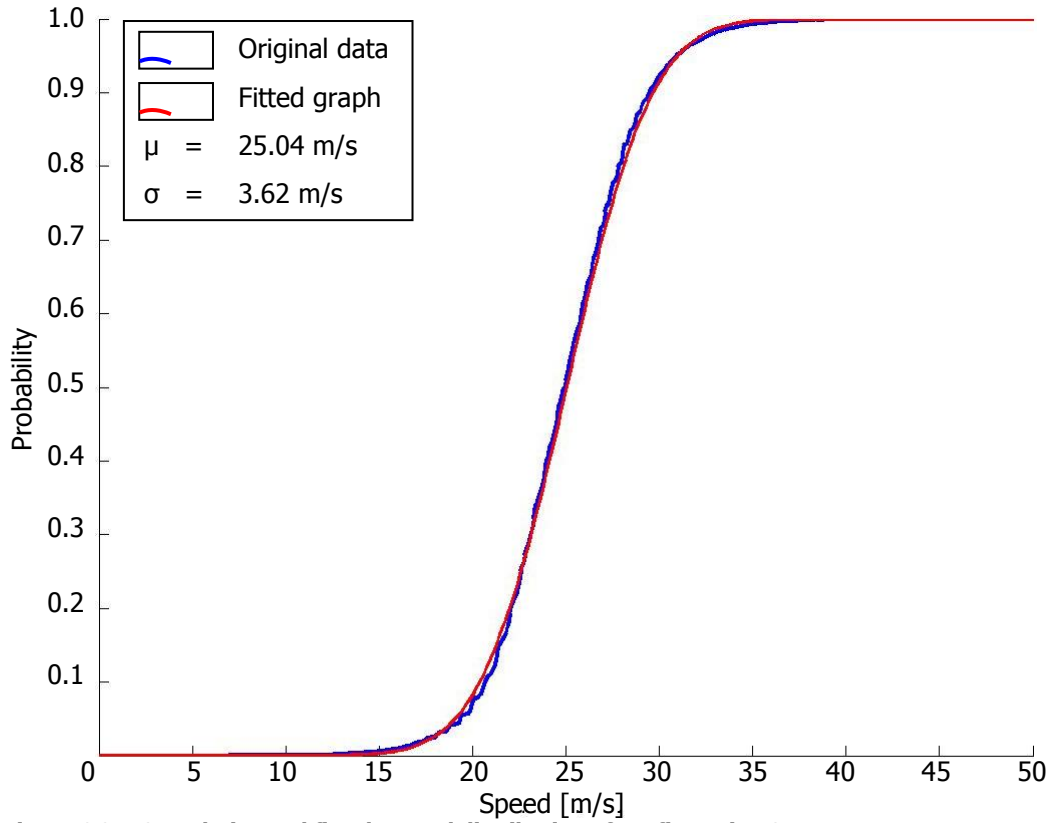


Figure 6.25: Cumulative and fitted normal distribution of configuration 2.

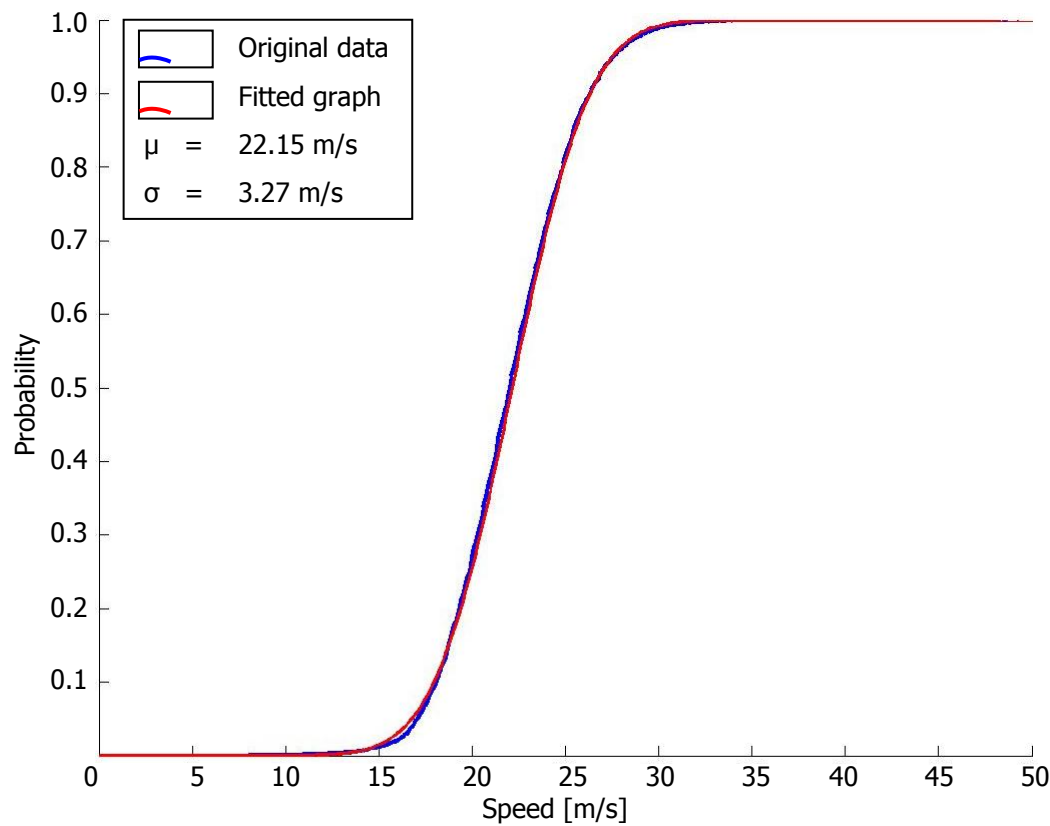


Figure 6.26: Cumulative and fitted normal distribution of configuration 4a.

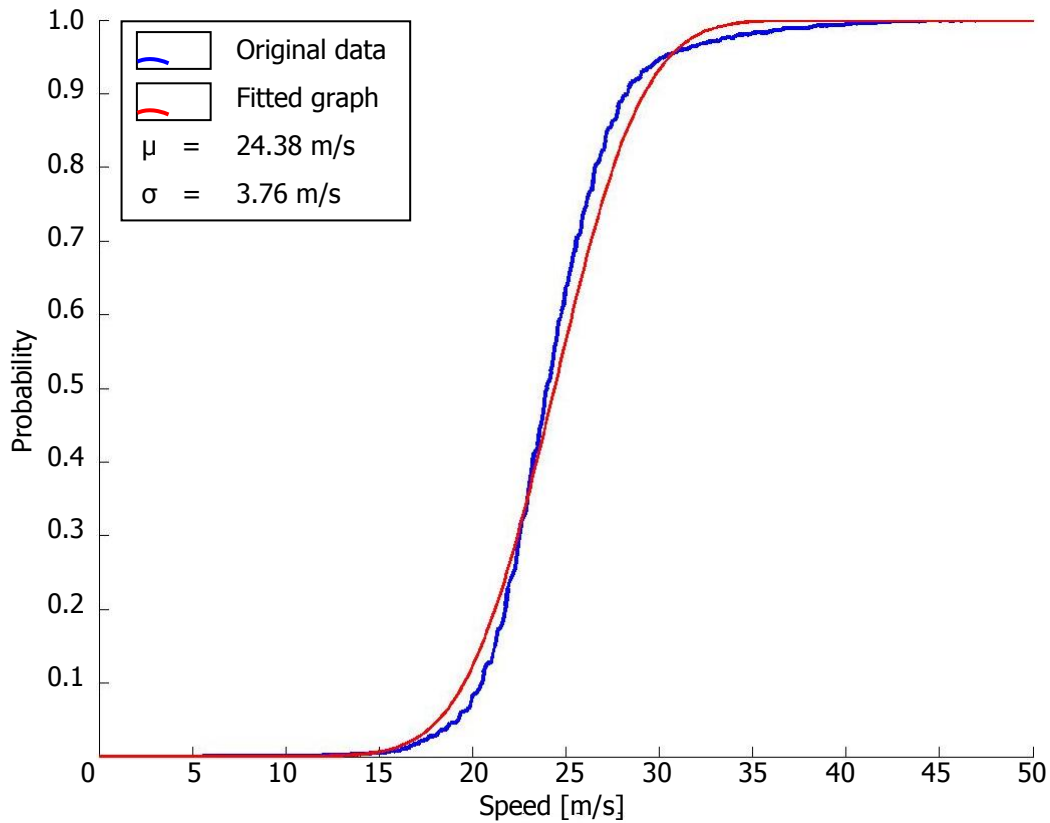


Figure 6.27: Cumulative and fitted normal distribution of configuration 4b.

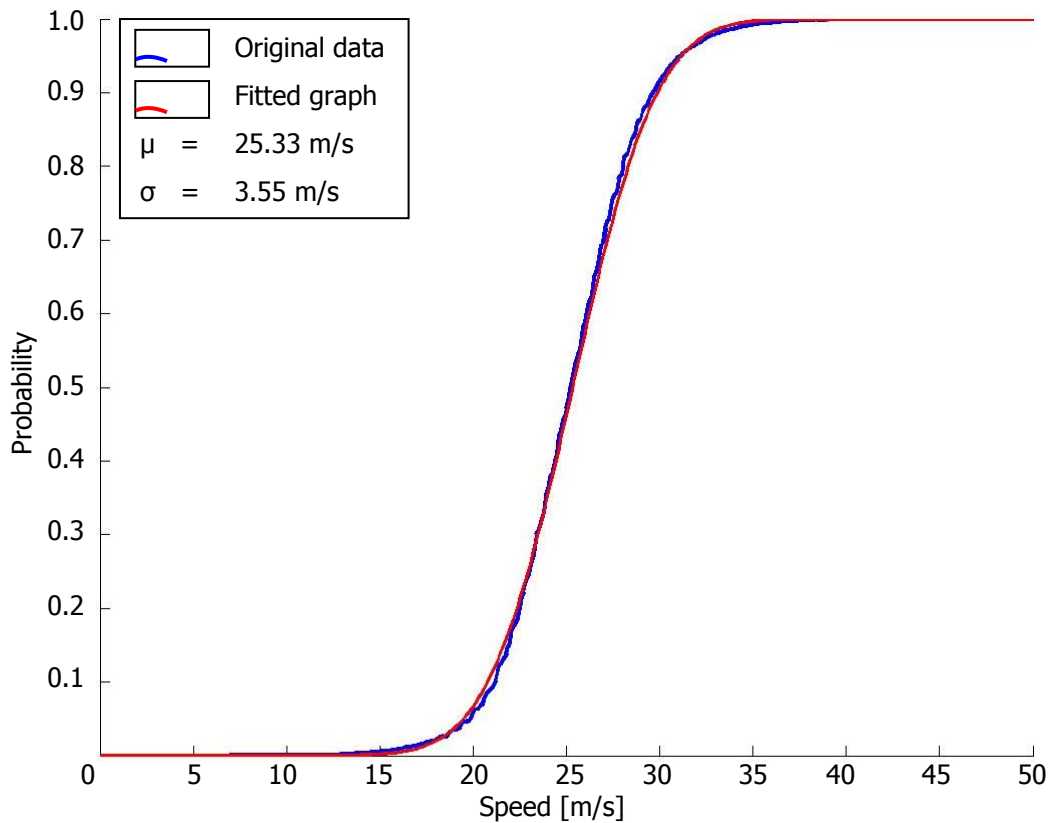


Figure 6.28: Cumulative and fitted normal distribution of passenger cars, configuration 2.

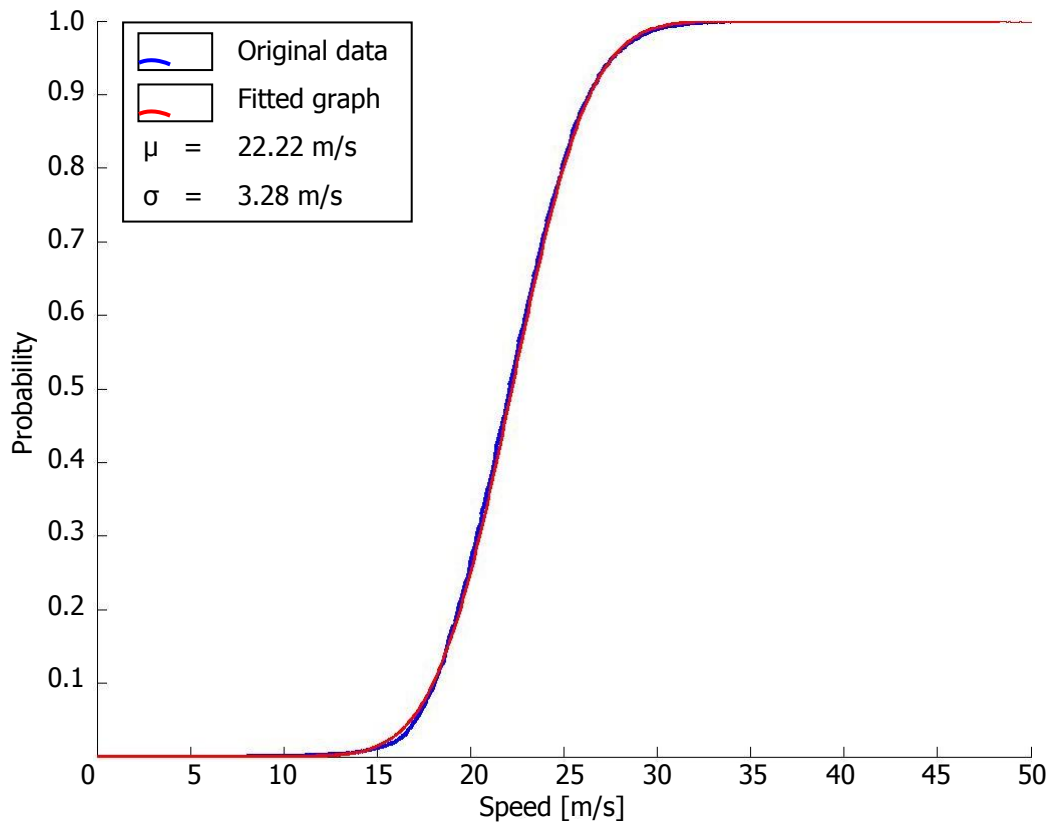


Figure 6.29: Cumulative and fitted normal distribution of passenger cars, configuration 4a.

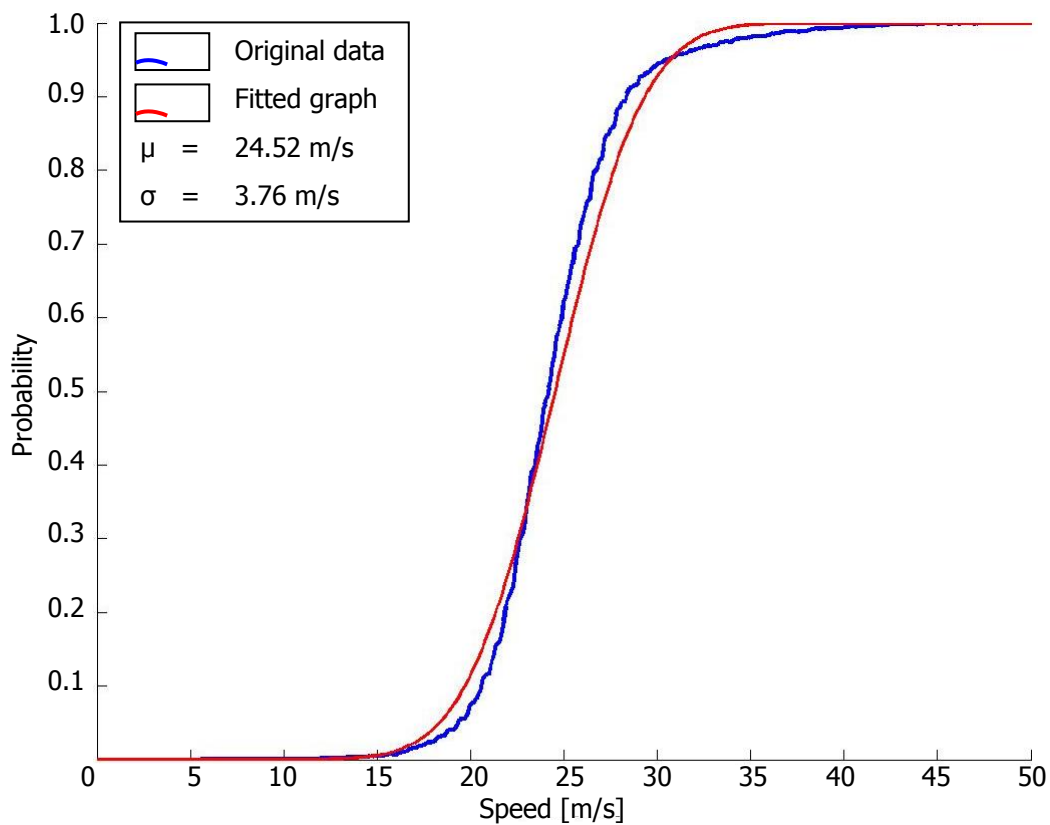


Figure 6.30: Cumulative and fitted normal distribution of passenger cars, configuration 4b.

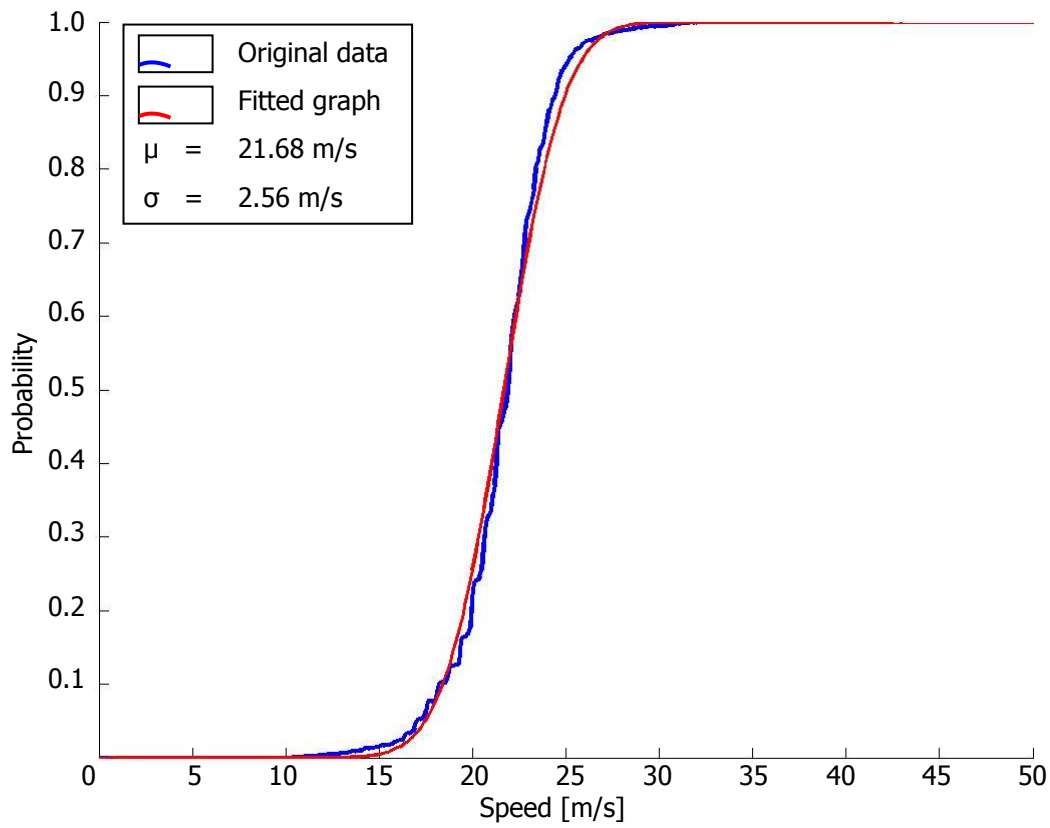


Figure 6.31: Cumulative and fitted normal distribution of heavy vehicles, configuration 2.

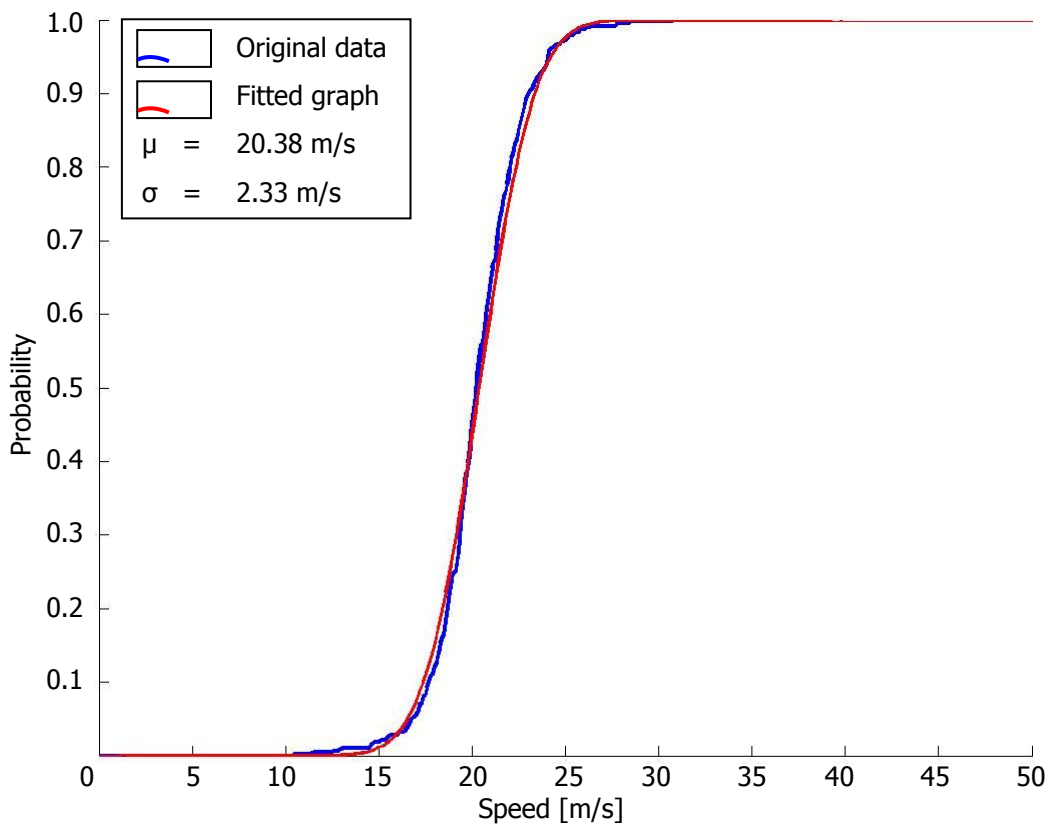


Figure 6.32: Cumulative and fitted normal distribution of heavy vehicles, configuration 4a.

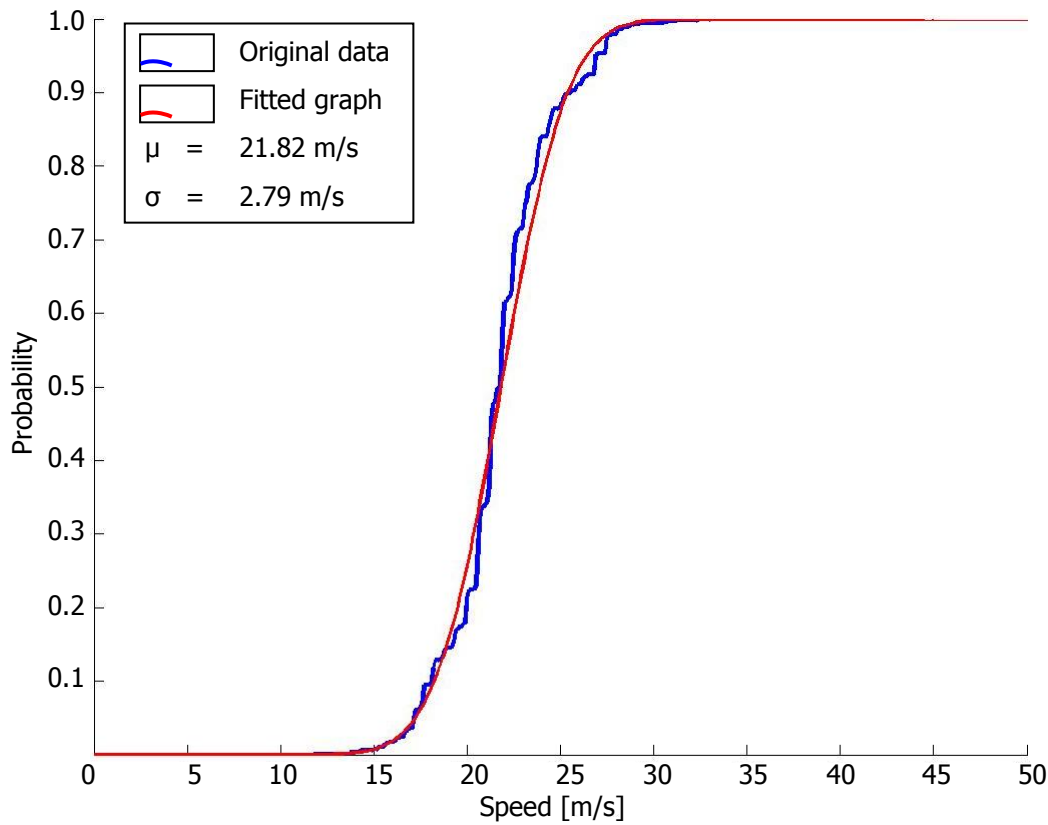


Figure 6.33: Cumulative and fitted normal distribution of heavy vehicles, configuration 4b.

Configuration	μ (m/s)	σ (m/s)
2	25.04	3.62
4a	22.15	3.27
4b	24.38	3.76
2: Passenger cars	25.33	3.55
4a: Passenger cars	22.22	3.28
4b: Passenger cars	24.52	3.76
2: Heavy vehicles	21.68	2.56
4a: Heavy vehicles	20.38	2.33
4b: Heavy vehicles	21.82	2.79

Table 6.3: Results of fitted normal distributions (mean value and standard deviation).

Comparing the control situation (configuration 2) with the work zone situation (configuration 4a and 4b), speeds are in general lower at same following distances with an applied work zone (1-3 m/s), which imply lower desired speeds of individual drivers, which meets the hypothesis.

Comparing speed distributions of the two different work zone configurations, configuration 4a consistently showed lower speeds (about 2 m/s) than configuration 4b. This indicates that presence of a small reverse curve has a large in impact on the driving speeds.

Significance of speed differences

To check if speed differences between configurations and vehicle types are significant, speeds between vehicles and within single vehicles have to be compared. This has been done using a 'Mixed

Model', which deals with a different number of vehicles per configuration and can deal with a different number of observations per single vehicle. In this case, a nested anova is used (McDonald (2006)), which is implemented in a Matlab program. Fortunately for all tests, the differences were significant ($P \leq 0.05$).

Heterogeneity

The results for heterogeneity between configurations, do not meet the hypothesis. No large differences have been observed between configurations: A small decrease in variance has been observed between configuration 2 and 4a and a small increase between 2 and 4b. The decrease in speed yields generally speaking for each driver, causing overall no difference in car heterogeneity.

The largest differences in driver heterogeneity appeared between values of heavy vehicles and passenger cars, which is understandable, because the variety between heavy vehicle drivers is much less than between passenger car drivers (e.g. gender, age, trip purpose), and often is a speed limiter installed in the vehicle.

6.1.5 Lane occupancy distributions

In this section, densities at right and corresponding left lanes are plotted against each other for each time instance. By comparing lane densities for different road configurations, the influence of differences in road configurations for lane occupancy are analysed.

This research focusses on car-following driving behaviour. To legitimate that adaptation effects in lane changing behaviour are not incorporated, it is checked that lane occupancy distributions between configurations do not significantly differ.

Densities are calculated as the number of observed vehicles, divided by the length of observed road stretches. To prevent strange values at low densities, a minimal three vehicles had to be present (left and right lane together) for calculating densities. If three or more vehicles were observed, flows are calculated by multiplying density by the mean speed of present vehicles.

Lane occupancy distributions results

The fraction of flow on the right and left lane are plotted against the total density of the left and right lane (see figure 6.34 to figure 6.36). To present results, bubble plots and line graphs are used, in which the size of the marker in the bubble plots indicate the number of observations for that specific value. The larger marker size, the more observations were collected for that density combination. The line graphs plot median fractions of lanes at a specific densities. Beside of median fractions, also the 20 and 80 percentiles are plotted.

The graphs displaying lane distributions show consistent results: At low densities almost all flow is on the right lane, and the flow shifts to the left lane if total density increases.

Figure 6.37 shows the density at each lane for each configuration when the total density increases.

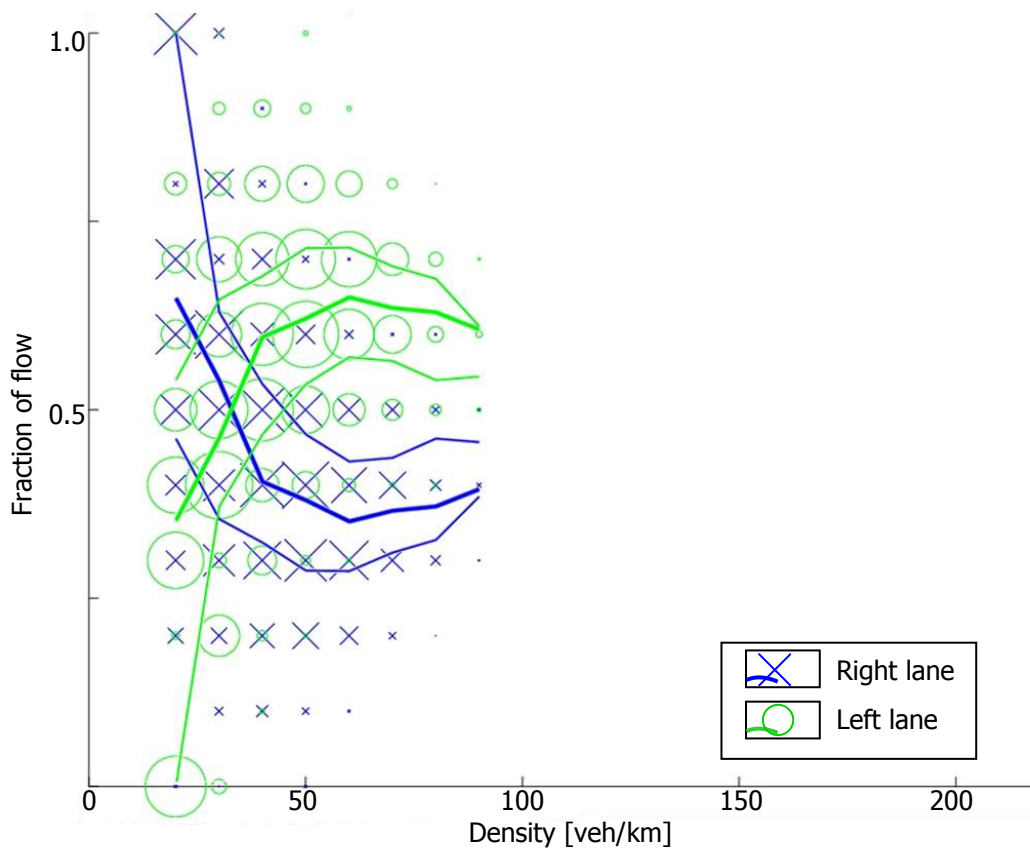


Figure 6.34: Lane density distribution, configuration 2.

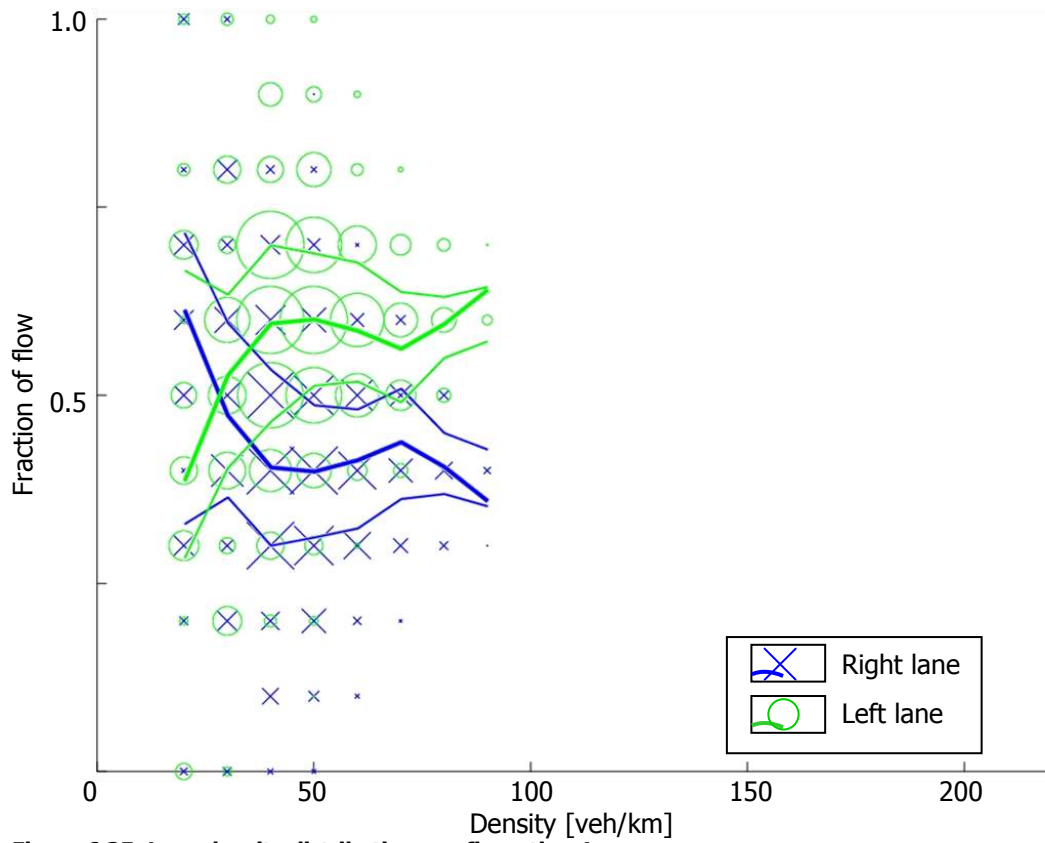


Figure 6.35: Lane density distribution, configuration 4a.

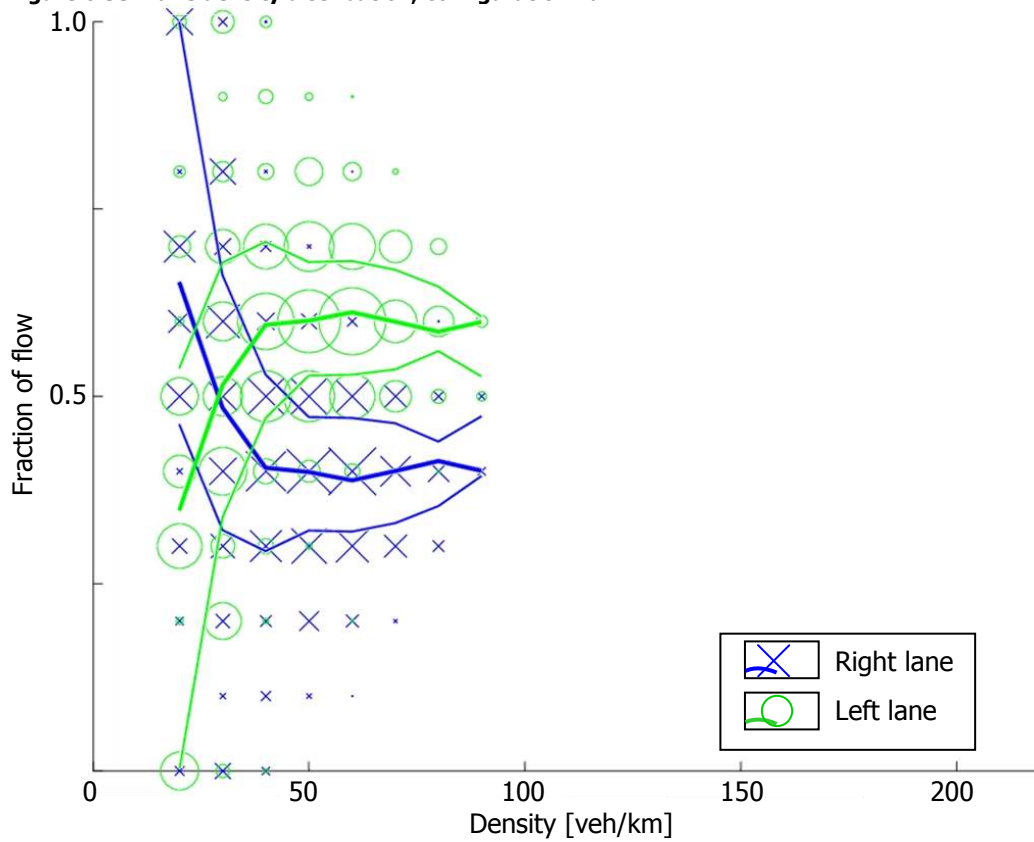


Figure 6.36: Lane density distribution, configuration 4b.

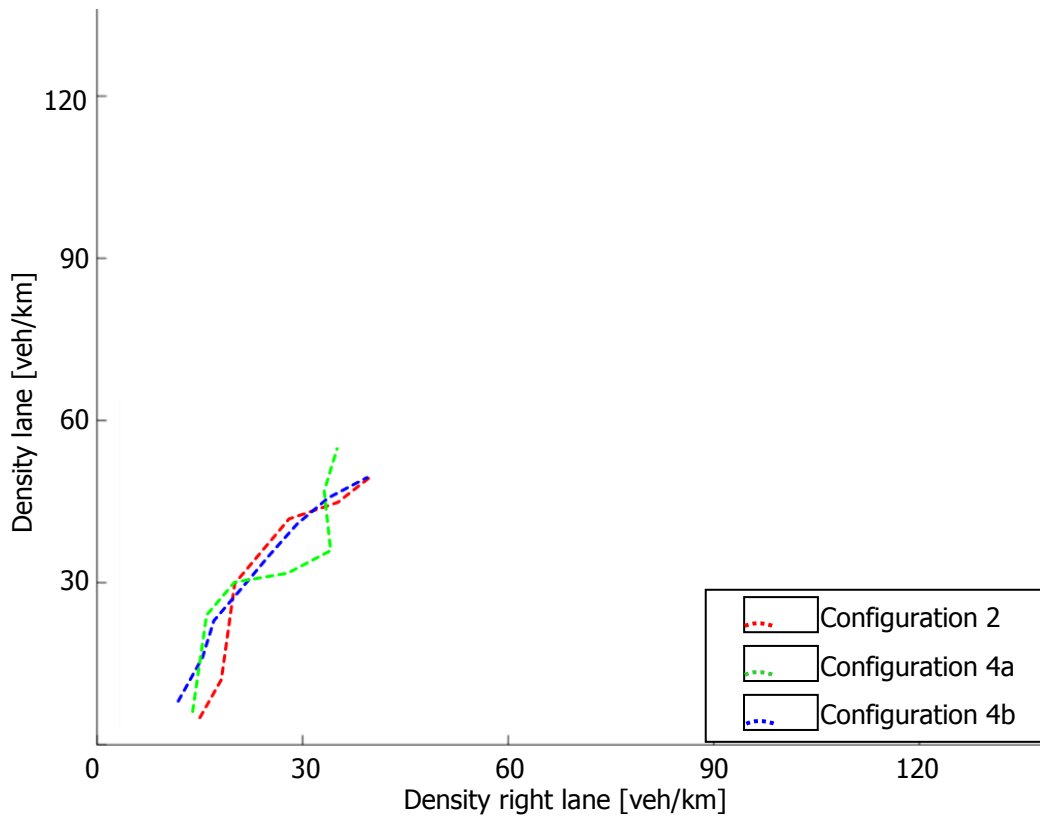


Figure 6.37: Right lane densities plotted against left lanes densities of all configurations.

No significant differences are observed between the control situation and when a work zone is applied. Because this equality between the configurations, it is legitimate to exclude changes in lane choice and lane changing behaviour.

6.1.6 Fundamental diagram of observations

Based on calculated flows of the previous section, plotted in figure 6.38 to figure 6.40, capacities of work zone configurations vary from 4000 to 7000 veh/h. When looking at reported capacities in literature (e.g. Zheng (2009)), these capacity values are about 1.5 times the expected value. A reason for this is that data used to estimate these capacity values are static counted vehicles instead of counted visible vehicles and observed road lengths.

More important, periods for which mean densities are calculated are relatively short compared to loop data averages used by induction loop data, because of vehicles' short retention periods in the observed system.

Therefore, results using a method that is based on the induction loop method, are presented in figure 6.41 to figure 6.43. These figures plot one data point for every stabilized period, if the duration was longer than 50 s. From these figures, it can be concluded that due to absence of congested traffic it is not possible to, based on collected data, directly determine capacity values and therefore the shape of the fundamental diagram.

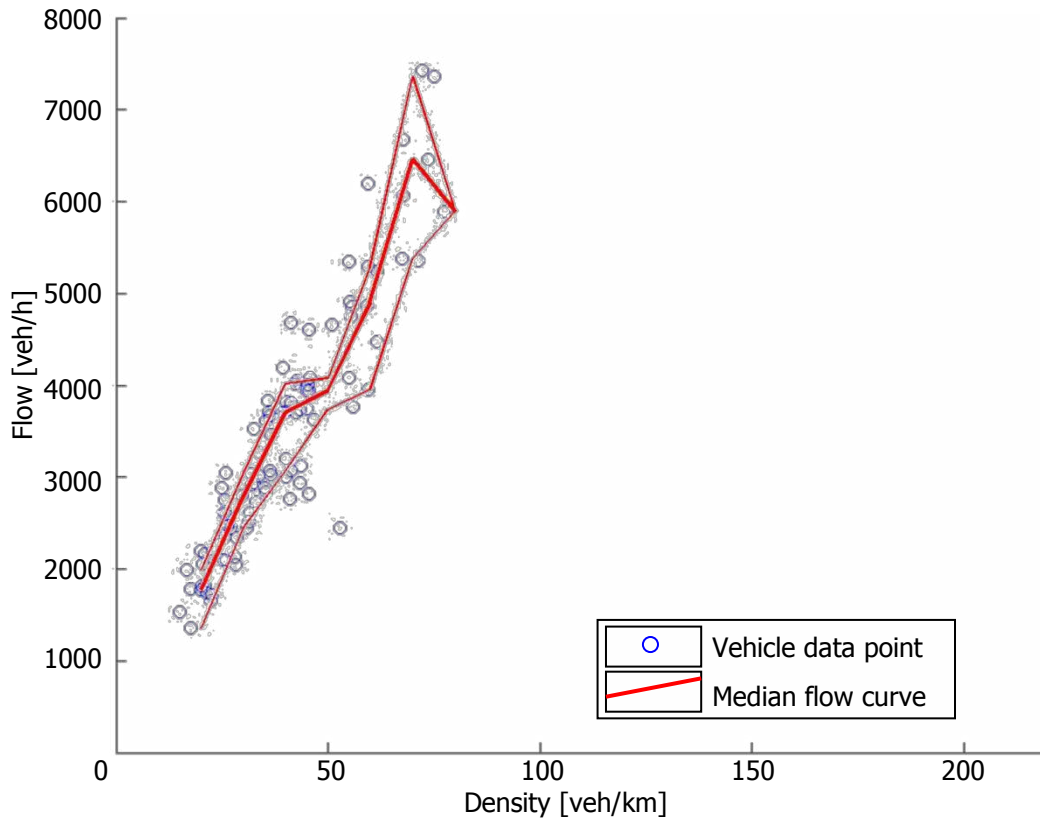


Figure 6.38: Flow-density relation with per vehicle 1 data point, configuration 2.

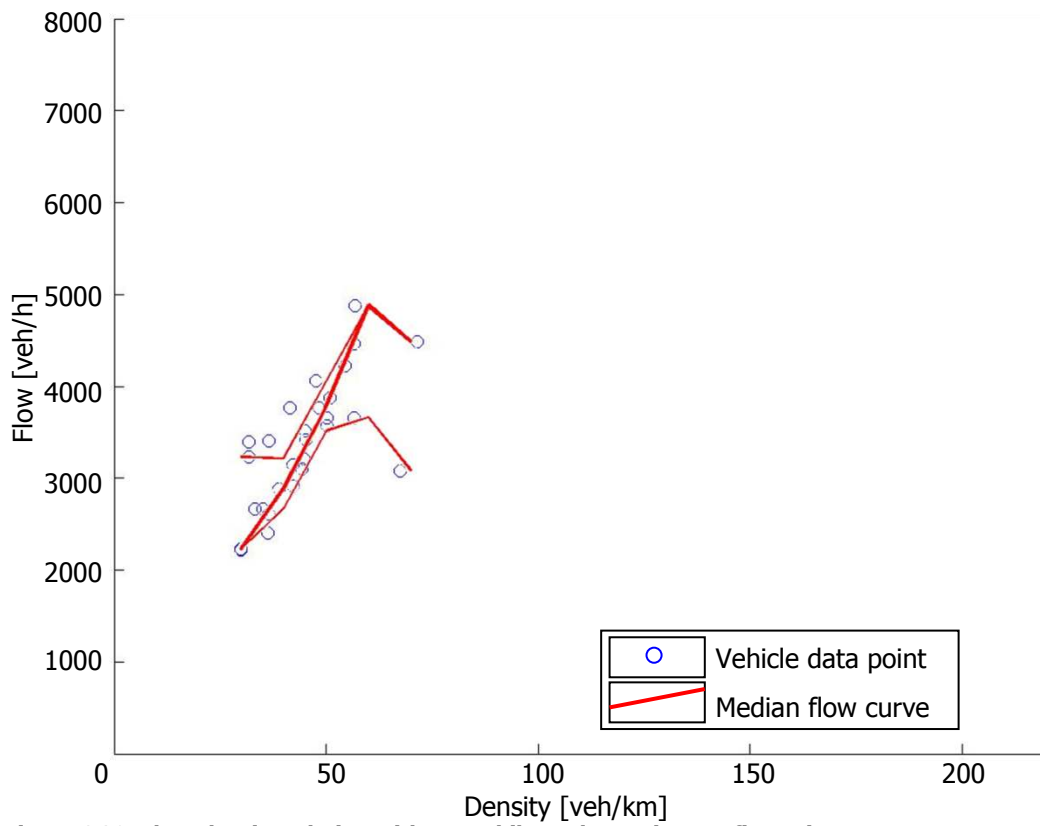


Figure 6.39: Flow-density relation with per vehicle 1 data point, configuration 4a.

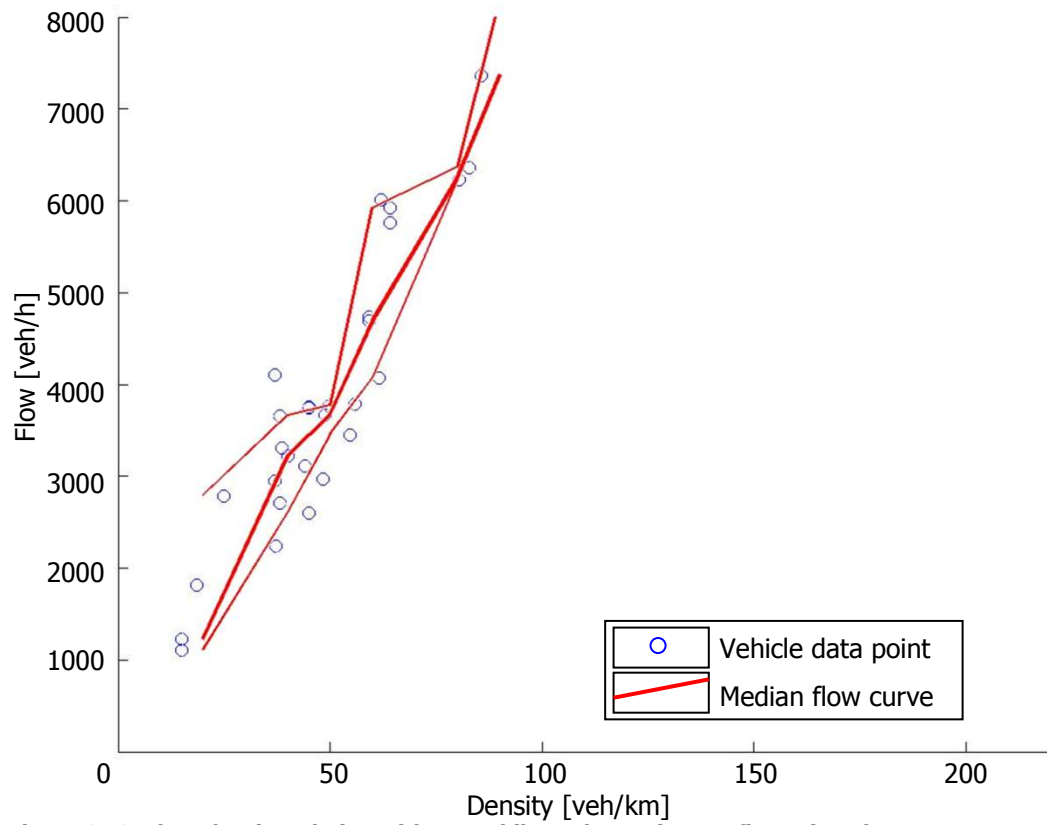


Figure 6.40: Flow-density relation with per vehicle 1 data point, configuration 4b.

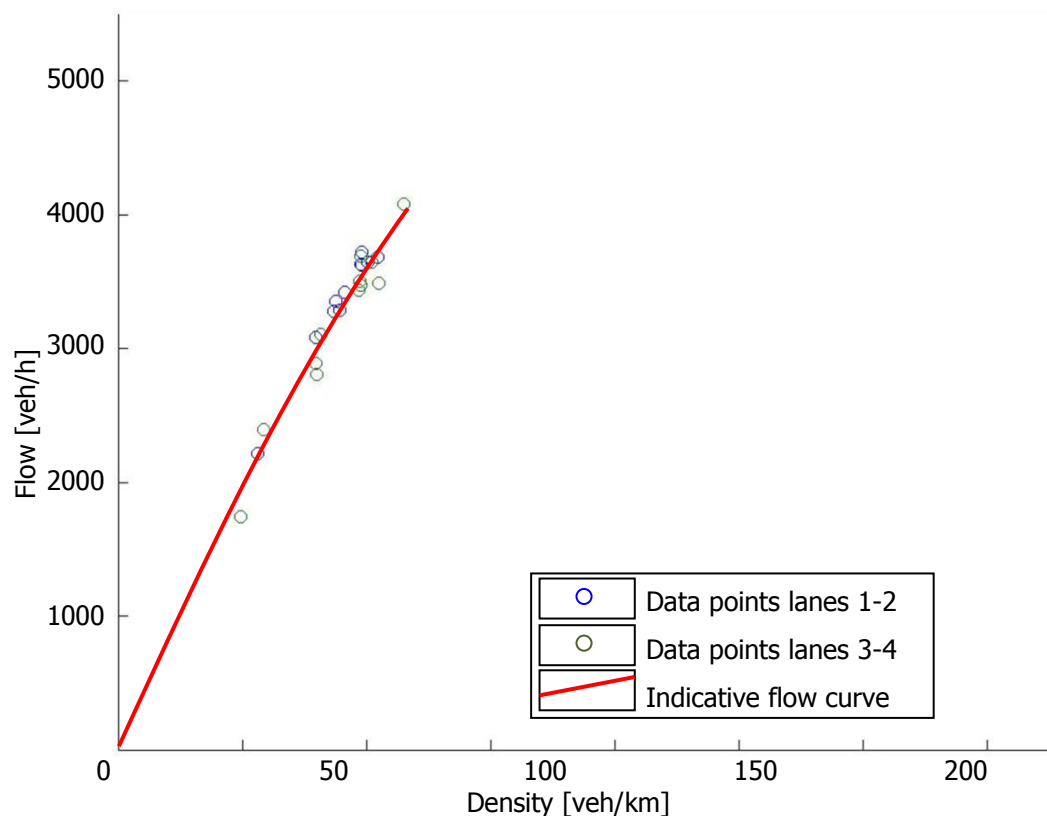


Figure 6.41: Flow density relation based on induction loop method, configuration 2.

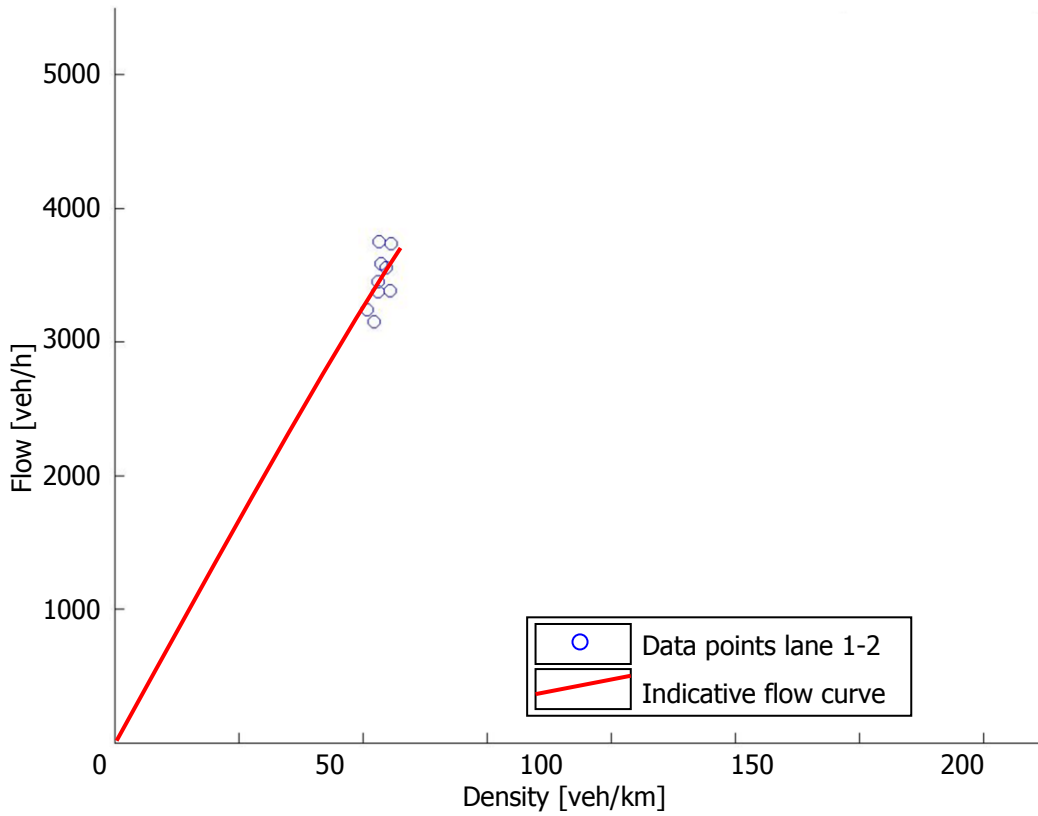


Figure 6.42: Flow density relation based on induction loop method, configuration 4a.

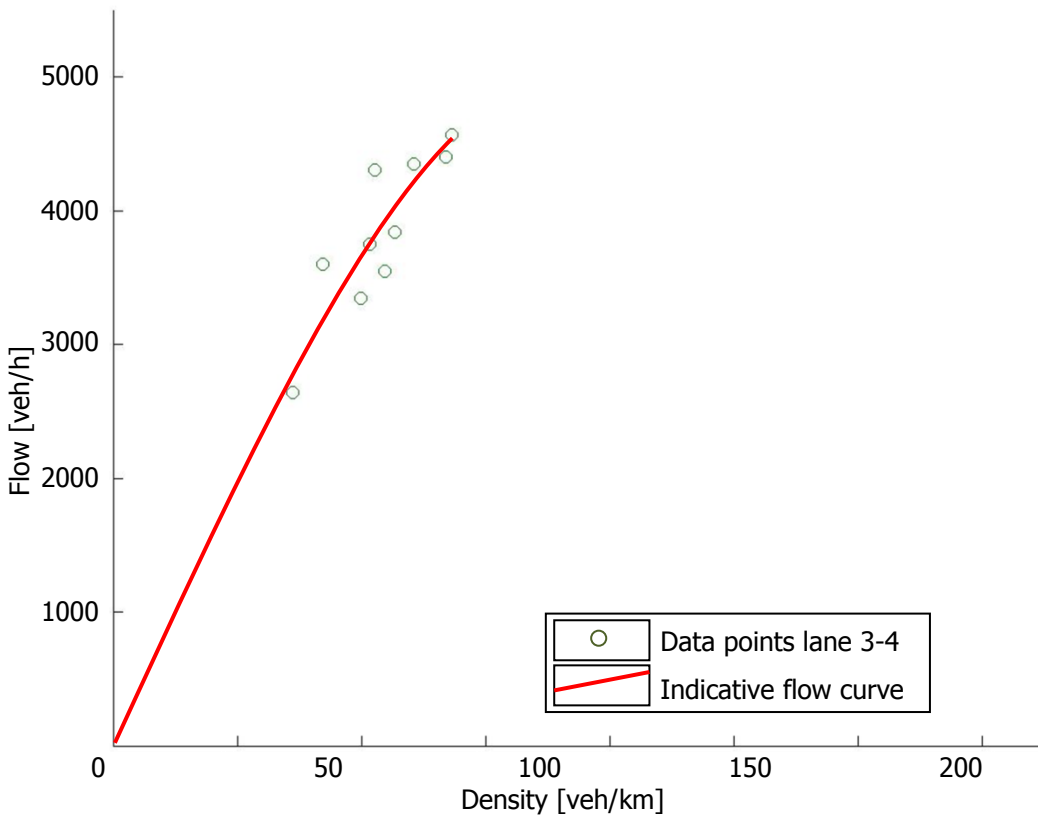


Figure 6.43: Flow density relation based on induction loop method, configuration 4b.

6.2 Simulating individual driving behaviour

It has been concluded that macroscopic effects of applied observed work zones cannot be determined directly out of the collected data, so these effects have to be investigated by simulations.

As mentioned before, this is possible by calibrating parameters of the simulation model using data of different configurations, which is described in section 6.2.1, after which the simulation process and simulation outcomes are described in 6.2.2.

6.2.1 Parameter estimation of car-following models

Integrally estimating model parameters

To analyse individual driving behaviour and changes in this behaviour between different configurations, parameter values of the Extended IDM are estimated. The estimation process searches for the best fit of estimated accelerations (using calibrated model parameters), and observed accelerations for the complete dataset of each configuration.

Unfortunately, all estimated parameters ended at predefined boundaries, which implies that it was not possible to estimate parameters of the Extended IDM, which is caused by the absence of observed congested traffic. Outside the congested traffic state, drivers do not react heavily on their leader, because they drive close to or at their desired speed.

Estimating single model parameters

In the ensuing, parameters of simulation model are estimated separately, in order to investigate macroscopic effects using simulations.

Based on empirical results (see section 6.1), parameters that have to be calibrated are selected. The absence of congested traffic makes it hard to estimate model parameters which are dealing with this part of driving. Therefore the 'Ceteris Paribus' approach (based on the values provided by Schakel) is applied for:

- T_r : Reaction time;
- n : Number of anticipated leaders;
- a_0 : Maximum acceleration;
- b_0 : Comfortable deceleration;

Which left the three to be estimated parameters:

- v_0 : Desired speed [m s^{-1}];
- s_0 : Minimal stopping distance [m];
- T_{des} : Desired time headway [s].

Estimating v_0 and s_0

To estimate v_0 and s_0 the relationship between speed and following distances have been used. By fitting a curve with a horizontal and a vertical asymptote the desired speed and minimal stopping distance are estimated: At large following distances mean speeds of vehicles do not increase, which return desired speeds at the horizontal asymptote. The minimal stopping distances are distances where speed values of the curves are 0 (i.e. the s where $v(s) = 0$). This value is close to the vertical asymptote. The formula that is used to estimate the asymptotes is of following form:

$$v(s) = \frac{a \cdot s - \text{abs}(b)}{c \cdot s - \text{abs}(d)}$$

The median speed at following distance s is given $v(s)$, coefficients a , b , c , d , have to be estimated.

The horizontal asymptote (v_0) is mathematically described by $v_0 = \lim_{s \rightarrow \infty} \frac{a \cdot s - \text{abs}(b)}{c \cdot s - \text{abs}(d)} = \frac{a}{c}$.

The value of s_0 is given by the value of s where $v = 0$. This can be described as $a \cdot s - \text{abs}(b) = 0$, which means that $s_0 = \frac{a}{b}$. By using a built-in Matlab function, the curves are fitted and parameters have been estimated (see figure 6.44 to figure 6.49).

Estimating T_{des}

The estimated desired headway times are equal to the expected value of the fitted distribution in section 6.1.2.

Parameter estimation results

The results of the single parameter estimation of v_0 , s_0 and T_{des} , and other parameters are presented in table 6.4.

Parameter	Passenger Cars			Heavy vehicles		
	Config 2	Config 4a	Config 4b	Config 2	Config 4a	Config 4b
v_0 [m/s]	25.8	22.6	24.7	22.7	21.1	23.1
s_0 [m]	0.6	7.7*	0.6	0.6	0.3*	0.6
T_{des} [s]	1.51	1.65	1.53	2.45	2.42	2.37
T_r [s]	0					
n [-]	1					
a_0 [m/s ²]	1.25					
b_0 [m/s ²]	2.09					
* Lack of observations cause this deviation in stopping distance, so 0.6 m is used.						

Table 6.4: Single parameter estimation results.

Comparing hypothesis of empirical variables with values of their corresponding estimated parameters, lead to consistent results. Desired headways slightly increase and desired speeds decrease when a work zone is applied compared to the control situation.

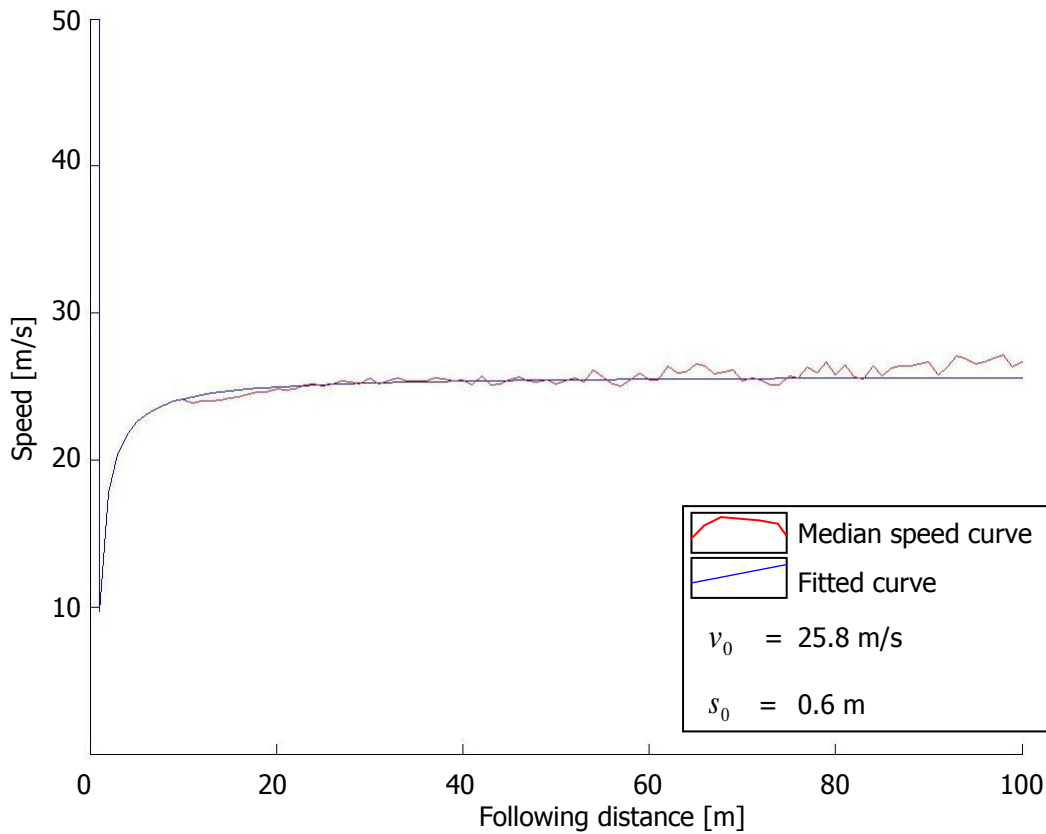


Figure 6.44: Fitted curve through speed - following distance data, configuration 2, passenger cars.

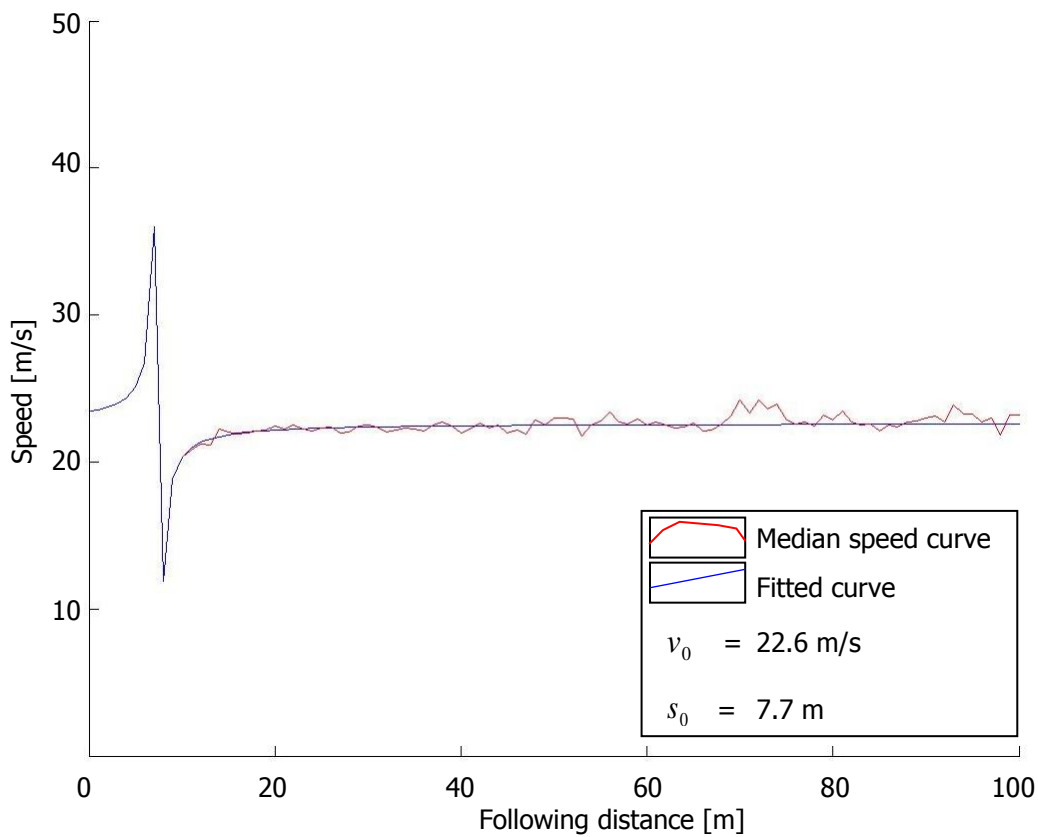


Figure 6.45: Fitted curve through speed - following distance data, configuration 4a, passenger cars.

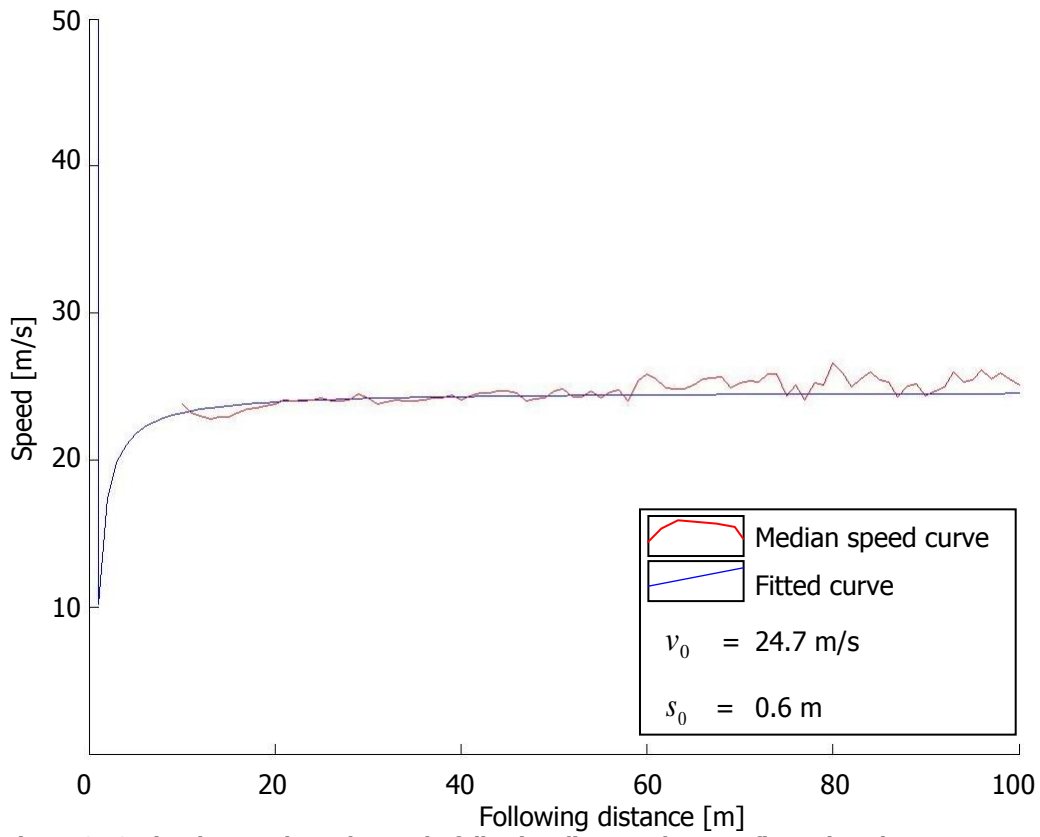


Figure 6.46: Fitted curve through speed - following distance data, configuration 4b, passenger cars.

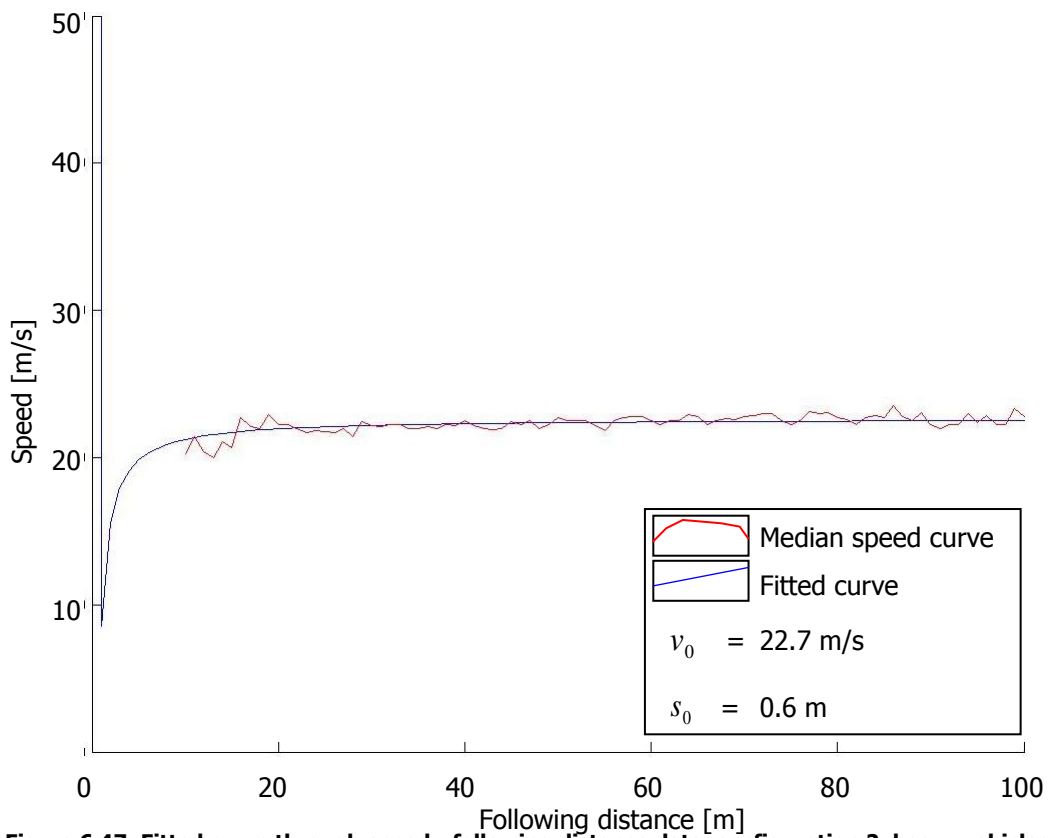


Figure 6.47: Fitted curve through speed - following distance data, configuration 2, heavy vehicles.

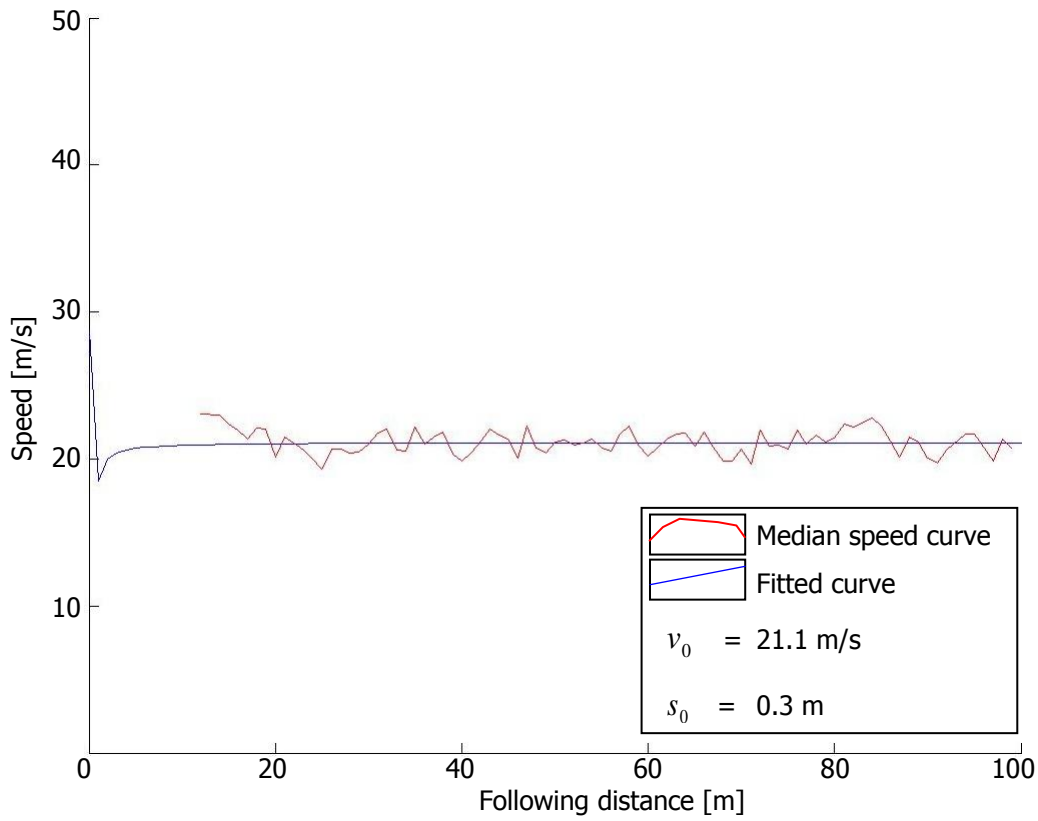


Figure 6.48: Fitted curve through speed - following distance data, configuration 4a, heavy vehicles.

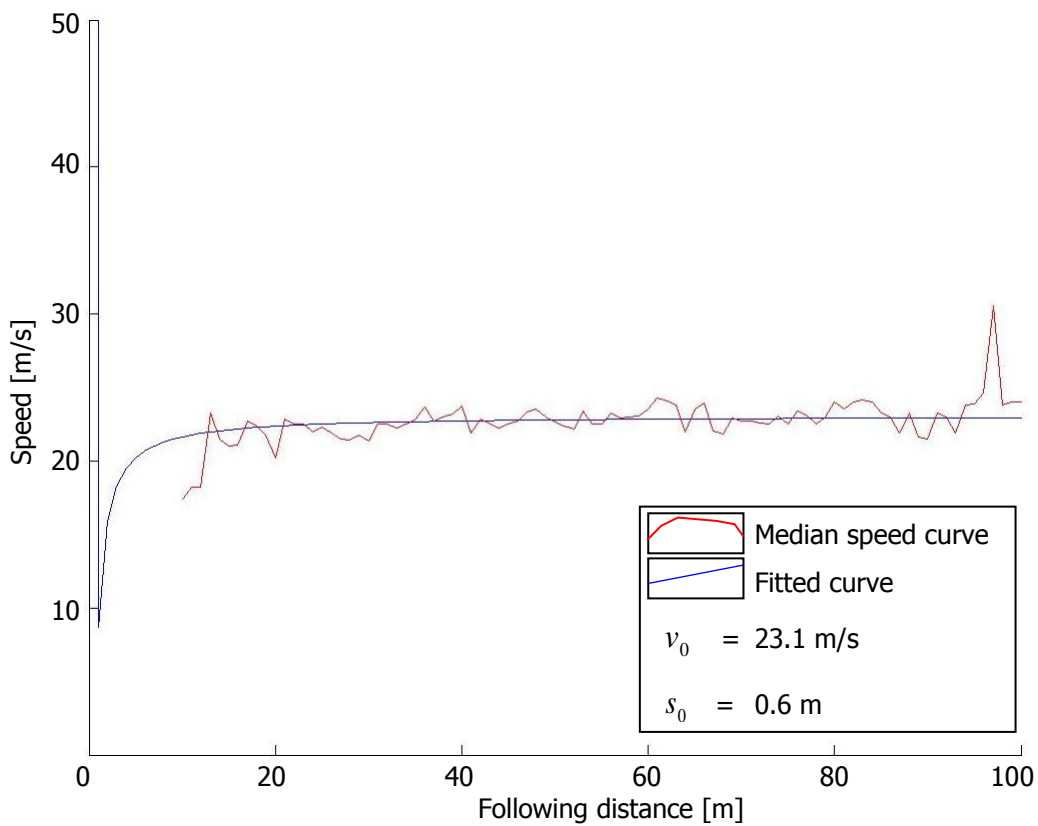


Figure 6.49: Fitted curve through speed - following distance data, configuration 4b, heavy vehicles.

6.2.2 Simulation process and results

From figures and results of the previous section can be seen that much less data of heavy vehicles are available compared to amount of passenger car data. This lack of data causes distributions of heavy vehicles to be unsmooth, and therefore parameter estimations are less accurate. Despite inconsistent results (desired speed is higher in the work zone configuration than in the control situation), differences for heavy vehicles between configuration 4b and 2 are relatively small. Therefore, for simulation only passenger cars are simulated.

Simulation program

The simulation tool which has been used is a Java based program, which can be run from Matlab. The car-following behaviour is simulated using the Extended IDM and the LMRS of Schakel et al. (2011) deals with the lane changing behaviour.

The tool simulates traffic in a two-lane freeway with an onramp. By allocating vehicles via the onramp to the two-lane freeway, a bottleneck is created (see figure 6.50 for an example of the GUI (the driving direction is from left to right)). The length of the road segments and duration of the runs can be manually adjusted, but are left unchanged for these simulation runs:

1. Two lane freeway over 2500 m;
2. Over 500 m additional lane for onramp, without merging possibility;
3. Over 250 m merging lane;
4. 1750 m two lane freeway downstream of merging zone.

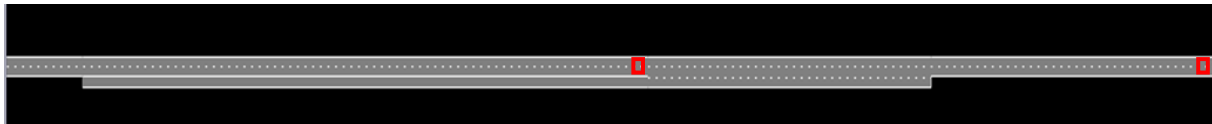


Figure 6.50: Example of the simulation tool GUI (detection loops in red), with onramp.

6.2.3 Fundamental diagram of simulation results

Per configuration a total of 30 runs have been performed, for which at two locations detector data have been saved. The first location is just downstream of the bottleneck, which is selected to determine the bottlenecks' capacity value and thus of the work zone configuration. The second detector location is upstream of the bottleneck, to investigate the congested branch of the fundamental diagram and capacity drop. Those two locations have been drawn in figure 6.50.

An example of the results of one simulation (in this case for configuration 2), is given in figure 6.51 (downstream detector) and figure 6.52 (upstream detector). In figure 6.53, maximum flows for all 30 simulation results (for both detector locations) are combined.

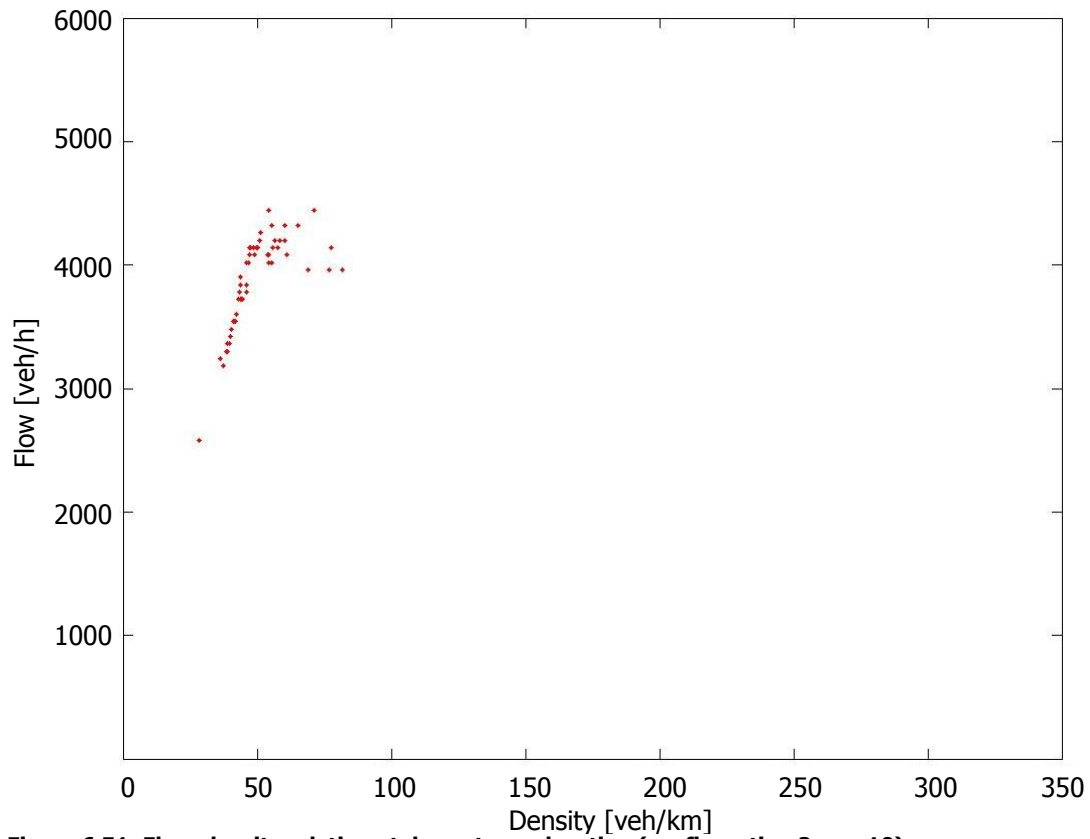


Figure 6.51: Flow-density relation at downstream location (configuration 2, run 10).

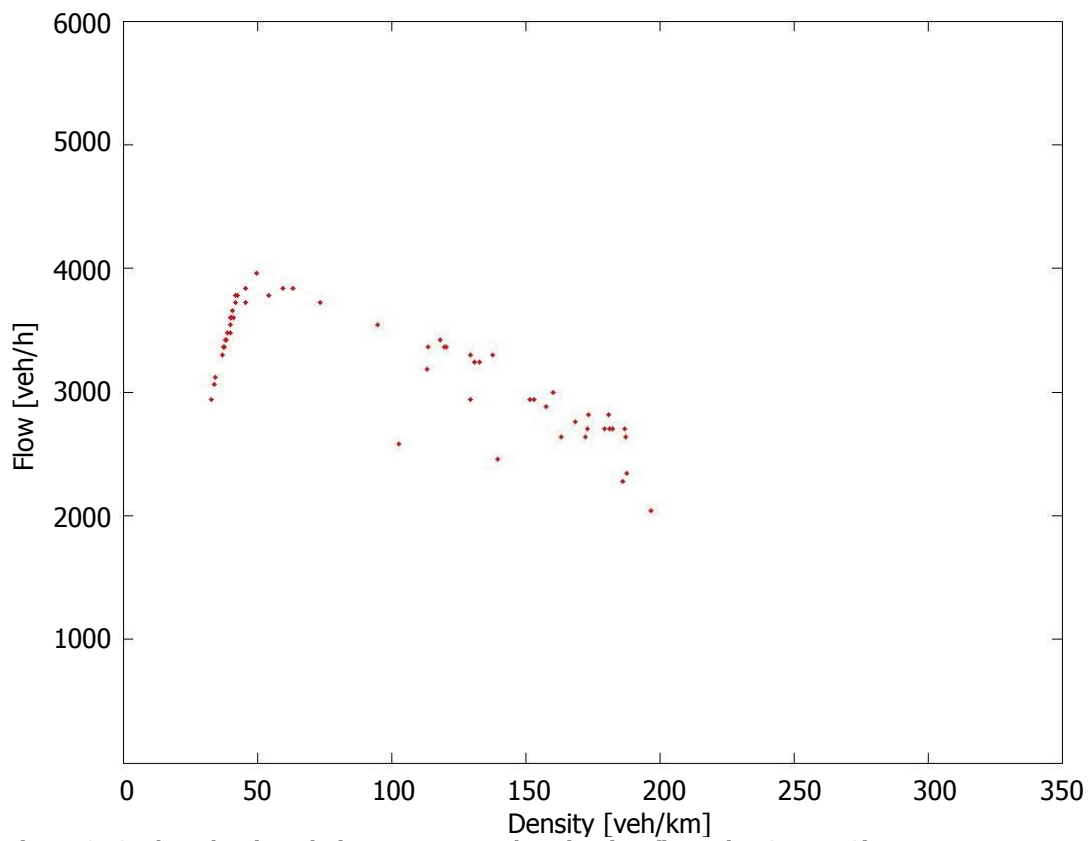


Figure 6.52: Flow-density relation at upstream location (configuration 2, run 10).

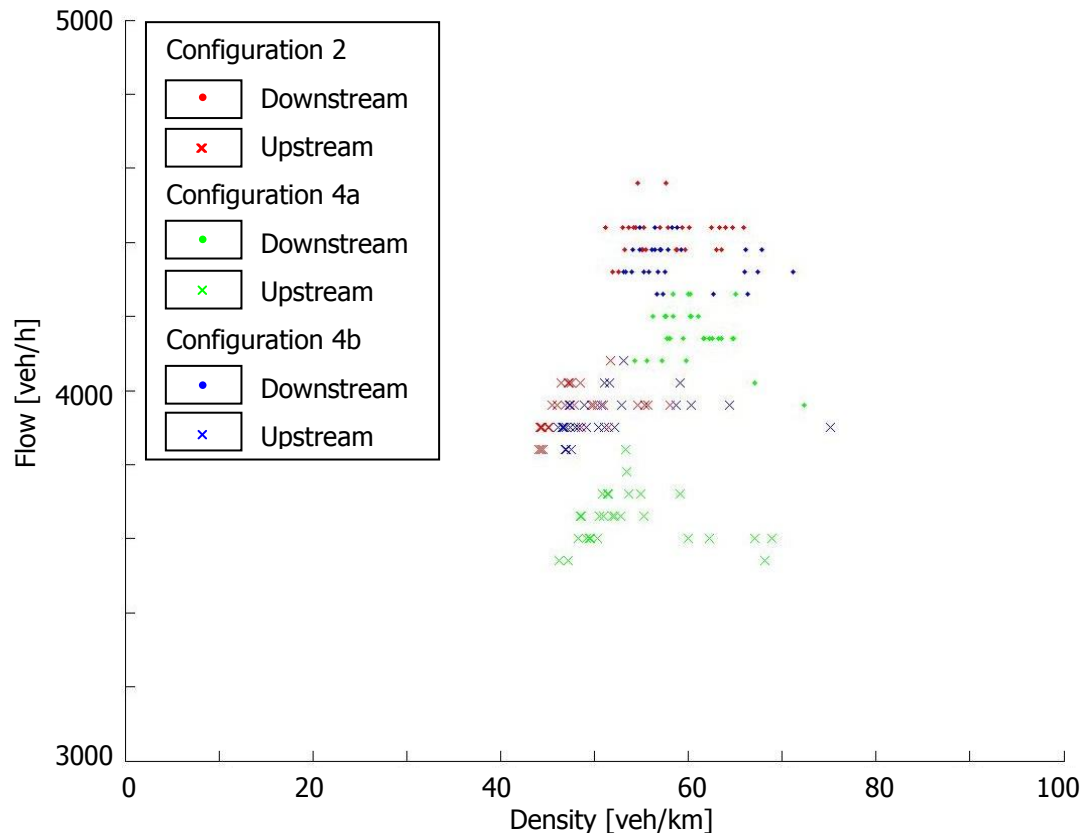


Figure 6.53: Maximum flows for all simulations, detectors and configurations.

The median maximum flow downstream is defined as the capacity value, and the difference between this value and the median maximum flow upstream is defined as the capacity drop. The results are summarized in table 6.5.

Configuration	Median capacity free flow	Median congested capacity	Capacity drop
2	4422	3944	478
4a	4150	3652	498
4b	4350	3928	422

Table 6.5: Values for capacity and capacity drop for each simulated configuration.

6.3 Conclusions

From the two previous sections it is concluded that applied work zone configurations have a significant influence on individual driving behaviour and capacity of the road section.

6.3.1 Results of analysing empirical data

Driving speeds have been significantly lower when a work zone configuration is applied at all following distances, indicating lower desired speeds. At the range of following distances of 25 - 30 m, smaller lane widths and a barrier close to the carriageway instead of a normal guard rail caused an average decrease in the median value of 2.4 km/h, from 90.1 to 87.7 km/h. When a small reverse curve is also

present in the lateral alignment, the decrease has even been 10.4 km/h. These lower speeds imply lower capacities at applied work zone configurations.

Differences among drivers did not significantly differ, i.e. the heterogeneity between drivers did not differ due to changes in work zone configurations or road layout.

By investigating lane occupancy distributions, whereby no significant differences between configurations have been found, it has been legitimate for this research not to investigate lane choice and lane changing behaviour.

Unfortunately it was not possible to investigate differences in the shape of the fundamental diagram based on observations only, because not all traffic states have been observed. Differences in capacity between configurations have been investigated by simulations.

6.3.2 Results of analysing data collected from simulations

Despite that it has not been possible to integrally estimate model parameters, different configurations have been simulated using single parameter estimations. Using these estimations and an existing simulation tool, macroscopic effects have been investigated.

The reduced lane widths from 2x3.5 m to 3.25 and 3.0 m in combination with a barrier close to the carriageway instead of normal guard rail resulted in a reduced capacity of 1.5%. A relatively large change in capacity when relatively small lateral change in the alignment is present. In this case, the small reverse curve has been responsible for a decrease in capacity of 6.2%.

With respect found capacity values of Zheng (2009) and the original Table of capacity (see appendix 2), which show capacity changes of +1% to -30% for comparable configurations, these reductions fall within acceptable boundaries.

The result indicate that to optimize the capacity of a work zone, it is recommended to pay specific attention to locations at critical cross-sections to prevent small changes in the layout of work zones.

7 Conclusions and recommendations

In this Chapter conclusions of this graduation study are presented, after which practical recommendations and recommendations for future research are given.

7.1 Conclusions

7.1.1 Analysing methods for adaptation effects

Empirical driving behaviour has been described as real time observed vehicle movements of individual drivers and their interaction with other drivers. This behaviour in work zones can be described best by microscopic analysis at a tactical level, because it includes all measurable driving behaviour at work zones (e.g. speed and following distance) and can be related to macroscopic effects.

Different methods have been selected to analyse individual driving behaviour and corresponding adaptation effects.

Analysing adaptation effects in individual driving behaviour and their distributions

Differences in empirical variables describe adaptation effects of individual driving behaviour and are an indication for macroscopic effects. The following variables have been selected to be investigated:

- Headway distributions;
- Speed distributions;
- Speed (differences) against corresponding following distances;
- Speed distributions at specific following distances;
- Lane occupation distributions.

Analyse macroscopic effects

Macroscopic effects can be investigated using empirical variables and by simulating calibrated driving behaviour models. With empirical data of all vehicles, macroscopic variables (e.g. density) can be computed and analysed as well. To analyse non-observed parts of macroscopic variables the Extended IDM as car-following model has been selected for simulating longitudinal individual driving behaviour and analysing macroscopic variables. The LRMS has been selected to simulate the lane changing part of individual driving behaviour.

7.1.2 Data collection and processing

Data collection

Based on selected methods for analysing individual driving behaviour, it has been required to observe positions of vehicles during a specific period, which requires a high observation location using a video camera. To reduce costs for data collection and thereby collecting more data, an innovative collection method has been chosen: Collect data using an unmanned helicopter.

At road works, carried out by 'De Utrechtse Tulp' at the A28 freeway, interesting and comparable configurations were present and therefore this project has been chosen for doing measurements. For the three configurations that have been fully worked out, one control situation and two configurations with applied work zone, values of research determinants are given in table 7.1.

Configuration	Location		
	2	4a	4b
Speed limit (km/h)	90	90	90
Contra Flow	No	No	No
Channelizing Device	Left	Guard rail	Barrier
	Right	Guard rail	Guard Rail
Hard Shoulder	Yes	Yes	Yes
Lane width (m)	2x3.5	3.25-3.00	3.25-3.00
Reverse Curve	No	Yes (small)	No

Table 7.1: Determinant values of worked out configurations.

Data processing

To analyse empirical variables and calibrate parameters of the driving behaviour model, video recordings have been converted into individual vehicle trajectories and corresponding individual data. This process consisted out of two steps:

1. Image pre-processing;
2. Vehicle detection & tracking.

The first step consisted stabilizing images and correcting them for pincushion and perspective distortion, which led to large difficulties, because the stabilization program did not work properly. Therefore, only three out of five observed configurations have been fully elaborated.

For these three configurations, longitudinal cross-sections have been extracted and combined for each lane, which already made trajectories visually observable. Then, for this type of research, innovate methods have been implemented to detect vehicles and track these vehicles over their paths:

- Edge detection, which detects possible vehicle locations from combined longitudinal cross-sections by comparing colour intensities of adjacent pixels;
- A program that stores mouse click locations has been developed for selecting start and end points of trajectories and to correct trajectories if they were faulty tracked;
- Furthermore, the Dijkstra algorithm (a shortest path algorithm) has been programmed to connect vehicle starts and ends over found edges.

After transforming pixel locations to real life distances using pavement markings, this detecting and tracking process resulted in 8355 useful trajectories of individual vehicles of approximately 8 seconds (100 separate observations) per vehicle:

- Configuration 2 included 4827 vehicles, of which 611 were heavy vehicles (13%);
- Configuration 4a included 1707 vehicles, of which 264 were heavy vehicles (15%);
- Configuration 4b included 2051 vehicles, of which 347 were heavy vehicles (17%).

7.1.3 Adaptation effects in individual driving behaviour

Headway distributions have been investigated as they indicate changes in capacity. The results showed an increase in time headway if a work zone was applied compared to the control situation.

Observed driving speeds at all following distances have been significantly lower at work zone configurations than at the control configuration, indicating lower desired speeds. At the range of following distances of 25 - 30 m, smaller lane widths and a barrier close to the carriageway instead of a normal guard rail caused an average decrease in the median value of 2.4 km/h, from 90.1 to 87.7 km/h. With also a small reverse curve installed in the lateral alignment, the decrease has even been 10.4 km/h. These lower speeds imply lower capacities at applied work zone configurations.

Differences among drivers did not significantly differ, i.e. the heterogeneity between drivers did not differ due to changes in work zone configurations or road layout. The decrease in speed did apply for each driver, causing overall no difference in car heterogeneity.

By investigating lane occupancy distributions, no significant differences between configurations have been found, which does legitimate not investigating lane changing behaviour for this research.

It has not been possible to investigate differences in the shape of the fundamental diagram based on observations only, because not all traffic states have been observed. Therefore, differences in configurations capacity could be investigated only by performing simulations.

7.1.4 Effects in macroscopic traffic flow operations

Due to lack of congested data, parameter values of the selected car-following model, the Extended IDM, could not be integrally estimated. Therefore, parameters of the Extended IDM that describe non-congested driving have been estimated (the desired speed, desired time headway and minimal stopping distance).

Desired speed and minimal stopping distance have been estimated by fitting a double asymptotic function to the speed – following distance relation, in which the horizontal asymptote represents the desired speed, and where the function crosses x-axis represents the minimal stopping distance (see next table for estimation results). The desired headways have been estimated using the expected value of the log-normal distribution fitted to empirical headways. The observed headways were relatively small that indicate car-following behaviour, which allowed using the log-normal distribution.

The results of the parameter estimation process are presented in table 7.2.

Parameter	Passenger Cars			Heavy vehicles		
	Config 2	Config 4a	Config 4b	Config 2	Config 4a	Config 4b
v_0 [m/s]	25.8	22.6	24.7	22.7	21.1	23.1
s_0 [m]	0.6	7.7*	0.6	0.6	0.3*	0.6
T_{des} [s]	1.51	1.65	1.53	2.45	2.42	2.37

Table 7.2: Single parameter estimation results.

Effects for possible differences in not estimated parameters a_0 and b_0 , should have been root squared, reducing the impact of the non-investigated changes.

For investigating macroscopic effects for differences in estimated car-following parameters, an existing simulation tool combined the Extended IDM with the lane changing model LMRS:

- Reduced lane widths from 2x3.5 m to 3.25 and 3.0 m in combination with a barrier as channelizing device instead of normal guard rail resulted in a reduced capacity of 1.5%;
- A small reverse curve is responsible for an additional decrease in capacity of 6.2%.

7.2 Practical recommendations

7.2.1 Choice of observation method and locations

The choice of the observation method depends on the purpose of the collected data, but when considering the unmanned helicopter to collect data, it is highly recommended to visit locations before doing observations to check observation possibilities and restrictions. Therefore, it is important to be informed by the company carrying out unmanned helicopter flights about this observing process and limitations (e.g. presence of approach routes of airports). When possibilities towards observation locations are clear, next checks can be performed:

1. To ascend and land the helicopter, an open area has to be present close to the freeway to prevent occlusion as much as possible. It is desirable that the unmanned helicopter cannot easily be spotted by road users when it ascends and descends (e.g. behind a sound wall), to prevent drivers from getting distracted from their driving task.
2. Locations should best be outside rural areas to minimize the number of spectators.
3. Visually observe traffic streams from ground level before actually carrying out flights, to determine time spans, in which all traffic states are observed during actual flights.

7.2.2 Stabilization

Adjust observed top view

As described in section 5.1.2, 'ImageTracker' fits frames by rotating and stretching them on a reference frame. To prevent that errors in during stabilization occur, reference points could be

manually placed in the landscape, (e.g. unicolor squared surfaces and/or your car) if they are missing in the natural top view.

Adjust stabilization program

As mentioned before, stabilizing individual frames caused large problems during this graduation research, and because of the large amount of data, it was not possible to correct all revealed errors. To limit these problems in future researches, it is recommended to adjust the stabilization program, so this program deals with these problems itself. This should be possible, because errors have been easily detected by comparing differences between successive stabilized frames:

1. Differences in pixel intensity (for each pixel) between the current and the first frame should be calculated;
2. This difference should be compared with the previous frame. If the difference is smaller than the boundary value, continue with the next frame. If the difference exceeds the boundary, redo this frame by using another frame as reference frame. If this results in a large error as well, use the second last successfully stabilized frame;
3. Register frame if this did not work either and continue with next frame.

Perform perspective corrections after stabilization

Do all required other perspective corrections, except lens corrections, after stabilization instead of doing this simultaneously: Do not stretch or compress pixel values before images have been stabilized, so wrongly stabilized parts can easily be projected on the first stabilized frame.

7.2.3 Simulations

For simulating individual driving behaviour models, it is recommended to separate combined car movements from estimated individual driving behaviour, so different car-following and lane changing models can easily be implemented and combined into the simulation tool.

7.2.4 Recommendations for setting up work zone configurations

It is recommended to pay specific attention to locations of changing cross-sections. If small changes appear abrupt for road users, these relatively small changes can have large consequences for capacity values of road sections. Therefore smoother changes over longer road stretches are preferred over short changed cross-sections, even they include smaller lane widths over long road stretches, because the influence of a narrowed lanes has turned out be much less than of reverse curves, which are mostly used for narrowing these lanes.

7.3 Recommendations for future research

7.3.1 Determinant research

For this research it has only been possible to investigate influences of three varying determinant values, but to determine adaptation effects and the performance of work zones with other varying determinants, these determinant influences have to be investigated in future research.

Because changes in layout turned out having a large influence on performance of work zones, it is recommended that at these locations the observations take place.

7.3.2 Edge detection

Now, the used edge detection algorithm has been selected by reading the Matlab manual and best practice. This so-called 'Canny' algorithm produced good results, but was not scientifically supported being a fast and accurate algorithm. Therefore, research towards this algorithm is recommended.

7.3.3 Connecting vehicle starts and ends to extract trajectories

To connect the found/selected vehicle starts and ends, the relatively simple and slow Dijkstra algorithm has been used for this research. This shortest path algorithm has been chosen for programming convenience, but has turned into relatively high computational times. For limiting computational time in future researches it is essential that a faster method will be implemented and programmed to connect two pixels over the shortest path.

7.3.4 Select vehicle starts and ends

In this research starts and ends of vehicles have been manually selected. To limit the duration of this process, it is recommended that to create a program that makes a first selection out of selected edges. Recommended selection steps are:

- Check next to removed stabilization edge if a connected edge is of sufficient length;
- If so, select this pixel as vehicle start or end and skip observations for the next second (to prevent vehicles' front and back are selected as vehicle).
- Use average gradient of connected edge pixels (indicating mean speed) to find corresponding start and end points.

7.3.5 Car-following models

In this research unobserved traffic states caused problems for integrally estimating car-following model parameters. For future research, the relationship between driving behaviour under uncongested conditions and under congested conditions could be investigated, which could make it possible to estimate changes of driving behaviour under congested conditions based on changed behaviour under uncongested driving only.

References

Aerial Group, BV. (2012). <http://www.aerialtronics.nl/media/>. (accessed: 2012, June 6).

Ahmed, KI., Ben-Akiva, ME., Koutsopoulos, HN. & Mishalani, RG. (1996). *Models of Freeway Lane Changing and Gap Acceptance Behaviour*. Theory of Traffic Flow and Transportation. New York: Elsevier Science Publishing. pp. 501-515.

Al-Kaisy, A. & Hall, F. (2003). *Guidelines for Estimating Capacity at Freeway Reconstruction Zones*. Vol:129, no:5, pp. 572-577.

Bando, M., Hasebe, K., Nakayama, A., Shibata, A. & Sugiyama, Y. (1995). *Dynamical Model of Traffic Congestion and Numerical Simulation*. Vol:51, no:2, pp. 1035-1042.

Benekohal, R.F., Kaja-Mohideen, AZ. & Chitturi, MV. (2003). *Evaluation of Construction Work Zone Operational Issues: Capacity, Queue and Delay*.

Berry, DS. & Belmont, DM. (1951). *Distribution of Vehicle Speeds and Travel Times*. 2nd Berkely Symposium on Mathematical Statistics and Probability. Berkeley, California, USA: University of California Press. pp. 589-602.

Brackstone, M. & McDonald, M. (1999). *Car-Following: A Historical Review*. Vol:F, no:2, pp. 181-196.

Chandler, RE., Herman, R. & Montroll, EW. (1958). *Traffic Dynamics: Studies in Car Following*. Vol:6, no:2, pp. 165-184.

Cohen, S. (2004). *Using the Hard Shoulder and Narrowing Lanes to Reduce Traffic Congestion: Some Lessons from an Experience on the Paris Motorway Network*. Vol:2004, no:CP501, pp. 149-153.

Coifman, B., McCord, M., Mishalani, RG., Iswalt, M. & Ji, Y. (2006). *Roadway Traffic Monitoring from an Unmanned Aerial Vehicle*. Vol:153, no:1, pp. 11-20.

CROW (2005). *Maatregelen op autosnelwegen - Werk in Uitvoering 96a*. Ede: Van Grinsven Drukkers Venlo bv.

Dijker, T. & Knoppers, P. (2004). *FOSIM 5.0: Gebruikershandleiding*. Delft: Delft University of Technology.

Dijkstra, EW. (1959). *A Note on Two Problems in Connexion with Graphs*. Vol:1, pp. 269-271.

- Gazis, DC., Herman, R. & Potts, RB. (1959). *Car-Following Theory of Steady State Traffic Flow*. Vol:7, no:4, pp. 499-505.
- Gipps, PG. (1981). *A Behavioural Car-Following Model for Computer Simulation*. Vol:15, no:2, pp. 105-111.
- Gipps, PG. (1986). *A Model for the Structure of Lane-Changing Decisions*. Vol:20, no:5, pp. 403-414.
- Github (2012). <https://github.com/kevinvandervlist/tfa>. (accessed: 2012, March 3).
- Godley, ST., Triggs, TJ. & Fildes, BN. (2004). *Perceptual Lane Width, Wide Perceptual Road Centre Markings and Driving Speeds*. Vol:47, no:3, pp. 237-256.
- Google (2011). <http://maps.google.nl/>. (accessed: 2011, Januari 19).
- Green, P., Lin, B. & Bagian, T. (1993). *Driver Workload as a Function of Road Geometry: A Pilot Experiment*.
- Gunay, B. (2007). *Car Following Theory with Lateral Discomfort*. Vol:41, no:7, pp. 722-735.
- HCM (2000). *Highway Capacity Manual*.
- Helly, W. (1959). *Simulation of Bottlenecks in Single Lane Traffic Flow*. Theory of Traffic Flow. New York: Elsevier. pp. 207-238.
- Hidas, P. (2002). *Modelling Lane Changing and Merging in Microscopic Traffic Simulation*. Vol:10, no:5-6, pp. 351-371.
- Higgs, B., Abbas, M., Medina, A. & Yang, DCY. (2010). *Reconstruction the Wiedemann Model using Naturalistic Driving Data*. Virginia, USA: VirginiaTech Transportation Institute. p. 23.
- Hoogendoorn, RG. (2011). *State-of-the-Art Driving Theory and Modeling in case of Adverse Conditions*.
- Hoogendoorn, RG. (2012). *Empirical Research and Modeling of Longitudinal Driving Behavior Under Adverse Conditions*.
- Hoogendoorn, SP., Botma, H. & Minderhoud, MM. (2004). *Traffic Flow Theory and Simulation*. Delft: Delft University of Technology.

Hoogendoorn, SP. & Daamen, W. (2007). *FOSIM Smalle Rijstroken en 80 km/u Zones: Modelontwikkeling, Kalibratie en Validatie*. Delft: Delft University of Technology.

Hoogendoorn, SP., Ossen, S. & Schreuder, M. (2006). *Empirics of Multianticipative Car-Following Behavior*. Vol:1965, no:12, pp. 112-120.

Hoogendoorn, SP., Ossen, S. & Schreuder, M. (2007). *Properties of a Microscopic Heterogeneous Multianticipative Traffic Flow Model*. Transportation and Traffic Theory. Amsterdam: Elsevier Science. pp. 583-606.

Hoogendoorn, SP., Zuylen, HJ., Schreuder, M., Gorte, B. & Vosselman, GM. (2003). *Traffic Data Collection from Aerial Imagery*. Vol:1, pp. 779-784.

Jain, R., Kasturi, R. & Schunk, BG. (1995). *Machine Vision*. New York, USA: McGraw-Hill Incorporated.

Kesting, A., Treiber, M. & Helbing, D. (2007). *General Lane-Changing Model MOBIL for Car-Following Models*. Vol:2007, no:1999, pp. 86-94.

Kim, T., Lovell, DJ. & Paracha, J. (2001). *A New Methodology to Estimate Capacity for Freeway Work Zones*. Transportation Research Board Annual Meeting. Washington D.C., USA: University of Maryland. p. 27.

Knoop, VL., Duret, A., Buisson, C. & Van Arem, B. (2010). *Lane Distribution of Traffic near Merging Zones Influence of Variable Speed Limits*. 13th International IEEE Conference on Intelligent Transportation. Funchal, Madeira Island, Portugal: Intelligent Transportation Systems (ITSC). pp. 485-490.

Knoop, VL., Hoogendoorn, SP. & Van Zuylen, HJ. (2009). *Processing Traffic Data Collected by Remote Sensing*. Vol:2009, no:2129, pp. 55-61.

Knoop, VL., Hoogendoorn, SP. & Van Zuylen, HJ. (2009). *Macroscopic Behaviour near Incidents*. Proceedings of the International Symposium of Transport and Traffic Theory. Springer: New York. pp. 75-97.

Lenz, H., Wagner, CK. & Sollacher, R. (1999). *Multi-Ancitipative Car-Following Model*. Vol:7, no:2, pp. 331-335.

Luttinen, RT. (1996). *Statistical Analysis of Vehicle Time Headways*. Otaniemi, Finland: Transportation Engineering.

Maze, TH., Schrock, SD. & Kamyab, A. (2000). *Capacity of Freeway Work Zone Lane Closures*. Mid-Continent Transportation Symposium. Ames, Iowa, USA: Iowa Department of Transportation. pp. 178-183.

McDonald, J. (2006). <http://www.dmi.units.it/~inverniz/adir/statnested.html>. (accessed: 2012, September 11).

Michon, JA. (1985). *A Critical View of Driver Behavior Models: What do we know, what should we do*. pp. 485-520.

Ossen, SJL. (2008). *Longitudinal Driving Behavior: Theory and Empirics*. Gildeprint Drukkerijen: Enschede.

Research Development and Technology, O.o. (2012). <http://www.fhwa.dot.gov/publications/research/operations/its/06108/02.cfm>. (accessed: 2012, June 6).

Rijkswaterstaat (2010). *Werkwijzer MinderHinder, Het RWS-brede Kader voor Minder Hinder bij Werk aan de Weg*. Utrecht: Rijkswaterstaat.

Rijkswaterstaat (2000). <https://beeldbank.rws.nl/MediaObject/Details/200907>. (accessed: 2012, June 6).

Schaap, TW. (2012). *Driving Behaviour in Unexpected Situations*.

Schakel, WJ., Knoop, VL. & Van Arem, B. (2011). *LMRS: An Integrated Lane Change Model with Relation and Synchronisation*. Proceedings of the 91st Annual Meeting of the Transportation Research Board. Washington D.C.: Transportation Research Board. p. 21.

Schakel, WJ., Van Arem, B. & Netten, BD. (2010). *Effects of cooperative adaptive cruise control on traffic flow stability*. Proceedings of the 13th International IEEE Conference on Intelligent Transportation Systems. pp. 759-764.

Sun, X., Park, J., Tekell, D. & Ludington, N. (2006). *Impact of Pavement Edge Line on Vehicular Lateral Position on Narrow Rural Two-Lane Roadways in Louisiana*. Transportation Research Board. Washinton D.C., USA: National Research Council. pp. 1-24.

Tampère, CMJ. (2004). *Human-Kinetic Multiclass Traffic Flow Theory and Modelling*. Delft: TRAIL Research School.

Tampère, C., Van Arem, B. & Hoogendoorn, SP. (2005). *A Behavioural Approach to Instability, Stop & Go Waves, Wide Jams and Capacity Drop*. Vol:11, pp. 205-228.

Ter Kuile, R. (2006). *Rijgedrag en Verkeersafwikkeling bij Werk in Uitvoering met Versmalde Rijstroken*. Delft: Technische Universiteit Delft.

Toledo, T., Koutsopoulos, HN. & Ben-Akiva, M. (2009). *Estimation of an Integrated Driving Behavior Model*. Vol:17, no:4, pp. 365-380.

Traffic Assignment Manual (1964). *Traffic Assignment Manual*. Washington D.C.: Bureau of Public Roads, U.S. Dept. of Commerce, Urban Planning Division.

Treiber, M., Hennecke, A. & Helbing, D. (2000). *Congested Traffic States in Empirical Observations and Microscopic Simulations*. Vol:62, no:2, pp. 1805-1824.

Trucco, E. & Alessandro, V. (1998). *Introductory Techniques for 3-D Computer Vision*. Englewood Cliffs, New Jersey, USA: Prentice-Hall.

Van Begin, B. (2002). *Naar een Beter Onderbouwde Planning van Wegenwerken: Aanbevelingen om de Verkeershinder te Beperken*.

Van Hinsbergen, CPI., Van Lint, HWC., Hoogendoorn, SP. & Van Zuylen, HJ. (2009). *Bayesian Calibration of Car-following models*. 12th IFAC Symposium on Transportation Systems. Redondo Beach, California, USA: IFAC. pp. 91-97.

Van Loon, A., Hoogendoorn, SP., Schreuder, M. & Ossen, SJL. (2006). *Helikopter Blijkt op Verkeer*. Vol:57, no:1, pp. 22-27.

Wegenforum (2010). <http://www.wegenforum.nl/>. (accessed: 2011, Februari 10).

Wiedemann, R. (1974). *Simulation des Straßenverkehrsflusses*. Karlsruhe. Germany: University of Karlsruhe.

Wiedemann, R. & Leutzbach, W. (1986). *Development and applications of traffic simulation models at the Karlsruhe Institut für Verkehrswesen*. Vol:27, no:5, pp. 270-278.

Yang, Q. & Koutsopoulos, HN. (1996). *A Microscopic Traffic Simulator for Evaluation of Dynamic Traffic Management Systems*. Vol:4, no:3, pp. 113-129.

Zheng, N. (2009). *Freeway Work Zone Capacity Prediction: Develop and Test the Fuzzy Logic Based Method*. Delft: Delft University of Technology, Heijmans Techniek & Mobiliteit BV.

Appendixes

- Appendix 1 List of Figures and Tables I**
- Appendix 2 Table of Capacity V**
- Appendix 3 Measurement registration forms VII**
- Appendix 4 Stabilization software manual XI**
- Appendix 5 Matlab programs..... XVII**
- Appendix 6 Images of Work Zone Configurations..... XXIX**

Appendix 1 List of Figures and Tables

List of Figures

Figure 1.1: Example of a freeway work zone.	1
Figure 1.2: Work zone layout (CROW (2005)).	1
Figure 1.3: Example of vehicle trajectories (Hoogendoorn et al. (2004)).....	3
Figure 1.4: Classification of driving tasks of Michon (1985), adapted by and copied from Schaap (2012).	4
Figure 1.5: Fundamental diagram (Hoogendoorn et al. (2004)).....	5
Figure 1.6: Data points collected by induction loops (Zheng (2009)).....	6
Figure 1.7: Data points with sketched fundamental diagram and capacity drop in pink (Zheng (2009)).....	6
Figure 1.8: Flow diagram research plan.	8
Figure 1.9: Data types from determinant to macroscopic effects.	8
Figure 2.1: Concrete barrier as channelizing device.	16
Figure 2.2: Narrow barricades as channelizing device.....	16
Figure 2.3: Traffic cones as channelizing device.	16
Figure 2.4: Example of reverse curve (Wegenforum (2010)).....	16
Figure 3.1: Lane occupancy distributions (Knoop et al. (2010)).....	21
Figure 3.2: Typical following pattern (left) and the Wiedemann threshold principle (right).	24
Figure 4.1: Unmanned helicopter.	30
Figure 4.2: Induction loops in pavement on a freeway.	30
Figure 4.3: Picture taken from the telescope mast.	31
Figure 4.4: Van with tripod of mast.....	31
Figure 4.5: Data validity against controllability for different collection methods (Hoogendoorn (2012)).....	32
Figure 4.6: Facet building.....	33
Figure 4.7: Remote control.....	35
Figure 4.8: Used helicopter for location 3 and 4.	35
Figure 4.9: Visual helicopter size at 200 m.	35
Figure 4.10: Used helicopter for location 1 and 2.	35
Figure 4.11: Measurement locations on the A28 (Google (2011)).....	36
Figure 4.12: Configuration 1, direction West-East.	37
Figure 4.13: Configuration 2, direction West-East.	37
Figure 4.14: Configuration 2, direction East-West.	38
Figure 4.15: Configuration 3, direction West-East.	38
Figure 4.16: Configuration 3, direction East-West.	38
Figure 4.17: Configuration 4a, direction East-West.	38
Figure 4.18: Configuration 4b, direction West-East.	38
Figure 5.1: Different observed stretches with same optic angles (left: top view, right: longitudinal view).	39
Figure 5.2: Example of interlaced frame	40
Figure 5.3: Corresponding deinterlaced frame.....	40
Figure 5.4: Chess board pattern, calibration picture of camera Aerialtake.....	41
Figure 5.5: Chess board pattern after calibrating.	42
Figure 5.6: Schematic sketch of the distortion introduced by the perspective vision.....	42
Figure 5.7: Illustration of a lens convexity correction for an isolated frame.	42
Figure 5.8: Frame 1, corrected for lens convexity.	43
Figure 5.9: Object contours of frame 1.	43
Figure 5.10: Frame 2, ready for stabilisation.	43

Figure 5.11: Frame 2, with contours of frame 1 in red.....	43
Figure 5.12: Frame 2 fitted best on frame 1.....	43
Figure 5.13: Useful part in yellow.	43
Figure 5.14: Detecting jumps in stabilized frames.....	44
Figure 5.15: Example of stabilized frame.	45
Figure 5.16: Curve in real stabilized image.	46
Figure 5.17: Corrected and stabilised frames with connected points on right lane.	46
Figure 5.18: Picture of one longitudinal cross-section.	46
Figure 5.19: Pictures of a number of time steps of a longitudinal cross-section.	46
Figure 5.20: Average colour along the longitudinal section.	47
Figure 5.21: Example of combined cross-sections (top) and found corresponding (negative) edges (bottom). ..	47
Figure 5.22: Example of removed edges.	48
Figure 5.23: Result of connected trajectories.	49
Figure 6.1: Lane numbering.	51
Figure 6.2: Cumulative speed distributions for each observed location.....	52
Figure 6.3: Cumulative speed distributions per lane.....	53
Figure 6.4: Cumulative speed distributions per vehicle type.	53
Figure 6.5: Speed over distance plots for configuration 2, lane 3.	54
Figure 6.6: Cumulative speed distributions without discarded data.	55
Figure 6.7: Fitted and empirical time headway distribution, configuration 2, passenger cars.	56
Figure 6.8: Fitted and empirical time headway distribution, configuration 4a, passenger cars.....	56
Figure 6.9: Fitted and empirical time headway distribution, configuration 4b, passenger cars.	57
Figure 6.10: Fitted and empirical time headway distribution, configuration 2, heavy vehicles.	57
Figure 6.11: Fitted and empirical time headway distribution, configuration 4a, heavy vehicles.	58
Figure 6.12: Fitted and empirical time headway distribution, configuration 4b, heavy vehicles.	58
Figure 6.13: Relation Speed - Following distance for configuration 2.	59
Figure 6.14: Relation Speed - Following distance for configuration 4a.	60
Figure 6.15: Relation Speed - Following distance for configuration 4b.	60
Figure 6.16: Relation Speed - Following distance for configuration 2 and passenger cars.....	61
Figure 6.17: Relation Speed - Following distance for configuration 4a and passenger cars.....	61
Figure 6.18: Relation Speed - Following distance for configuration 4b and passenger cars.....	62
Figure 6.19: Relation Speed - Following distance for configuration 2 and heavy vehicles.	62
Figure 6.20: Relation Speed - Following distance for configuration 4a and heavy vehicles.	63
Figure 6.21: Relation Speed - Following distance for configuration 4b and heavy vehicles.	63
Figure 6.22: Relative speeds – following distance, configuration 2.....	65
Figure 6.23: Relative speeds – following distance, configuration 4a.	65
Figure 6.24: Relative speeds – following distance, configuration 4b.....	66
Figure 6.25: Cumulative and fitted normal distribution of configuration 2.....	67
Figure 6.26: Cumulative and fitted normal distribution of configuration 4a.....	67
Figure 6.27: Cumulative and fitted normal distribution of configuration 4b.....	68
Figure 6.28: Cumulative and fitted normal distribution of passenger cars, configuration 2.	68
Figure 6.29: Cumulative and fitted normal distribution of passenger cars, configuration 4a.	69
Figure 6.30: Cumulative and fitted normal distribution of passenger cars, configuration 4b.....	69
Figure 6.31: Cumulative and fitted normal distribution of heavy vehicles, configuration 2.	70
Figure 6.32: Cumulative and fitted normal distribution of heavy vehicles, configuration 4a.....	70
Figure 6.33: Cumulative and fitted normal distribution of heavy vehicles, configuration 4b.	71
Figure 6.34: Lane density distribution, configuration 2.	73
Figure 6.35: Lane density distribution, configuration 4a.	74
Figure 6.36: Lane density distribution, configuration 4b.	74
Figure 6.37: Right lane densities plotted against left lanes densities of all configurations.	75
Figure 6.38: Flow-density relation with per vehilce 1 data point, configuration 2.	76

Figure 6.39: Flow-density relation with per vehicle 1 data point, configuration 4a.....	76
Figure 6.40: Flow-density relation with per vehicle 1 data point, configuration 4b.	77
Figure 6.41: Flow density relation based on induction loop method, configuration 2.	77
Figure 6.42: Flow density relation based on induction loop method, configuration 4a.	78
Figure 6.43: Flow density relation based on induction loop method, configuration 4b.	78
Figure 6.44: Fitted curve through speed - following distance data, configuration 2, passenger cars.....	81
Figure 6.45: Fitted curve through speed - following distance data, configuration 4a, passenger cars.....	81
Figure 6.46: Fitted curve through speed - following distance data, configuration 4b, passenger cars.....	82
Figure 6.47: Fitted curve through speed - following distance data, configuration 2, heavy vehicles.	82
Figure 6.48: Fitted curve through speed - following distance data, configuration 4a, heavy vehicles.	83
Figure 6.49: Fitted curve through speed - following distance data, configuration 4b, heavy vehicles.	83
Figure 6.50: Example of the simulation tool GUI (detection loops in red), with onramp.....	84
Figure 6.51: Flow-density relation at downstream location (configuration 2, run 10).	85
Figure 6.52: Flow-density relation at upstream location (configuration 2, run 10).....	85
Figure 6.53: Maximum flows for all simulations, detectors and configurations.....	86

List of Tables

Table 2.1: Determinant trade-off (+: matches criterion, 0: partly matches criterion, -: not matching criterion). 14	14
Table 3.1: Car following model comparison (performance scale: + high; 0:neutral; -: low).....	27
Table 3.2: Lane changing model comparison (performance scale: + high; 0:neutral; -: low).....	27
Table 4.1: Required data for each parameter.....	29
Table 4.2: Explanation and quantification judgement symbols.	32
Table 4.3: Comparison of data collection methods.	33
Table 4.4: Determinant values of all locations.	37
Table 6.1: Expected headway times for different configurations and vehicle types.	55
Table 6.2: Speeds at specific following distances at each configuration for each vehicle type.	64
Table 6.3: Results of fitted normal distributions (mean value and standard deviation).	71
Table 6.4: Single parameter estimation results.....	80
Table 6.5: Values for capacity and capacity drop for each simulated configuration.	86
Table 7.1: Determinant values of worked out configurations.	90
Table 7.2: Single parameter estimation results.....	92

Appendix 2 Table of Capacity

	Capacity recommended values by CIA	Speed Limit (km/h) with average lane width 3.5			Average lane width (m) with 70 speed limit		
		70	80	90	(3.2,3.4)	(3.4,3.6)	3.75
	1500	NA	NA	NA	NA	NA	NA
	3300	3370	3250	3300	3370	3370	3030
	3400	3330	3320	3330	3330	3330	3350
	1400	Case not included, NA					
	1500	Case not included, NA					
	2870	2230	2060	2000	2860	2230	2000
	1350	Case not included, NA					
	2700	2970	3690	3690	2950	2970	2980
	(2700,3300)	3330	3320	3330	3330	3330	3350
	(1100,1500)	Case not included, NA					
	(2400,3300)	Case not included, NA					
	(2850,3330)	2650	2050	2000	2960	2650	1980
		Case not included, NA					
	>4000	3620	3740	3770	4240	3620	3600
	<1300	Case not included, NA					
	<1300	Case not included, NA					

(Note: NA stands for not available. In this study, there is no single-lane work zone case with lane width lower than 3.5 meter. Neither is occupying hard shoulder for extra lane. 4-0 system and parallel reroute system is applied in the studied projects, however no detector can be matched to obtain relative data.)

Appendix figure 1: CIA recommendation table extended with values from the research of Zheng (2009).

Appendix 3 Measurement registration forms

Measurement Registration Form TU Delft			Form No: /
Observer:		Tel:	
Location number			
Time Start			
Time End			
Date			
Day			
Temperature (°C)			
Weather			
Incidents			
Activity Intensity			
Landing location			
Direction			
Speed Limit			
Channelizing device (2x)			
Number of lanes			
Marking (2x)			
Duration of figuration			
Remarks			

Measurement Registration Form TU Delft			Form No: 1/2
Observer:	Rosco Voorrips	Tel	+31 (0)6 40303405
Location number	1	2	
Time Start	7:10	9:15	
Time End	8:45	11:00	
Date	June 17th 2011		
Day	Friday		
Temperature (°C)	12-16	16-18	
Weather	Sunny	Heap clouds	
Incidents	n/a	n/a	
Activity Intensity	0	0	
Landing location	De Bilt: Upsalapad	Soesterberg: Kampweg	
Direction	West --> East	Both	
Speed Limit	90 km/h	90 km/h	
Channelizing device (2x)	Guardrail (L), small barricades (R)	Guardrail 4x	
Number of lanes	2	2x2	
Marking (2x)	White, discontinued	White, discontinued	
Duration of figuration	3 weeks	n/a	
Remarks			

Measurement Registration Form TU Delft			Form No: 2/2
Observer:	Rosco Voorrips	Tel	+31 (0)6 40303405
Location number	3		4
Time Start	13:45		15:10
Time End	14:50		16:00
Date	September 15th 2011		
Day	Thursday		
Temperature (°C)	17		17
Weather	Cloudy		Cloudy
Incidents	n/a		n/a
Activity Intensity	0		0
Landing location	A28 exit 8		Soesterberg kamweg
Direction	Both		Both
Speed Limit	90 km/h		90 km/h
Channelizing device (2x)	Barrier 3x (L-R), Guardrail 1x (R)		Barrier 1x (L) Guardrail 2x (R)
Number of lanes	2 and 3		2x2
Marking (2x)	Yellow, parts continued		Yellow, discontinued
Duration of figuration	6 months		2 weeks
Remarks			
Location 4: Direction W-E, small reserve curve to pass viaduct			

Appendix 4 Stabilization software manual

In the next few pages, the usage of the stabilization software is explained.

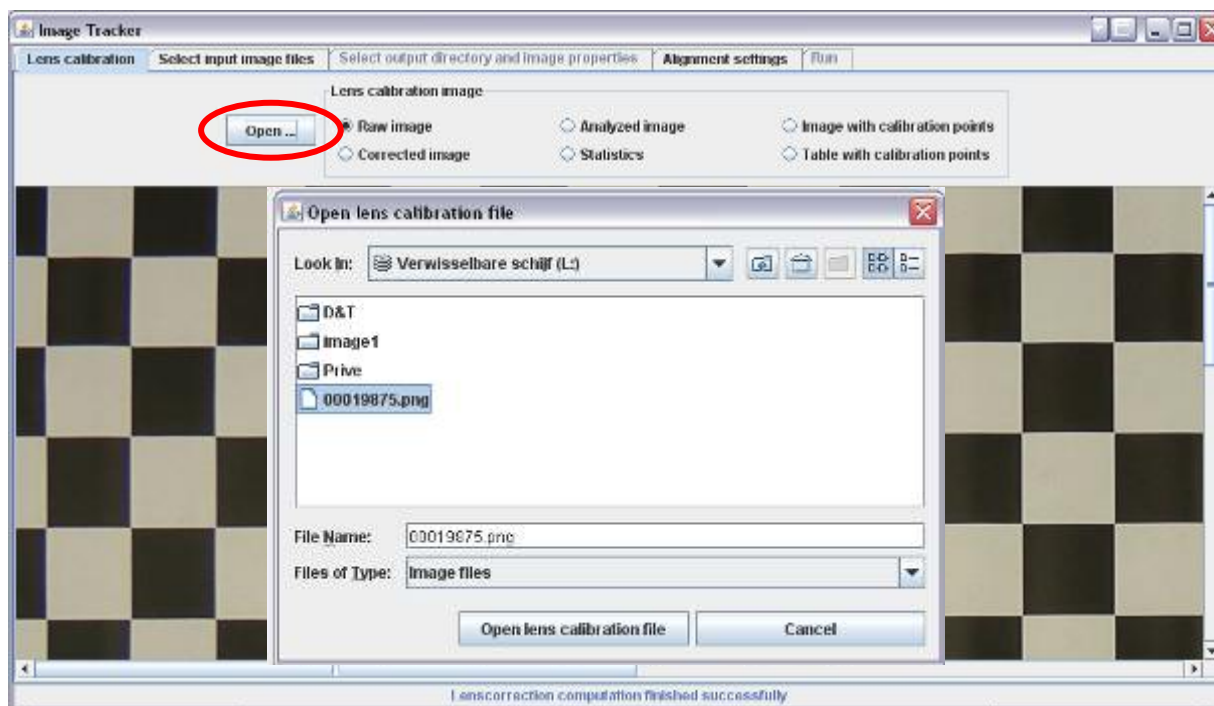
The latest manual is available at:

<http://www.regiolab-delft.nl/?q=node/76>

Condition for using the program is that the computer runs Java applications.

- Tab: Lens calibration:

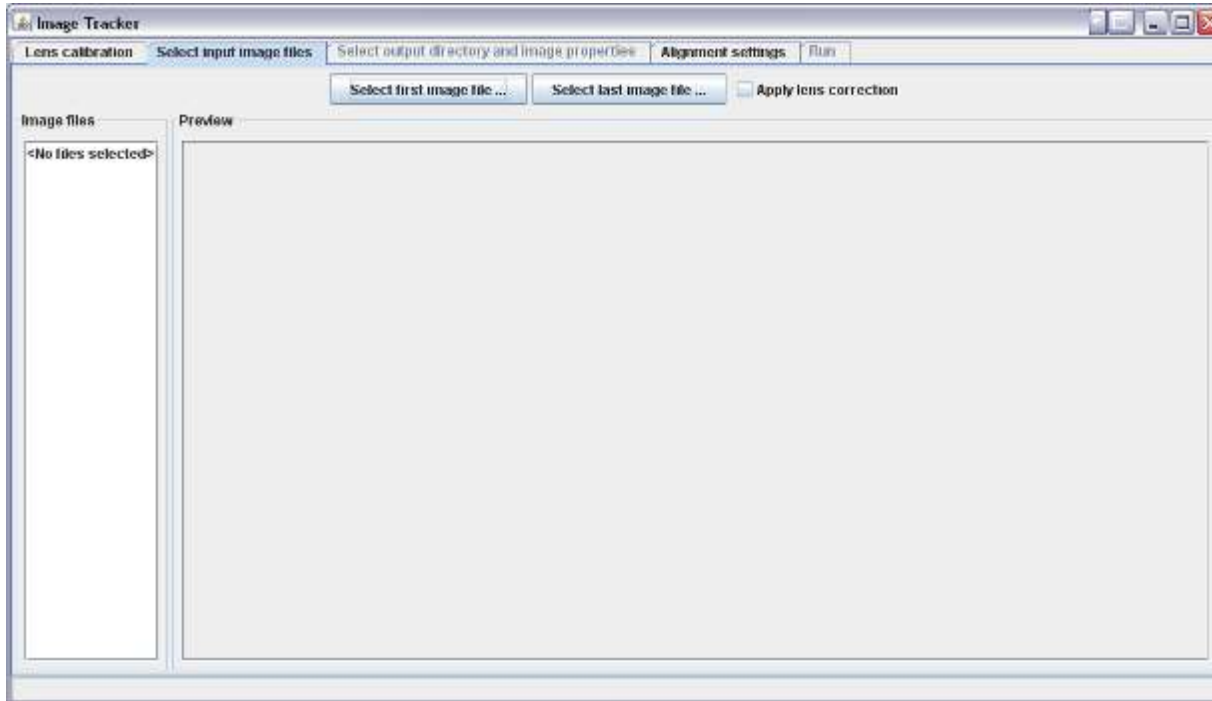
Open lens calibration file:



After opening calibration file and selecting another tab, the lens correction is automatically performed. At this tab you must add the height of the camera in pixels. If the calibration image recorded a width of 10m represented by 2000 pixels, and the camera was at a height of 5m, the elevation is 1000 pixels.

- Tab: Select input image files

By pressing the button 'Select first image file...' and 'Select last image file...' you can select the series of images which have to be stabilized. It selects all images in the same folder between the first and the last image.



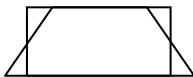
- Tab: Select output directory and image properties

Here, the output folder can be selected.

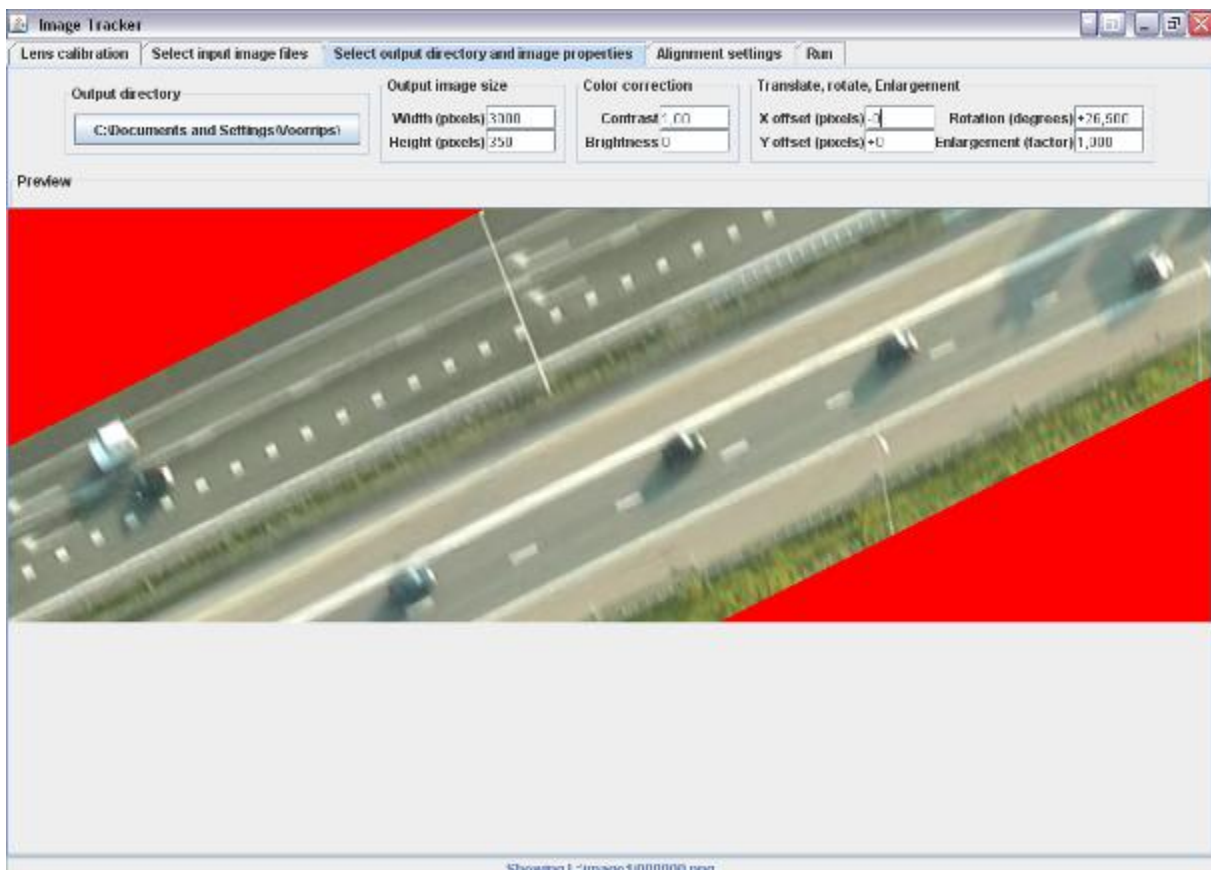
Furthermore the preferences for the movies can be configured. The way this leads to good results is described in the main report. You can change the size of output image, perform a colour correction, translate, rotate and enlarge the image.

Finally you can also change the wedge distortion parameters. By changing the x-wedge the images are rotated over the x-direction. As a result the distance per pixel can be configured to be equal over the lanes. By changing the y-wedge the distance per pixel over one lane can be adjusted:

- x-wedge (+): to change differences in distances in height of image:

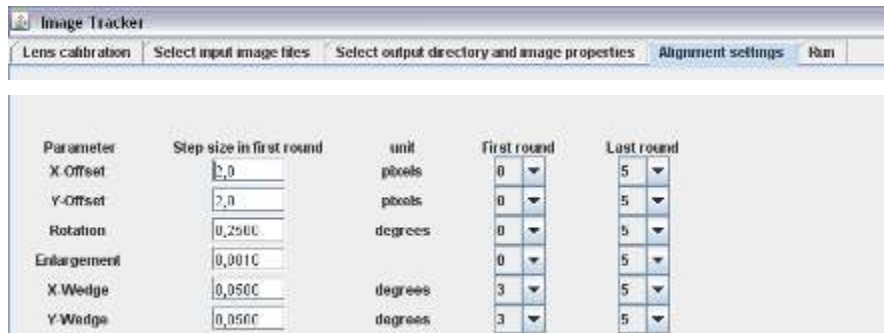


- y-wedge (+): to change differences in distances in width of image:



- Tab: Alignment settings

In this menu, the settings for the stabilization process can be changed. Normally the default values work out fine, but can be changed if necessary.



- Tab 5 Run

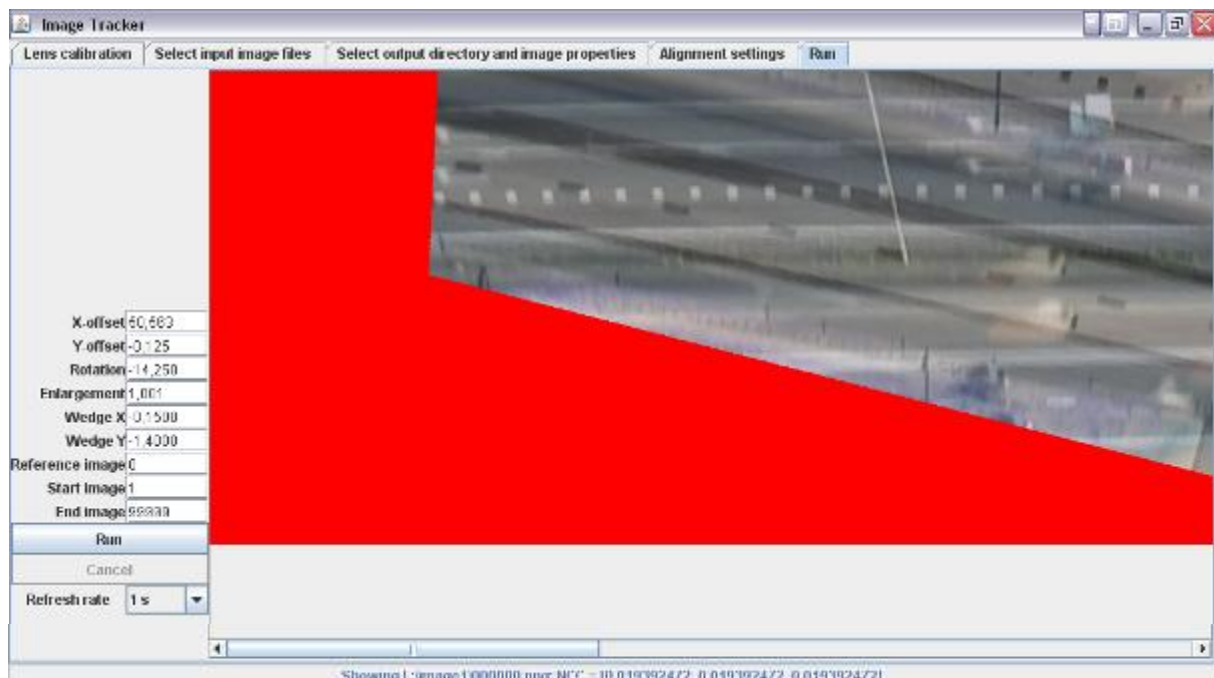
The values in this tab have to be changed if an interrupted stabilization process has to be continued.

For the first series of one movie, all values can be set 0, except 'Enlargement' which has to be set to 1, and 'End Image' which can be set to 99999. By pressing the 'Run' button the process starts.

During the stabilization process, for every stabilized image, all changes in parameter values are logged in a file called results.txt.

If an interrupted process has to continue, the values out of results.txt of the last stabilized image can be put into this tab. By setting the start image to the image number where the process has to continue, the process continues after pressing 'Run' again.

By using this feature, the process can be stopped and continued at every moment.



- Batch file.

The whole process can be run from a batch (.bat) file as well, which is efficient when having a large number of images/parallel processes.

An example of a command line in a batch is given below:

```
java -jar D:\Rosco\ImageTracker.jar Run Elevation=1752
LensCalibration=D:\Rosco\00019875.png StartImage=1 InitialWedgeY=0.575
InitialWedgeX=-0.6375 InitialEnlargement=0.98722 InitialRotation=1.3591
InitialXOffset=24.813 InitialYOffset=-15.938 OutputWedgeY=5 OutputWedgeX=-
35 OutputRotation=1.2 OutputYOffset=-100 OutputXOffset=0 OutputHeight=400
OutputWidth=3000 OutputDirectory=X:\rvoorrips\PNG"
"STREAM1\003A\Stabilized" "(1)\Output\ LastImage=X:\rvoorrips\PNG"
"STREAM1\003A\Stabilized" "(1)\00003775.png FirstImage=X:\rvoorrips\PNG"
"STREAM1\003A\Stabilized" "(1)\00001676.png
```


Appendix 5 Matlab programs

This appendix gives the basic source code for Matlab programs used for this study.

Exceptions etc. which are not necessary are deleted or left out to compress the amount of code

Program overview

- CheckStabilizedFrames: To find 'jumps' in images which are a result of the program ImageTracker.
- CreateCrossSections: To create cross-sections of individual stabilized frames with use of pixels located in the centre of the lane.

Programs based on cross-section images

- FindVehs: To find vehicles using an edge detection method, which results in Boolean value matrices (1 for possible vehicle, 2 if not).
- Remove Edges: To automatically remove left and right stabilization edges.
- Remove Viaduct: To remove region edges from found edges.
- Proposed Selection: To find most of the vehicles.
- Dijkstra: Find shortest paths with Dijkstra Algorithm.

CheckStabilizedFrames.m (Brief overview)

Repeated, but necessary parts which are not reported for notational convenience are marked bold.

```

%% CONFIGURATION
% Stabilized Images input directories
ImDir(1).DirName = 'G:\Rosco2\BackupStream2\00005A\Stabilized\';
ImDir(2).DirName = 'G:\Rosco2\BackupStream2\00007A\Stabilized\';
type = '.png'; % type of inputimages (extension)
% OutputStabilized serie names
ImDir(1).Serie = 'STR2_00005A';
ImDir(2).Serie = 'STR2_00007A';
% Limit of error (start with inf): can be set by viewing figure
Limit = inf;
% Outputdir(s)
DirOut(1).DirName = 'C:\Rosco\MatlabCode\Rosco\Stabilisatie\StabCheck\';
%% PROCESS
p = length(ImDir);
for q = 1:p
    qDir = ImDir(q).DirName;
    ImList = dir([qDir '*' type]);
    ImSt = imread([qDir filesep ImList(1).name]); % Load 1st image
    % Give size of image height+width in pixels, colours 2=BW 3=RGB
    [height,width,colour] = size(ImSt);
    %% Load every image, calculate error with first & compare with previous
    result = zeros((numel(ImList)-2),2); % Zero arrays for array
    Result = result(:,1:2);
    i4 = 0; % start value of error array
    % From 3, because for 1: error=0, and 2 compared to 1 error=very large
    for i1 = 3:(numel(ImList))
        % First, load the previous and calculate error compared to ImSt
        ImPr = imread([qDir ImList(i1-1).name]);
        errorPr = 0; % start error = 0
        for i2 = 1:colour % calculate error for each colour
            ImStC = ImSt(:,:,i2); % for 1st image
            ImPrC = ImPr(:,:,i2); % for previous image
            % Error = calculated error + error of previous colour(s)
            errorPr = sum(abs(ImStC(:)-ImPrC(:)) + errorPr;
        end
        % Second, load the current and calculate error compared to ImStart:
        errorCu
        % Difference in error towards 1st image of prev and current image
        delta_error = abs(errorCu - errorPr);
        i4 = i4+1; % give rownr of error matrix
        result(i4,:) = [i4 delta_error];
    end
    Result(:,1:2) = [result(:,1) result(:,2)/(height*width)];
    %% SAVE RESULTS
    save([DirOut(1).DirName ImDir(q).Serie],'Result','qDir')
    %% Figure of results
    close all, hold on;
    figure('Numbertitle','off','Name',['error differences of ' qDir]);
    plot(Result(:,1),Result(:,2),'.')
    if Limit ~= inf
        plot([1 i4], [Limit Limit],'r')
    end
    xlabel('image sequence'), ylabel('delta\_error');
    saveas(gca,[DirOut(1).DirName ImDir(q).Serie],'png');
end
end

```


PictureTransform.m (Brief overview)

```
%% CONFIGURATION
% Set main directories
AllMov(1).InDir = 'F:\Data1\Frames\';
AllMov(2).InDir = 'F:\Data1\Frames\';
% Set movienames (folder names)
AllMov(1).MovName = 'Movie1';
AllMov(2).MovName = 'Movie2';
% Set ZoneNames
AllMov(1).ZoneDir = '\\Stabilized\Zone';
AllMov(2).ZoneDir = '\\Stabilized\Zone';
% Set matrix with number of zones per movie
AllMov(1).ZoneNum = 5;
AllMov(2).ZoneNum = 4;
% Lanenums, if occlusion can appear, laneNum is higher than number of lanes
AllMov(1).LaneNum = 4;
AllMov(2).LaneNum = 4;
% Order of curve
AllMov(1).Order = 2;
AllMov(2).Order = 2;

% Maximum image length, to prevent matlab memory errors
ImHmax = 5000;
% Output dir
OutDir = 'C:\MatlabCode\D&T\CS\';
% Directory with pixelindices
pixDir = 'C:\MatlabCode\D&T\Pixels\';

%% PROCESS
for M1 = 1:length(AllMov) % for every movie
for Z1 = 1:AllMov(M1).ZoneNum % for every zone
% Load frames for this folder
FrameDir = [AllMov(M1).InDir AllMov(M1).MovName ...
    AllMov(M1).ZoneDir num2str(Z1) '\\'];
FramesFiles = dir([FrameDir '*.png']);
% Load pixels
pixels = dlmread([pixDir AllMov(M1).MovName 'Zone' num2str(Z1) ...
    '.txt'])+1; % +1 because pixels are 0-based, and matlab is 1-based
LaneNrs = size(pixels,1);
% Determine number of images and empty output image
% Load first image
fr = imread([FrameDir FramesFiles(1).name]);
% Number of colours (2=B&W or 3=RGB)
colour = size(fr,3);
% Order
Order = AllMov(M1).Order;
% For every lane
for LaneNr = 1:LaneNrs
% Load pixels and change row<->col
p1 = zeros(numel(pixels(LaneNr,:))/2,2);
p1(:,1) = pixels(LaneNr,2:2:end);
p1(:,2) = pixels(LaneNr,1:2:end);
% Remove empty rows
p1(sum(p1(:,1)+p1(:,2))==0,:) = [];
% Fit curves to defined polynomial order
warning('off', 'MATLAB:polyfit:RepeatedPointsOrRescale')
pfl = polyfit(p1(:,1),p1(:,2),Order);
warning on all
% Fit all points
x = 1:size(fr,2);
```

```

y1 = round(polyval(pf1,x));
y1(y1<1) = 1;
y1(y1>size(fr,1)) = size(fr,1);
% Set indices as 1 vector
sect(1).curve = size(fr,1)*((1:size(fr,2))-1)+y1;
% start values of output picture
ImNo = 0;
rownr = 0;
for fr_i = 1:length(FramesFiles) % For every frame
    rownr = rownr+1;
    if rownr == 1 % if first row, create empty output image
        comb = zeros([ImHmax size(fr,2) colour],'uint8');
    end
    fr = imread([FrameDir FramesFiles(fr_i).name]);
    for colour1 = 1:colour
        fr1 = fr(:, :, colour1); % colour matrix
        fr1 = fr1(sect(1).curve); % pixel indices old
        comb(rownr, :, colour1) = fr1; % save cross section
    end
    % Check if next frame needs new image
    NewImage = false;
    if rownr == 5000
        SaveImage = true;
    elseif fr_i == length(FramesFiles)
        SaveImage = true;
    elseif 1 ~= str2double(FramesFiles(fr_i+1).name(1:end-4)) - ...
        str2double(FramesFiles(fr_i).name(1:end-4))
        SaveImage = true;
    end
    % If image has to be saved
    if SaveImage == true
        comb(rownr+1:end, :, :) = [];
        % Determine image number
        ImNo = ImNo+1;
        rownr = 0;
        % Set Imagename
        fname = [OutDir AllMov(M1).MovName '_Z' num2str(Z1) ...
            '_L' num2str(LaneNr) 'No_' num2str(ImNo) '.png'];
        % Save image
        imwrite(comb, fname);
    end
end
end
end
close all

```

Find Vehicles (Brief overview of files)

Too prevent that the overview becomes too large, and large parts of code are used multiple times, more programs are explained. References to this program parts are capital bold. Per proces, change in and output directories, so all can be isolated be run.

```
clc,clear all,close all
%% A. CONFIGURATION
% Set input and output directory
InDir = 'C:\MatlabCode\D&T\CS\';
OutDir= 'C:\MatlabCode\D&T\FoundVehs\';
Ims = dir([InDir 'Im*']); % find number of vehicles
% Set thresholds for edge(), leave empty for default value
bnd = [];

%% B. PROCES
% For every image
for Im1 = 1:numel(Ims)
    im = imread([InDir Ims(Im1).name]); % Load image
    % PROCESSES
    EDGE DETECTION
    REMOVE STABILIZATION EDGES
    REMOVE AREA (VIADUCT)
    PROPOSED SELECTION (2 Parts)
    SHORTEST PATH
    CORRECT WRONG TRAJECTORIES
    fname = ['Vh#S' Ims(Im1).name(5:end-4)];
    fname1 = [OutDir 'Images\' fname '.png'];
    % Save image
    imwrite(im,fname1)
end

EDGE DETECTION
% Determine if image is color or b&w
[~,~,z]=size(im);
if z==1
    im=edge(im,'canny',bnd); % Edge Detection using Canny method
elseif z==3
    im=rgb2ycbcr(im);
    im=edge(im(:,:,1),'canny',bnd);
end

REMOVE STABILIZATION EDGES
[yn xn z] = size(im);
cs = imread([csDir 'Im' Ims(Im1).name(3:end)]); % load colour image
for y = 1:yn % for every row
    % If first pixel is edge (red = [255 0 0])
    if cs(y,1,1) == 255 && cs(y,1,2) == 0 && cs(y,1,3) == 0
        for x1 = 1:xn % for every column while pixel is edge
            if cs(y,x1,1) ~= 255 || cs(y,x1,2) ~= 0 || cs(y,x1,3) ~= 0
                break
            end
        end
        im(y,1:x1) = 0; % fill row with zero's
        SAVE x1 FOR PROPOSED SELECTION (edge1(y))
    end
    % Do same proces for other edge (right 2 left)
    if cs(y,xn,1) == 255 && cs(y,xn,2) == 0 && cs(y,xn,3) == 0
        for x1 = xn:-1:1
```

```

        if cs(y,x1,1) ~= 255 || cs(y,x1,2) ~= 0 || cs(y,x1,3) ~= 0
            break
        end
    end
    im(y,x1:end) = 0;
    SAVE x1 FOR PROPOSED SELECTION (edge4(y))
end
end
end

```

REMOVE AREA (VIADUCT)

```

% Set directory with viaduct location
InTxsDir = 'C:\MatlabCode\D&T\ViaductIndices\';
Tx = dlmread([InTxsDir Txs(Im1).name]); % load indices for this image
% Remove area
SAVE EDGES FOR PROPOSED SELECTION (edge2) & (edge3)
im(:,Tx(1)+1:Tx(3)+1) = 0;

```

PROPOSED SELECTION

```

%% PART 1
% Propose vehicles @ all edges (left+right (also @ viaduct)
[yn xn z] = size(im);
y1 = 0; y2 = 0; y3 = 0; y4 = 0;
vhE1 = 0; vhE2 = 0; vhE3 = 0; vhE4 = 0;
for y = 3:yn-2 % for every row (except first and last 2)
    Continue_edge2and3 = false; % Check which edges have to be performed
    if edge2 == 0 && edge3 == 0 % if both viaduct edges are zero
        Continue_edge2_3 = true;
    elseif edge2 < edge1(y) % if viaduct is smaller than left edge
        if edge1(y) < edge3 % and viaduct right is larger than left edge
            edge1(y) = edge3; % set new left edge as first edge
        end
        Continue_edge2_3 = true;
    elseif edge3 > edge4(y) % perform the same for right edge
        if edge2 < edge4(y)
            edge4(y) = edge2;
        end
        Continue_edge2_3 = true;
    end
end
% If edge is found @ image bound of edge 1,2,3,4.
if im(y,edge1(y)+2) == 1
    % Check if vehicle has found in 25 frames (1 sec) before
    if y-25 > y1 || y1 == 0
        % Check end of edge > .5*range: vehicle=found.
        % Edge length and arc
        [iniLength arc] = TRACKLINE(y, edge1(y)+2, xn, im);
        if Continue_edge2_3 == false && 2*iniLength > edge2(y) - edge1(y) - 2
            y1 = y;
            vhE1 = vhE1 + 1;
            vhsE1(vhE1,1:4) = [vhE1, y, edge1(y)+2 arc];
        elseif 2*iniLength > edge4(y) - edge1(y) - 2
            y1 = y;
            vhE1 = vhE1 + 1;
            vhsE1(vhE1,1:4) = [vhE1, y, edge1(y)+2 arc];
        end
    end
end
end
if im(y,edge2(y)+2) == 1 && Continue_edge2_3 == false
    % Perform same method as for edge 1, but backwards to edge 1
end
if im(y,edge3(y)+2) == 1 && Continue_edge2_3 == false

```

```
        % Perform same method as for edge 1, but from edge 3 to 4
    end
    if im(y,edge1(y)+2) == 1
        % Perform same method as for edge 1, but backwards from edge 4 to 1
    end
end
% save vhs matrices
save([Outdir Do Ims(Iml).name(3:end-4) '.mat'],'vhsE1:4')
% Plot all found vehicle starts and ends
for dot = 1:length(vhsE1)
    y1 = vhsE1(dot,2);
    x1 = vhsE1(dot,3);
    % Set vehicle start to white
    im(max(1,y1-5):min(y1+5,yn),max(1,x1-5):min(xn,x1+5)) = 1;
end
% Perform same operations for all vehicles
for dot = 1:length(vhsE2,E2 & E4)
end

%% PART 2: After checking with indices program
CorDir = 'C:\MatlabCode\D&T\Correction\' % directory with correction pixels
Dots = dlmread([CorDir 'Cr#' Ims(Iml).name(3:end-4) '.txt']);
% Delete wrong (start with 0 0) and calculate estimated arc
arcs = [];
for D1 = 1:numel(Dots)/4
    if ~(Dots(D1*4-3) == 0 && Dots(D1*4-2) == 0)
        continue
    end
    distMinE1 = [inf 0]; % set distance to infinity
    % Find closest point, checking every edge
    for dot = 1:length(vhsE1)
        dist = abs(Dots(D1*4)-vhsE1(dot,2))+abs(Dots(D1*4-1)-vhsE1(dot,3));
        if dist < DistMinE1(1)
            distMinE1 = [dist vhsE1(dot,1)];
        end
    end
    end
    for dot = 1:length(vhsE2:4)
        % Same for all edges to find closest
    end
    % Delete closest point
    if min(DistMinE1:4) == DistMinE1
        vhsE1(vhsE1(:,1)== distMinE1(2),:)=[];
    elseif % other edges
    end
end
EdgeRange = [1 xn/2 xn];
for D1 = 1:numel(Dots)/4
    % By adding new points, set edgeNo by clicking near image edge or mid
    if Dots(D1*4-3) == 0 && Dots(D1*4-2) == 0 % if delete, skip
        continue
    end
    EdgeSelection = abs(EgdeRang-Dots(D1*4-2));
    ind = find(EdgeSelection==min(EdgeSelection));
    if ind == 1 % save as E1
        vhsE1(end+1,1:4) = [max(vhsE1(:,1)+1),Dots(D1*4),Dots(D1*4-1),0];
    elseif ind == 3
        vhsE4(end+1,1:4) = [max(vhsE4(:,1)+1),Dots(D1*4),Dots(D1*4-1),0];
    else % ind ==2
        if Dots(D1*4-1) < Dots(D1*4-3) % save as edge2
            vhsE2(end+1,1:4) = [max(vhsE2(:,1)+1),Dots(D1*4),...
                Dots(D1*4-1),0];
        end
    end
end
```

```

        else % save as edge 3
            vhsE3(end+1,1:4) = [max(vhsE3(:,1)+1), Dots(D1*4), ...
                Dots(D1*4-1), 0];
        end
    end
end
save([Outdir SE Ims(Im1).name(3:end-4) '.mat'], 'vhsE1:4')

% Find expected destination using (mean) arc
% Plot matching starts-ends, with different colours/markers.
% Check+change manually, ends in 4 columns, 2 for Start and 2 for End point

% TRACKLINE
% Set start pixel active and visited.
% while any pixel is active & required path length is not reached,
%   pathlength+1
%   If connected pixels of active pixels exist, are not-visited, and == 1,
%   Set pixel active and visited
%   end if
%   Set current active pixel inactive
% end while

DIJKSTRA
% Function using the resistance map (im) and origin & destination (nodes)
function im = G1_Dijkstra(im,nodes)
global globalRows globalCols imActive imVisited imDirection imFilled
[globalRows globalCols] = size(im);
imActive = [];
imVisited = false(size(im));
imDirection = imVisited;
imFilled = zeros(size(imVisited),'uint8');
% File to find shortest path between 2 points
% Set start and end of paths
rowS = nodes(1); % indices
colS = nodes(2);
rowE = nodes(3);
colE = nodes(4);
% Check if start or end is out of bounds
if rowS > globalRows || rowS < 1 || rowE > globalRows || rowE < 1 ...
    colS > globalCols || colS < 1 || colE > globalCols || colE < 1
    error('nodes out of bounds')
elseif colS == colE || rowS == rowE
    error('Start point is the same as End point')
end
tripLength = 0; % distance of current trip: start = 0
tripLengthMax = (abs(rowE-rowS)+1+abs(colE-colS)+1)*double(max(im(:)));
imActive = [rowS colS]; % active pixel = only start pixel
imVisited(rowS,colS) = 1; % visited pixel = only start pixel
% direction of set pixels active
if colS < colE
    direction = [5 8 7]; %7 3 6 2 4 1];
else % colS > colE
    direction = [4 6 7]; %7 1 8 2 5 3];
end
% 2. While destination is not reached, set tripLength+
while ~imVisited(rowE,colE)
    tripLength = tripLength + 1;
    % Check to prevent while loop from endless looping
    if tripLength > tripLengthMax
        error('Length trip is too long')
    end
end

```

```
% Create matrix for removing pixel form active pixel list
setRemove = [];
% For all active pixels
N = size(imActive,1);
for n = 1:N
    P1 = imActive(n,1);
    P2 = imActive(n,2);
    if imFilled(P1,P2)<im(P1,P2)
        imFilled(P1,P2) = imFilled(P1,P2)+1; % add 1 if not filled
    elseif imFilled(P1,P2) == im(P1,P2)
        setRemove = [setRemove n]; % set active pixel on remove list
        % Find connected, existed, unvisited pixels
        % Save these pixels in imActive imVisited imDirection
        G2_Neighbours(P1,P2,direction)
    End
end
% Remove pixels which are not active any more, due to previous loop
for getRemove = setRemove'
    imActive(getRemove,:) = [];
end
end
% 3. Find shortest path, by travelling back to start by use of directions.
imActive = [rowE colE];
imVisited= false(globalRows,globalCols); % save path in imVisited
imVisited(rowE,colE) = 1; % Set end point as visited
tripBack = 0; % record length of backTrip
while ~imVisited(rowS,colS)
    tripBack = tripBack+1;
    convertedDirection = 9-imDirection(imActive(1,1),imActive(1,2));
    % 3.5 Get backward indices pixel and set visited & (only) active pixel
    G4_WayBack(imActive(1,1),imActive(1,2),convertedDirection)
end
im = imVisited;
end

function G2_Neighbours(row,col,direction)
global imActive imVisited imDirection
% Program to find connected, existed and unvisited pixels
% These pixels have to be set active, visited and direction has to saved
if isempty(direction)
    direction = [1 2 3 4 5 6 7 8];
end
for pixel = direction % for all 8 connected pixels (only first is given)
    if G3_IndExist(row-1,col-1) && ~imVisited(row-1,col-1) && pixel == 1
        % Set indices as visited in imVisited
        imVisited(row-1,col-1) = 1;
        % Set indices as active in imActive list
        imActive(end+1,:) = [row-1,col-1];
        % Set neighbour position as origin direction in imDirection
        imDirection(row-1,col-1) = 1;
        continue
    end
    % Do same for other 7 pixels
end
end

function R = G3_IndExist(row,col) % Check if indices exists
%% Subprogram (3rd) G0
global globalCols globalRows
R = 0;
% If row or column is outside image boundary
```

```

    if row < 1 || col < 1 || row >= globalRows || col >= globalCols
        return
    end
    % If not (so indices exists), return 1 as result
    R = 1;
end

function G4_WayBack(row,col,direction) % to find way back
global imActive imVisited
%% Subprogram (4th) of ConnectTraj.m
%% For all 8 possible neighbours positions (only first done)
% --- 1 ---
if direction == 1
    % Set indices as visited in imVisited
    imVisited(row-1,col-1) = 1;
    % Set indices as active as imActive
    imActive = [row-1,col-1];
elseif % has to be done for all directions
end

function Traj4 = G5_AdjustTraj(Traj)
vehicles = unique(Traj(:,1));
vehicleN = numel(vehicles);
TrajRow = 0;
Traj4 = zeros(size(Traj));
for vehicleI = 1:vehicleN
    vehicle = vehicles(vehicleI); % Select vehicle
    Traj2 = Traj(Traj(:,1)==vehicle,:);
    % Do same excersise only with steps ~ rows = 2nd col of traj
    steps = unique(Traj2(:,2));
    stepN = numel(steps);
    % Per vehicle per time instance: One row in final Trajectory matrix
    for stepI = 1:stepN
        TrajRow = TrajRow+1;
        step = steps(stepI);
        Traj3 = Traj2(Traj2(:,2)==step,:);
        meanCol = sum(Traj3(:,3))/size(Traj3,1);
        Traj4(TrajRow,1:3) = [vehicle step meanCol];
    end
end
end
% Delete unused rows
Traj4(TrajRow+1:end,:) = [];
end

```

Traj2CarFollow

```

% File converting trajectories converting original to new output format
%% CONFIGURATION
InMatDir = ['C:\Rosco\Detect&Track\D&T\Output\RawTraj\VL_Mat\'];
LocationInfo = ['C:\Rosco\DataLocation\Config\MovLaneLocations.txt'];
OutDir = 'C:\Rosco\DataLocation\Output\';
Mas = dir([InMatDir 'VL#*.mat']);
dF = 2; F1 = true; % Perform dT = 1 frame?
%% PROCES
fid = fopen(LocationInfo); % open information of movies
Movie.Info = textscan(fid,'%q %q %q %q %q %q %q');
fclose(fid);
Movie.Stream = cell2mat(Movie.Info{1});
Movie.Name = Movie.Info{2};
Movie.Loc = str2double(Movie.Info{3});
Movie.Lanes = [str2double(Movie.Info{4}) str2double(Movie.Info{5}) ...
    str2double(Movie.Info{6}) str2double(Movie.Info{7})];

```

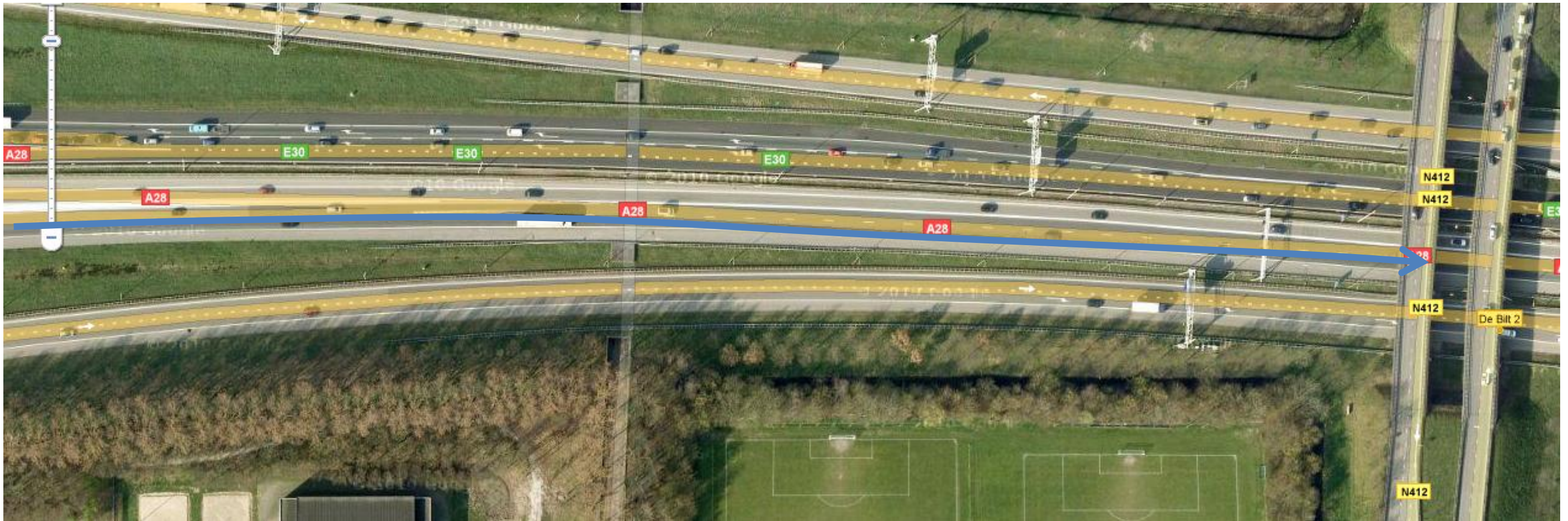


```
% Determine number of inputfiles
for Mat = 1:numel(Mas)
    % Load Trajectories matrix (Traj)
    load([InMatDir Mas(Mat).name], 'Traj') % inclusive extension (.mat)
    Traj(:, [6 7 8]) = Traj(:, [7 8 6]);
    % Format: VehNum, frameNum, LocPix, time, LocX, LengthPix, LengthX, VType
    Traj(:, 9:15) = 0;
    Traj(:, 16) = Traj(:, 3);
    Traj = sortrows(Traj, [1,2]); % Sort matrix first by vehID, then by time
    % Information of current image file
    Image.Info = regexp(Mas(Mat).name, '_', 'split');
    Image.Stream = Image.Info{1}(5:end);
    Image.Name = Image.Info{2};
    Image.Lane = str2double(Image.Info{4}(2:end));
    % Movie selection
    getMov = (Image.Stream==Movie.Stream) .* strcmp(Image.Name, Movie.Name);
    % Now, convert to required data
    Traj(:, 2) = Traj(:, 4); % new is time in seconds
    Traj(:, 3) = Traj(:, 7); % new is vehicle length in meters
    Traj(:, 4) = Traj(:, 8); % new is vehicle type
    Traj(:, 7) = Traj(:, 5); % new is position of vehicle in meters
    Traj(:, 5) = sum(getMov .* Movie.Loc); % new is observation location
    Traj(:, 6) = sum(getMov .* Movie.Lanes(:, Image.Lane)); % new is lane
    % Determine unique vehicles and calculate speed and accelerations
    Mtot = find(strcmp({Mas.name}, Mas(Mat).name));
    vehIDs = unique(Traj(:, 1));
    vehN = numel(vehIDs);
    for vehI = 1:vehN % for every unique vehicle
        veh = vehIDs(vehI);
        % Start iteration original matrix, only this vehicle
        N = Traj(Traj(:, 1)==veh, :);
        % If too little observations, do not calculate speed & acceleration
        if size(N, 1) < 3, continue, end
        N(2:end, 8) = (N(2:end, 7)-N(1:end-1, 7))./(N(2:end, 2)-N(1:end-1, 2));
        N(3:end, 9) = (N(3:end, 8)-N(2:end-1, 8))./(N(3:end, 2)-N(2:end-1, 2));
        % Copy from first calculated observation
        N(1:2, 9) = N(3, 9); % just copy acceleration
        N(1, 8) = N(2, 8) + N(3, 9) * (N(2, 2) - N(1, 2));
        if N(1, 4) < Bound.VT(Mtot)
            N(:, 4) = 1;
        end
    end
end
% Add leader information, determine number of observations
Traj(:, 15) = 1:size(Traj, 1); % number matrix with rows
rowN = size(Traj, 1);
for rowI = 1:rowN
    N = Traj(Traj(:, 1)~=Traj(rowI, 1), :);
    % Observations with same time as original in selected matrix
    N = N(N(:, 2)==Traj(rowI, 2), :);
    Nn = size(N, 1); % determine minimum location difference
    DisLeader = inf; % start with infinite distance
    for Ni = 1:Nn % For every left observation
        % Distance must be > 0 between possible leader and current veh
        if N(Ni, 7)-Traj(rowI, 7) > 0
            % If selected distance is larger than current, replace
            if DisLeader > N(Ni, 7)-Traj(rowI, 7)
                DisLeader = N(Ni, 7)-Traj(rowI, 7);
                rowLeader = N(Ni, 15);
            end
        end
    end
end
end
```

```
    if ~isinf(DisLeader) % determine if leader is defined
        % If defined load from original matrix
        Traj(rowI,10:14)= [Traj(rowLeader,3) Traj(rowLeader,4) ...
            Traj(rowLeader,7) Traj(rowLeader,8) Traj(rowLeader,9)];
    else % leader is not selected fill with NaN
        Traj(rowI,10:14) = [NaN NaN NaN NaN NaN];
    end
end
% Delete auxiliary column with rownumbers
Traj(:,15) = Traj(:,16);
Traj(:,16) = [];
%% Save
% File name based on original name
fname = ['Cf#' Mas(Mat).name(4:end)];
save([OutDir 'Total\' fname],'Traj')
end
```

Appendix 6 Images of Work Zone Configurations

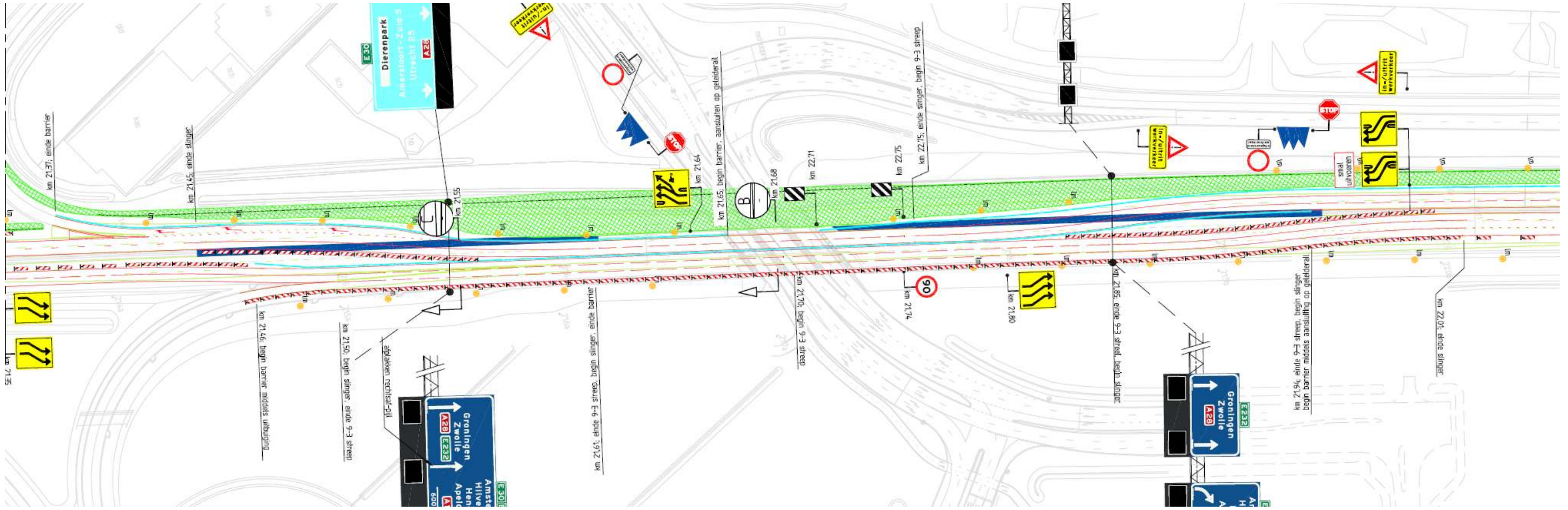
Location 1



Location 2



Location 3



Location 4

